NIPBL's role in building cohesion

Isobel Gretel Johns

Wolfson College

Department of Biochemistry

University of Oxford

A thesis submitted for the degree of Doctor of Philosophy

Trinity 2024

Abstract

Cohesin is integral to life through its ability to organise our duplicated DNA until it is segregated between two daughter cells. Equal segregation is ensured through a process called sister chromatid cohesion, which is essential to all eukaryotic life. The process of building sister chromatid cohesion, however, is not well understood. In this thesis, we explore the role of one of cohesin's main regulatory proteins, NIPBL, in facilitating this process. NIPBL associates cohesin with DNA, a process which underpins all of cohesin's activities. It also stimulates cohesin's ATPase activity which underpins some of its DNA organising abilities. To explore NIPBL's role in cohesin regulation, we develop the first internal NIPBL degron that allows acute depletion of all known isoforms of the protein. We find that NIPBL is essential and required for cohesion. We use this tool to explore the dependency of cohesion on NIPBL throughout the cell cycle to learn how NIPBL aids cohesin. We find that NIPBL is required for the establishment of cohesion, predominantly through its role as a cohesin loader, but not the maintenance of cohesion once it is built. We identify the critical window in the cell cycle where NIPBL first associates cohesin with DNA, and hence when NIPBL is essential for cohesion. In this thesis, we reveal a simple but powerful idea, that once NIPBL has fulfilled its task before S-phase of associating cohesin with DNA, it is no longer required for cohesion establishment or maintenance.

Acknowledgements

The PhD was a very unexpected path for me, and one which has taught me a lot about myself. A massive part of that journey was the people I came across who made it worth it, who have shaped who I am today, and would mean I wouldn't change a second of it. With that in mind, I want to say some thanks.

Firstly, I want to say thank you to those weird and wonderful people who initially drew me to the Nasmyth lab. Thank you to Jean Metson and Martin Houlard for looking after me from when I was a wee duckling, and for teaching me three very important principles: focus, be square, anticipate. Thank you to Fena Ochs for always believing in me, even when I didn't do so myself. Thank you to James Rhodes for being a consistent sounding board. Thank you to Mafalda Almeida for always checking in on a 'scientist at work'.

Thank you to James Collier for setting me on this path.

Thank you to my friends, who are (in my humble opinion) some of the greatest people on planet earth. Thank you to Meryem, Seren and Octavia. You make life wild and full of love. Thank you to Emma and Peru for your beautiful minds. Thank you to Jimmy and Nino for making my degree unforgettable. Thank you to Matt for our musings on life. Thank you to Scott, Ruari and George for the family we created. Thank you to Jen and Julius for putting me in hysterics, for always having my back, and for generally being the soundest people I know.

I am extremely lucky to have you all in my life.

Thank you to Elizabeth Edginton for getting me through the last leg of this PhD. You have the patience of a saint and a wisdom I can only one-day hope to achieve.

I want to say thank you to my family. Thank you to my mum and dad - I wouldn't have become the person I am today without your infinite love and the examples you both set with your fascination for life. Thank you to Richi for the soul we share, your emotional intelligence and depth of insight. Thank you to Rog for constantly making me laugh, and for being there for me when I need it most. Thank you also for letting me borrow one rather lovely little kitty in times of need.

Thank you to Grant Rowley for accepting and loving me for who I am, for supporting me, and for making me happy. You are light and goodness. I admire you every day, and I am blessed to have lived life and found my heart.

Finally, I want to thank my supervisors, Kim Nasmyth and Madhu Srinivasan. It was 8 years ago, whilst sitting in an undergraduate lecture, that I was taken by the topic of DNA organisation by a charismatic lecturer who would later become my boss. I have always appreciated the clarity of thinking, the straightforward approach to science, and the boldness to say things as they are, even if it goes against the grain. I have learnt a huge amount about what good science looks like from both of you, and I will always be grateful for the way you have taught me to think.

Table of Contents:

List of Common Abbreviations:

Aa	**Amino acid**
APC/C^{Cdc20}	**Anaphase-promoting complex/ cyclosome associated with Cdc20**
BSD	**Blasticidin**
CDK	**Cyclin-dependent kinase**
CdLS	**Cornelia de Lange syndrome**
ChIP	**Chromatin Immunoprecipitation**
CTCF	**CTCC-binding factor**
FRAP	**Fluoresence recovery after photobleaching**
G1	**Gap Phase 1**
G2	**Gap Phase 2**
HAWKS	**HEAT proteins associated with kleisin**
HEAT	**Huntington, elongation factor 3 (EF3), protein phosphatase 2A (PP2A), and the yeast kinase TOR1**
HU	**Hydroxyurea**
IF	**Immunofluorescence**
M	**Mitosis**
mAID	**miniAID**
MCC	**Mitotic checkpoint complex**
NIPBL	**Nipped-B like protein**
P2A	**Porcine teschovirus-1 2A**
PBS	**Phosphate-buffered saline**
PI	**Propidium Iodide**

Plk1	**Polo-like Kinase 1**
RFC	**Replication factor C**
S Phase	**Synthesis phase**
SAC	**Spindle assembly checkpoint**
SCC1	**Sister chromatid cohesion protein 1**
SGO1	**Shugoshin 1**
SiRNA	**Small interfering RNA**
SMC	**Structural Maintenance of Chromosomes**
Scs-Hi-C	**Sister-chromatid-sensitive Hi-C**
TAD	**Topologically Associated Domain**
WT	**Wild type**
4sT	**4-thio-thymidine**

Chapter I: Introduction

The Eukaryotic cell cycle

The founding principle of life is the ability of an organism to double from one to two. On the simplest level, this process starts with a cell which is able to replicate its genome and divide equally passing identical copies to two daughter cells. Organisms can exist on the single cellular level, such as bacteria or archaea, or can cooperate in larger multicellular organisms, where cells double and divide continuously to maintain the organism at large. In an average healthy human male between 20-30 years old, the process of doubling happens 330 billion times per day, and will happen with near perfect accuracy every time (Sender & Milo, 2021).

The fidelity of successful duplication is ensured through a highly choreographed series of events across the lifetime of a cell, collectively known as the cell cycle. The somatic eukaryotic cell cycle can be broadly described by two eras; interphase and mitosis. Interphase is the time in which the cells grow and duplicate their contents, and mitosis is the dramatic point at the end of the cell cycle when the cell divides in two. Interphase can be further subdivided into three phases: Gap1 phase (G1), synthesis phase (S) and gap 2 phase (G2), with the cell cycle of a newly divided daughter cell starting in G1 (**Fig. 1-1**). G1 and G2 are the growth phases where the cell gets larger in size and synthesises all the components necessary for the critical phases of S phase and mitosis. S phase is when the genome is replicated and mitosis is when the genome divides into two new daughter cells.

Critical to the cell cycle is the notion of directionality, where the cell progresses irreversibly in one direction through the series of phases (G1→S→G2→M→G1). The purpose of unidirectionality is to ensure that the genome is duplicated and segregated only once per cell cycle, to ensure genomic stability through the generations. Two families of proteins govern the transitions throughout the cell cycle: the cyclin-dependent kinases (CDKs) and their partner cyclins (Evans et al., 1983; Lee & Nurse, 1987). Oscillations in the concentrations of cyclins

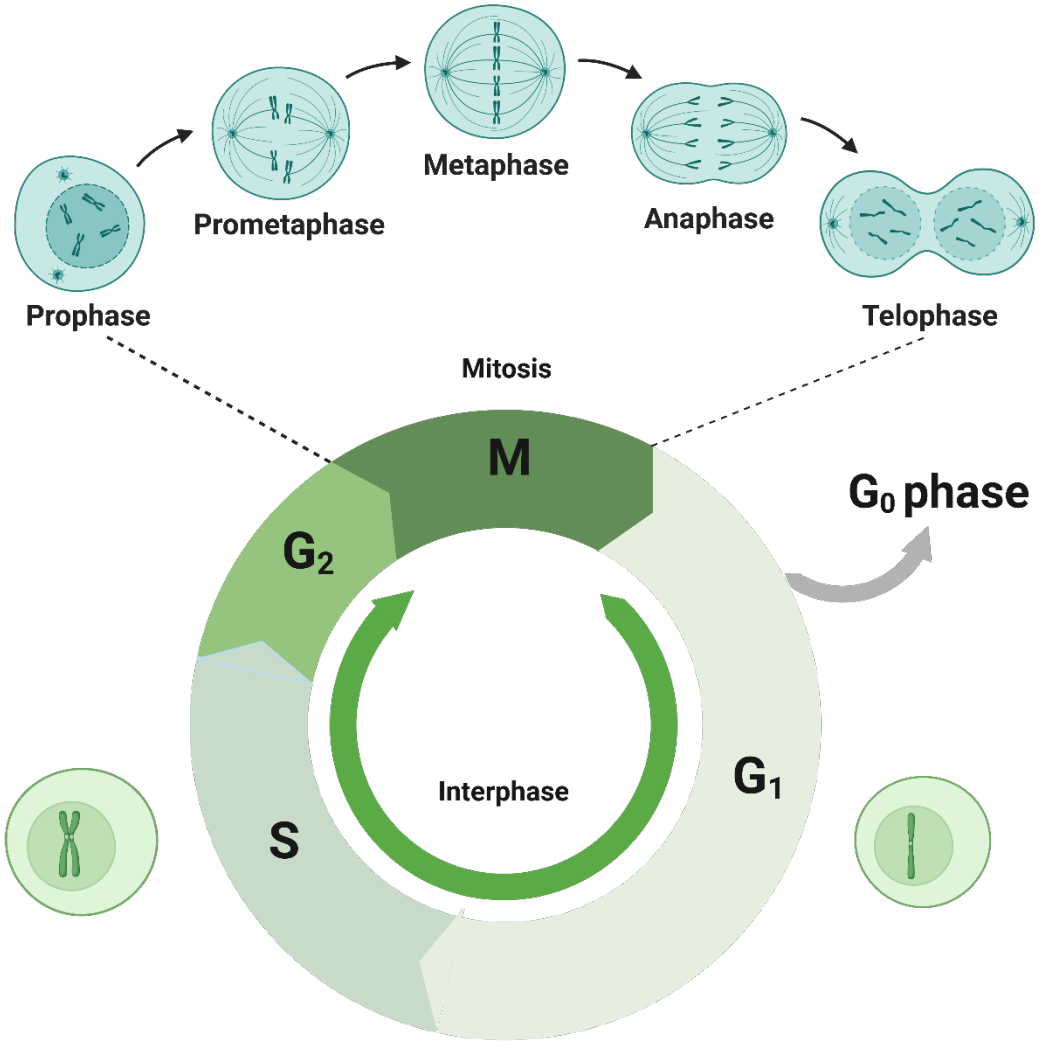

Figure 1-1. The eukaryotic cell cycle. Interphase begins clockwise from G1, moving to S and G2. Mitosis is composed of 5 phases. DNA doubles in S phase (n → 2n) and divides during mitosis to give a complete copy to two daughter cells (2n → n).

specific to each cell cycle stage regulate CDK activity, which in turn promotes progression through the cell cycle through the phosphorylation of key downstream substrates (Suryadinata et al., 2010). The irreversibility is generated through a "bistable switch" mechanism, where phosphorylation events either generate a positive or a negative feedback loop which ensure on a system level that the cell cannot move backwards (Novak et al., 2007). Before progressing, the cell ensures that it is ready for each transition through a series of checkpoints between critical phases, notably between G1/S and G2/M, which ensure the cell is ready before committing to cell division and the dramatic events of genetic duplication and segregation.

Dramatic moments for DNA: Replication, condensation and segregation

Genetic information is stored in double stranded DNA (dsDNA) molecules. In humans, this information is stored across 46 linear molecules of DNA called chromosomes, collectively known as the genome, whilst some organisms such as the Atlas Blue Butterfly possesses as many as 452 chromosomes (current animal Guinness world record holder). Each molecule of DNA is an extremely long polymer, only 2nm in width but collectively spans >1m in length in a human cell (M. D. Wang, 2021). The genome lives within a subcellular compartment of the a cell called the nucleus spanning only 6μM, which for context, is the equivalent of 40 km of string fitting into a vessel the size of a tennis ball (Alberts et al., 2002). Given its length, it is no wonder that DNA is a highly organised molecule, with hundreds of proteins devoted purely to its maintenance and architecture.

Throughout a cell cycle, DNA will undergo two major organisational feats. The first is during S phase, when DNA replication takes place. Here, each dsDNA molecule is unzipped and a new DNA molecule is synthesised along each of the unzipped strands creating two new DNA

molecules through a process of semi conservative replication. The cell is then left with two identical copies of DNA which are known as sister chromatids. The DNA content of the cell is now temporarily doubled with the intention of dividing later in the cell cycle. In the case of bacteria, equal segregation of the sister DNAs is ensured by simultaneous replication and segregation (Webb et al., 1997). The same is not possible to eukaryotic DNA due to its length and linear structure, therefore sister DNAs must instead remain associated from their synthesis in S phase until their segregation in mitosis. This process is called sister chromatid cohesion, and allows identical pairs of sister chromatids to be recognised so that one copy can be inherited to each daughter cell for a complete copy of the genome.

The second major organisational feat for DNA is during mitosis, when DNA first condenses and sister DNAs are then segregated. Mitosis occurs in 5 distinct phases; prophase, prometaphase, metaphase, anaphase and telophase. At the onset of prometaphase, the nuclear envelope of the cell breaks down, which allows all proteins to access DNA. The DNA compacts from an elongated and highly amorphic structure into a linear and highly compact structure called a chromosome. This individualises the chromosomes and condenses the DNA both laterally and longitudinally into a unit which can withstand forces and be moved around the cell (Earnshaw & Laemmli, 1983).

This is essential for its next feat in prometaphase where biorientation of the sister chromatids occur. Here, chromosomes become attached by microtubules emanating from spindle poles at opposite ends of the cell. Microtubules attach at a discrete locus on the chromosome called the centromere via large proteinaceous structure which assembles on its surface called a kinetochore (Cleveland et al., 2003). Kinetochores will attach to microtubules and once attached, will be pulled poleward along the microtubule (Tanaka & Desai, 2008). Vitally, it is essential that each sister chromatid kinetochore becomes attached by microtubules coming

from opposite poles. By doing this, sister chromatid cohesion can resist the opposing pulling forces from the spindle microtubules and this creates bi-orientation, ensuring that equal tension is applied across the sister chromatids, and lines the chromosomes along a central axis of the cell in metaphase (Tanaka, 2010). Whilst the microtubules are searching from their correct attachment, mono-orientation (the unequal binding of a microtubules to a kinetochore) may occur. In this case, tension is not applied across the complex and the attachment destabilises (Nicklas, 1997).

Only when all sister chromatids are fully bi-oriented will the cell progress to the next, and arguably most dramatic, step of the cell cycle which is anaphase. Here, the attachment holding the two sister chromatids together is broken, allowing the microtubules to pull one copy of each sister chromosome to either end of the cell. Through segregation, effectively two identical and independent copies of the genome become spatially separated. Finally, the cell moves to telophase, where the nuclear envelope reforms around each copy of the genome and the cell membrane divides into two through a process called cytokines until you have two independent identical daughter cells. At this point, chromosomes are able to decondense, and the cell cycle restarts in G1.

SMC complexes

Key to these two major organisational feats are the structural maintenance of chromosomes (SMC) proteins, an ancient family of proteins found in every phylum of life from prokaryotes to eukaryotes, which are dedicated to the organisation of chromosomes throughout the cell cycle (Soppa, 2001; Strunnikov et al., 1993). SMC proteins share a universal structure, forming a large ring shaped protein complex composed of a pair of SMC proteins and a kleisin subunit

(Gruber et al., 2003) (**Fig. 1-2**). SMC proteins are ~ 50nm long intramolecular antiparallel coiled-coils, which form a "hinge" domain at their apex and a "head" domain with their N and C termini (Haering et al., 2002). The hinge domain facilitates dimerization, allowing two SMC monomers to form a V-shaped dimeric complex, which are homodimeric in prokaryotes but heterodimeric in eukaryotes (Anderson et al., 2002). The head domain of each monomer forms half of an ATPase domain, containing a walker A and a walker B motif. Together, the dimerised pair form an ATP-binding cassette (ABC)-like ATPase domain, which enables the binding and hydrolysis of ATP (Löwe et al., 2001). The kleisin is an unstructured subunit that bridges the SMC dimers through binding to neck (just above the head domain) of one SMC with its N-terminus, and the base of the ATPase head domain on the other SMC protein with its C-terminus, and thus completing the ring structure (Gligoris et al., 2014; Haering et al., 2004).

In eukaryotes, three notable SMC proteins exist which catalyse sister chromatid cohesion, chromosome condensation and DNA repair through topologically interacting with DNA (Yatskevich et al., 2019). Cohesin is the protein responsible for aiding DNA's first organisational feat of sister chromatid cohesion from S phase until mitosis (Guacci et al., 1997; Michaelis et al., 1997). Condensin in responsible for DNA's next organisational feat of condensing DNA into manoeuvrable chromosomes in mitosis (Hirano et al., 1997; Hirano & Mitchison, 1994). Finally, SMC 5/6 is involved in DNA's repair pathway throughout the cell cycle (Palecek, 2019).

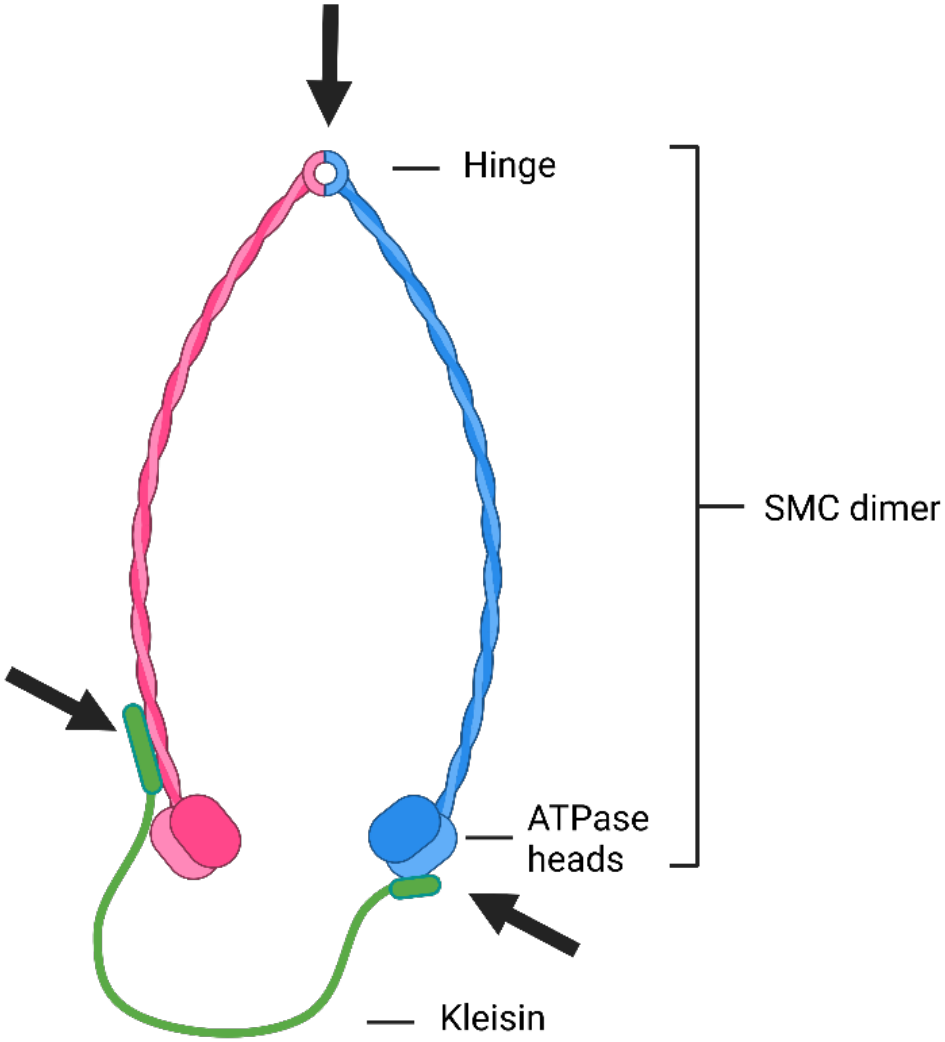

Figure 1-2. Basic structure of an SMC protein complex. Two SMC 50nm coiled coil proteins dimerise at the hinge domain and form an ATPase head with their N and C termini. They are connected by an unstructured Kleisin subunit which completes the tripartite ring. SMC complexes have three interfaces, marked with black arrows.

Cohesin: Sister chromatid cohesion and loop extrusion

Sister chromatid cohesion is essential to life, and without it cells are unable to receive a complete copy of the genome to each daughter cell. Cohesin builds sister chromatid cohesion exclusively during S phase when DNA replication takes place, and will associate with chromosomes but fail to build cohesion if loaded later in the cell cycle in G2 or M (Haering et al., 2004; Uhlmann & Nasmyth, 1998).

The cohesin complex is forms a tripartite ring from a heterodimer of SMC3 and SMC1 and a kleisin subunit RAD21^{SCC1}, yeast name in superscript (Haering et al., 2002). Cohesin's ring like structure provided a possible mechanism for cohesion, lending itself to the idea that both sister DNAs could be topologically entrapped within the 35nm diameter of the cohesin ring. Indeed, it was found in anaphase that SCC1 becomes cleaved and that sister chromatid disjunction could be recapitulated using a TEV-cleavable version of SCC1 or of the SMC3 coiled coil, showing that the integrity of the ring was vital (Gruber et al., 2003; Uhlmann et al., 1999, 2000). It was shown that DNA could be topologically entrapped within a cohesin ring through work in yeast using circular minichromosomes where cleavage of either cohesin, or the minichromosome lead to the dissolution of the cohesin/ minichromosome structure (Ivanov & Nasmyth, 2005). This topological entrapment was proven in the context of DNA replication, when a entrapment of single minichromosomes perfectly correlated with the co-entrapment of a dimer of minichromosomes (duplicated DNA) as cells passed through S phase (Haering et al., 2008; Srinivasan et al., 2018). Other than work using minichromosomes, more recently microscopy evidence visualising chromosomes illustrated that points of sister chromatin cohesion coincide with a single cohesin ring (Ochs et al., 2024).

Whilst cohesin was originally identified for its role in sister chromatid cohesion, it was more recently realised that it also shared a secondary activity with other SMCs like condensin, which

is the ability to create chromatin loops in DNA (Tedeschi et al., 2013) (**Fig. 1-3**). This looping process is called loop extrusion, and relies on the principle of binding pieces of the same DNA molecule to processively enlarge loops (Davidson et al., 2019; Ganji et al., 2018; Kim et al., 2019). Unlike condensin which generates very large chromatin loops in mitosis to condense DNA, cohesin is able to make more modest loops during interphase. A product of this interphase looping is the creation of regions of DNA that interact with a higher frequency (Dixon et al., 2012; Nora et al., 2012). These regions are bordered by convergently oriented insulating elements bound by CCCTC-binding factor (CTCF) proteins and are called topologically associating domains (TADs) (Fudenberg et al., 2016; Sanborn et al., 2015). Together with cohesin, it was shown in the *H19-IGF2 locus* (Wendt et al., 2008) and the *β-globin locus* (Parelho et al., 2008) that TADs provide transcriptional microenvironments, aiding in insulting promoters and enhancers within a TAD to prevent aberrant promoter-enhancer interactions. Cohesin has especially been shown to have an impact on the expression of inducible genes where dynamic loop extrusion and cohesin turnover enables tracing along the DNA which aids communication between enhancers and promoters for induction (Liu et al., 2021). Furthermore, processive loop extrusion was shown to have a vital role in the mechanism of V(D)J recombination for MHC antibody elements, where recruitment to the start of the V(D)J locus and the generation of loops of varying lengths aids in the variety of recombination spots selected (Ba et al., 2020; Dai et al., 2021)

Whilst these two cellular activities appear to have very different purposes, they may function by a similar mechanistic principle: the ability to associate with two pieces of DNA. In the case of sister chromatid cohesion, these two pieces of DNA are in *trans* as two separate sister DNA molecules are entrapped. In the case of loop extrusion, this behaviour is in *cis*, where you are interaction with two DNAs pieces of the same molecule to form a loop.

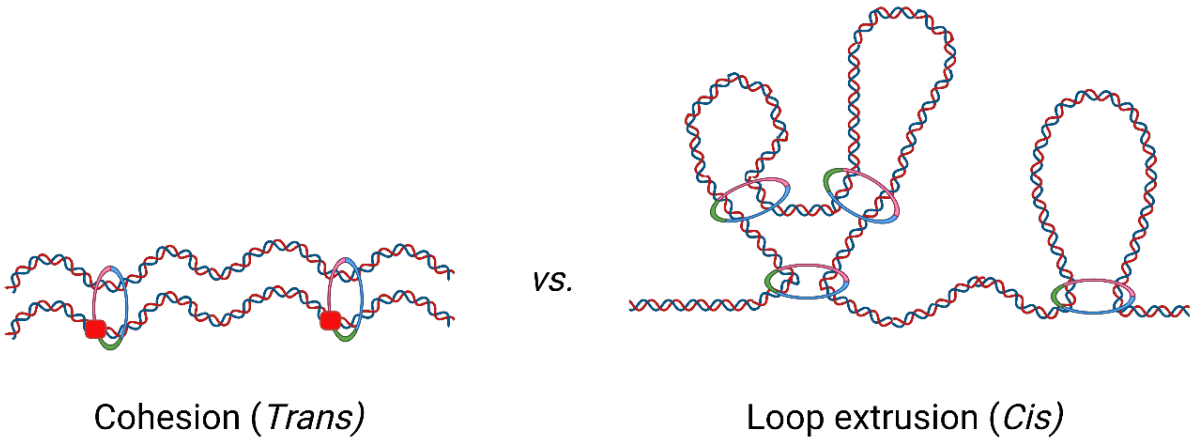

Figure 1-3. Cohesion vs. loop extrusion. Cohesive cohesin marked by acetylation (red box) holds sister DNAs in *trans*. Loop extruding cohesin makes chromatin loops on a single DNA stand in *cis*.

HAWK regulatory proteins

To perform these different functions, cohesin is regulated by a series of accessory proteins. One group of these proteins are called the HEAT proteins associated with kleisins (HAWK) proteins which are characterised by a series of helical Huntington/EF3/PP2A/TOR1 (HEAT) repeats which form a large hook-like structure (Wells et al., 2017). The three major HEAT repeat proteins that regulate cohesin in mammalian cells are known as NIPBL^{Scc2}, STAG1 / 2^{Scc3} and PDS5, with the yeast names is superscript (**Fig. 1-4**). Evidence suggests that STAG1/2 remains constitutively bound to the cohesin complex, often thought of as a quaternary complex, whilst NIPBL and PDS5 appear to bind interchangeably with the SCC1 kleisin (Kikuchi et al., 2016; Losada et al., 2000; Petela et al., 2018; Tóth et al., 1999). Collectively, these proteins help to associate cohesin with DNA, release cohesin from DNA, and facilitate loop extrusion by activation of cohesin's ATPase, or cohesion.

NIPBL: the cohesin loader and processivity factor

One of cohesin's main regulatory HAWKS is NIPBL^{Scc2}. NIPBL binds to a partner protein called Mau2^{Scc4} at its N-terminus which together form the cohesin loading complex and drives cohesin's association with DNA (Ciosk et al., 2000; Hu et al., 2015). NIPBL has a vital role as the ATPase activator of cohesin (Petela et al., 2018). The ability to bind and hydrolyse ATP is essential for cohesion to associate with chromosomes (Arumugam et al., 2003; Weitzer et al., 2003). Once cohesin has associated, cohesin's ability to translocation along DNA away from points of loading are also NIPBL and ATP dependent (Hu et al., 2011; Lengronne et al., 2004). This description became better understood when both NIPBL and ATP hydrolysis were shown to be required for loop extrusion *in vitro* (Davidson et al., 2019; Kim et al., 2019). Thus, a

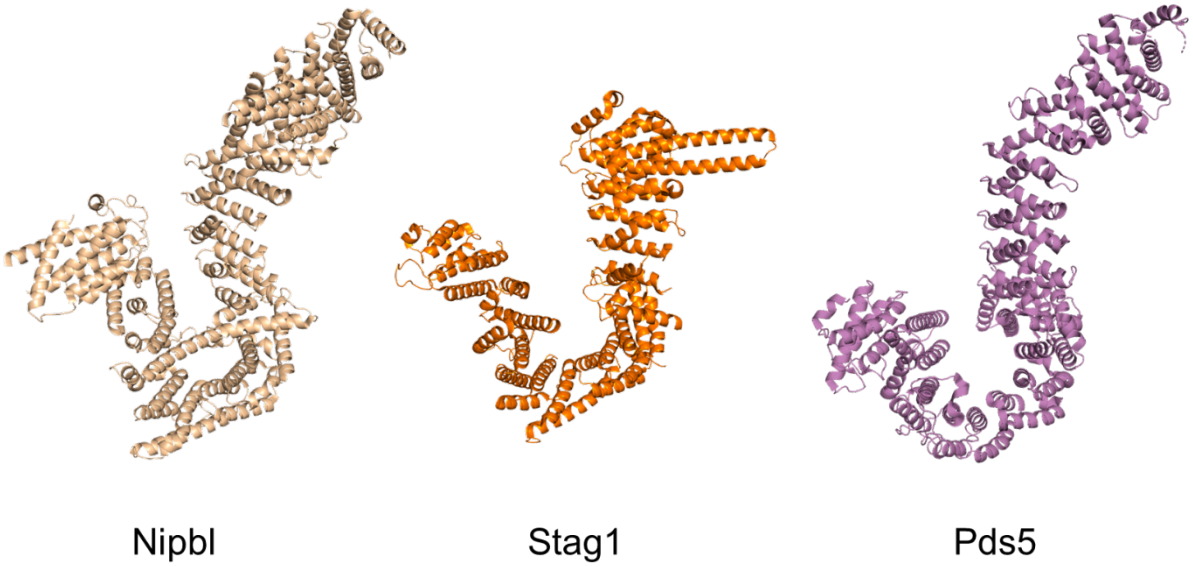

Figure 1-4. The HAWK proteins. Left to right: Structures of Human NIPBL^{Scc2} (*PDB: 6WG3*), STAG1^{Scc3} (*PDB: 6WG3*) and PDS5B (*PDB: 6WG3*), all share a hook structure formed from HEAT repeats.

model was determined whereby NIPBL both associates cohesin complexes with DNA, and then remains actively bound to facilitate ATP hydrolysis and loop extrusion. The requirement of NIPBL for loop extrusion was further evidenced by data from *in vivo* Hi-C experiments where NIPBL knock-down produced a similar pattern of chromatin loop loss as seen in RAD21 knock-outs (Rao et al., 2017; Schwarzer et al., 2017). It could be debated, however, that the loss of loops was due to a loss of cohesin from DNA from NIPBL knockdown. To show NIPBL's processivity then, it was found that if NIPBL's antagonist was depleted, the release factor called WAPL, then not only did cohesin begin to hyper-load, but chromatin loops increased in length until the DNA condensed into chromosome-like structures called "vermicelli" (Haarhuis et al., 2017; Tedeschi et al., 2013; Wutz et al., 2017).

In light of the findings that NIPBL activates cohesin's ATPase and promotes loop extrusion, its definition purely as the "cohesin loader" has come under scrutiny, with discussion as to whether it should instead be described as the cohesion processivity factor. To understand NIPBL's role in associating cohesin with DNA, we first have to describe what is meant by "cohesin loading".

It is known that cohesin can topologically bind around DNA (Ivanov & Nasmyth, 2005; Srinivasan et al., 2018). *In vitro* studies initially established that NIPBL was required to topologically entrap minichromosomes inside of cohesin's ring (Murayama & Uhlmann, 2014). It was therefore assumed that until cohesion was established, cohesin would be topologically loaded by NIPBL and entrap one single DNA. In order to topologically load cohesin onto DNA, either one of the three interfaces of the tripartite ring, namely SMC3/SCC1, SMC1/SCC1 or the SMC3/SMC1 hinge must open, or DNA must be cleaved and ligated into the ring. Logically, opening of DNA is a very high risk and elaborate a process requiring repair factors, therefore it was reasoned that the cohesin complex must open. This entrapment was

proposed to occur through the SMC hinge domain, as this was the only cohesin interface to abolish loading upon fusion (Collier & Nasmyth, 2022; Gruber et al., 2006). It was only in later work studying the cohesin hinge *in vivo* that it was found that if residues in the hinge were neutralised (they are usually acidic), then cohesin could associate with and translocate along DNA but not entrap it (Srinivasan et al., 2018). Furthermore, *in vitro* work showed that cohesin could still associate with DNA and do loop extrusion, even if all the interfaces of cohesin were artificially closed using cysteine crosslinks (Davidson et al., 2019). Thus, it is proposed that cohesin can associate with DNA through both topological and non-topological mechanisms.

Structural studies revealed that an intermediary state exists where NIPBL is able to create a pseudo-topological association with DNA. Here, NIPBL facilitates a clamping state where the ATPase heads open and close around DNA, thus creating an transition state where DNA sits in the coiled coil region of the ring (between the heads and the hinge) and in the kleisin section of the ring (between the heads and the kleisin) (Collier et al., 2020; Shi et al., 2020).

After this pseudo-topological state is created, it is supposed that one of the cohesin interfaces opens to allow DNA to pass out and make a true topological entrapment. This mechanism is however still under examination (Collier & Nasmyth, 2022). Furthermore, the mechanism of loop extrusion, which would first involve DNA binding, then processively enlarging loops is still unknown. It analogous condensin complexes, a “safety belt” mechanism was proposed using a condensin HAWK protein, Ycg1, and the kleisin forming an anchor point from which loops are extruded asymmetrically (Ganji et al., 2018; Kschonsak et al., 2017). Alternatively, in cohesin, symmetrical extrusion has been observed in *in vitro* extrusion assays (Davidson et al., 2019; Kim et al., 2019). Interestingly, microscopy studies in human cells revealed the majority of non-cohesive cohesin complexes on DNA existed in dimeric pairs (Ochs et al., 2024). Whether these cohesin complexes are loop extruding whilst dimerised both in an

asymmetrical manner which overall gives symmetrical extrusion is yet to be determined. Also, the nature of association with DNA by loop extruding complexes has yet to be determined, be it through a similar safety belt mechanism as condensin, or a system more similar to NIPBL clamping which creates a pseudo-topological embrace and does not require opening of any of the interfaces. Whilst NIPBL can allow cohesin to loop extrude non-topologically *in vitro* when the complex is fully circularised, this does not mean that the behaviour is also non-topological *in vivo* (Davidson et al., 2019).

When describing cohesin's role as a loader therefore, we currently describe it as NIPBL's ability to associate cohesin with DNA, be it topological or non-topological. We can safely describe it as thus, as we know that if NIPBL is knocked-down we have a dramatic reduction in cohesin association with DNA (Alonso-Gil et al., 2023; Hu et al., 2015; Petela et al., 2018; Schwarzer et al., 2017). Similar effects have also been described with the knockout of NIPBL's loading partner, Mau2 (Haarhuis et al., 2017; Watrin et al., 2006). NIPBL is known to have a number of chromatin-bound recruitment partners involved in transcription and chromatin remodelling, such as Mediator and BRD4, which stabilise NIPBL on DNA and thus promote cohesin loading (Linares-Saldana et al., 2021; Mattingly et al., 2022; Muñoz et al., 2019). It appears to especially load at enhancers and the promoters of active genes, thus facilitating cohesin's role in gene expression (Luna-Peláez et al., 2019; Vian et al., 2018; Zhu et al., 2021). Scc4 has also been shown to recruit the Scc2/Scc4 loading complex to the pericentromeres of yeast via its interaction with Ctf19 kinetochore complex (Fernius et al., 2013; Hinshaw et al., 2015). Whist NIPBL facilitates the association of cohesin with DNA, it can also facilitate loop extrusion, and will therefore likely play a role as both the cohesin loading factor and a processivity factor (**Fig. 1-5**).

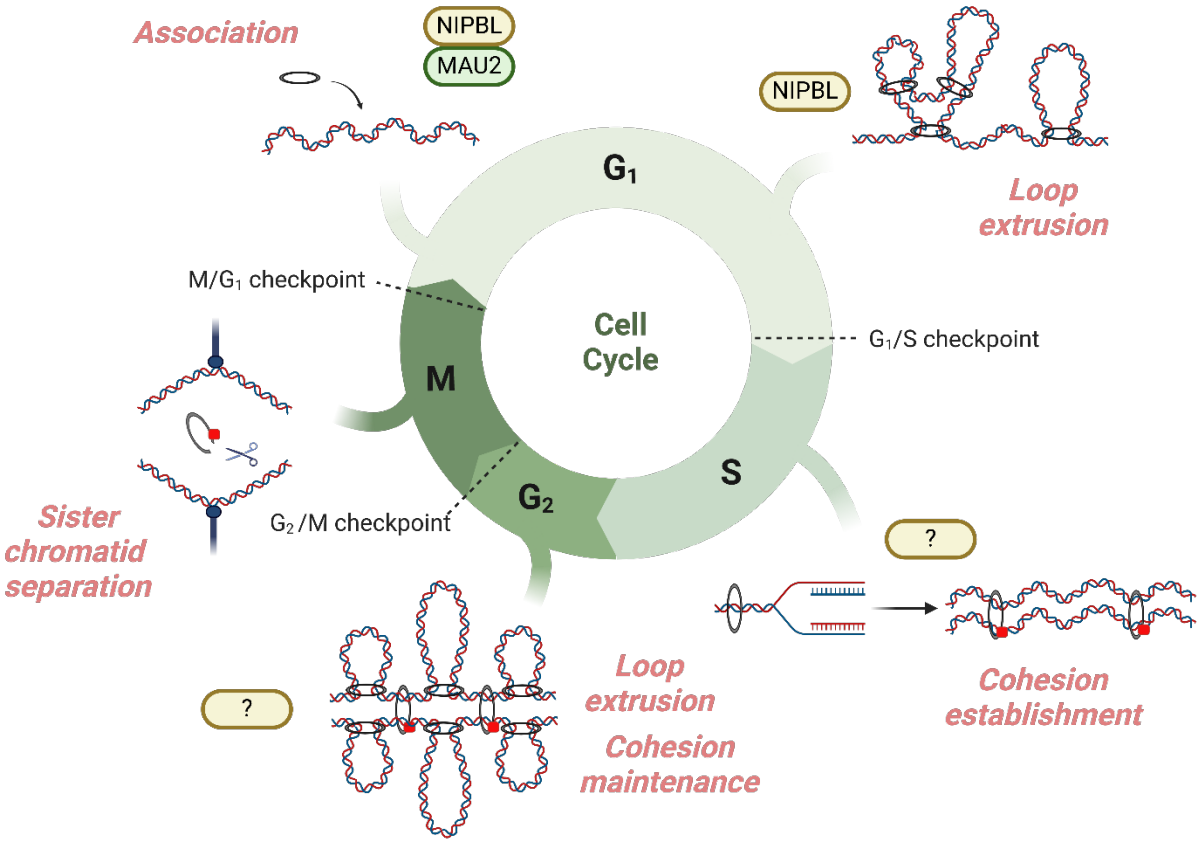

Figure 1-5. NIPBL throughout the cell cycle. NIPBL loads cohesin in G1 and facilitates loop extrusion. NIPBL's role in cohesion establishment is unknown. NIPBL keeps loop extruding through to G2.

NIPBL in developmental disorders

The importance of NIPBL as a loading and processivity factor is especially evidenced by its incidence in the development disease Cornelia de Lange Syndrome (CdLS). CdLS is one of a family of "cohesinopathies" which show mutations predominantly linked to the cohesin pathway. In the case of CdLS, over 60% of the mutation are found within NIPBL (Krantz et al., 2004). These mutations often result in a haploinsufficiency of NIPBL, disrupting typical loading and extrusion of cohesin, which in turn affects the transcriptional regulation of developmental genes leading to aberrant gene expression patterns during critical stages of development (Garcia et al., 2021; Tonkin et al., 2004). This dysregulation is thought to underlie the diverse phenotypic manifestations observed in CdLS (Mannini et al., 2013). CdLS is therefore also often termed a "transcriptopathy", rather than an issue pertaining to sister chromatid cohesion. NIPBL disease models with CdLS mutations have demonstrated that cohesin accumulates transcriptional start sites and is unable to translocate away, causing global changes to the transcriptome landscape (Garcia et al., 2021; Zuin et al., 2014) Thus, studying disease models elucidate critical mechanisms supported by NIPBL in the cell.

WAPL: the cohesin release factor

The loading and processivity of cohesin on DNA by NIPBL is directly opposed cohesin's release factor, WAPL (Gandhi et al., 2006; Kueng et al., 2006). WAPL is a shorter, lobed shaped protein with a flexible N-terminus and a conserved C-terminus containing HEAT repeats (Ouyang et al., 2013). WAPL binds cohesin's kleisin subunit via interaction with cohesin's two other HAWK subunits, STAG1/2 and PDS5 (Shintomi & Hirano, 2009). Mutations in PDS5S81R and scc3K404E abolish WAPL binding and release (Beckouët et al.,

2016; Chan et al., 2012). Interestingly, NIPBL and PDS5 have been shown to bind cohesin in a mutually exclusive manner (Kikuchi et al., 2016; Petela et al., 2018). In order to release the cohesin complex from DNA, it is therefore likely that NIPBL must first be replaced with PDS5 which can then recruit WAPL. Once bound, WAPL / PDS5 facilitates cohesin's release through disengaging the SMC3 neck / SCC1 interface, thereby opening the cohesin ring and releasing cohesin from DNA (Beckouët et al., 2016; Gligoris et al., 2014; Murayama & Uhlmann, 2015). Indeed, if this SMC3/SCC1 interface is fused, the mechanism of release is blocked (Chan et al., 2012).

WAPL operates throughout the cell cycle to release cohesin from DNA and notably, abrogating WAPL's release reaction is a major factor in protecting cohesion. Studies which deplete WAPL observe that cohesin is hyper-loaded onto DNA but does not turnover (Kueng et al., 2006; Tedeschi et al., 2013). Together then, NIPBL and WAPL work to balance each other's activities and maintain cohesin turnover on DNA which appears to be essential for the correct organisation of interphase chromatin.

The cohesion cycle:

1. G1

Throughout the cell cycle cohesin will perform its specific activities according to the DNA organisational needs of the cell. Cohesin begins its association with DNA at the very start of the cell cycle, before cells have even entered into G1. As soon as sister DNAs are segregated and the nuclear envelope begins to reforms around each genome of the daughter cells in telophase, cohesin begins to reload onto DNA rapidly (Gerlich et al., 2006; Sumara et al., 2000; Watrin et al., 2006). Over the course of G1, cohesin is associated with DNA by NIPBL/Mau2

and released from DNA by WAPL/PDS5 (**Fig. 1-6**). Cohesin will topologically entrap single DNA molecules and will also be loop extruding forming TADs along DNA, a process driven by NIPBL. Whilst cohesin is predominantly being loaded during this time, it is important to note that cohesin is also highly dynamic so will be going through cycles of loading and offloading with a residency time of 20-30 minutes (Hansen et al., 2017). PDS5 has been shown to limit the expansion of loops and provide loop stability through both WAPL recruitment and acetylation during G1 by the acetyltransferase Eco1 which converts cohesin into a PDS5-bound state (Bastié et al., 2022; Dauban et al., 2020; van Ruiten et al., 2022).

2. Cohesion establishment

After the G1/S checkpoint where the cell ensures that the cell has grown to a sufficient size and that there is no DNA damage, the cell progresses to S phase and DNA replication begins. It is during S phase that cohesion is established, however the exact mechanism of cohesion establishment is still under investigation. Cohesion appears to be built concurrently with DNA replication, which ensures that sister DNAs are still in close spatial proximity. Delays in DNA replication correlated with delays in cohesion establishment (Beckouët et al., 2010). Indeed a series of non-cohesin proteins that are important, but not essential, for sister chromatid cohesion were found to traverse with the replication fork (Bermudez et al., 2003; Lengronne et al., 2006). Synthetic lethality studies in yeast making pairwise depletions of these replisome-associated proteins revealed two groups of proteins which appeared to operate in separate pathways (Xu et al., 2007). The first group contained the proteins Chl1, Ctf4, Csm3 and Tof1, components which can bind DNA pol α and the GINS complex to form part of the replication progression complex (Gambus et al., 2006). The other group contained Mrc1, Ctf8, Ctf18 and Dcc1, which all form part of the Ctf18-replication factor C (RFC) complex which loads PCNA

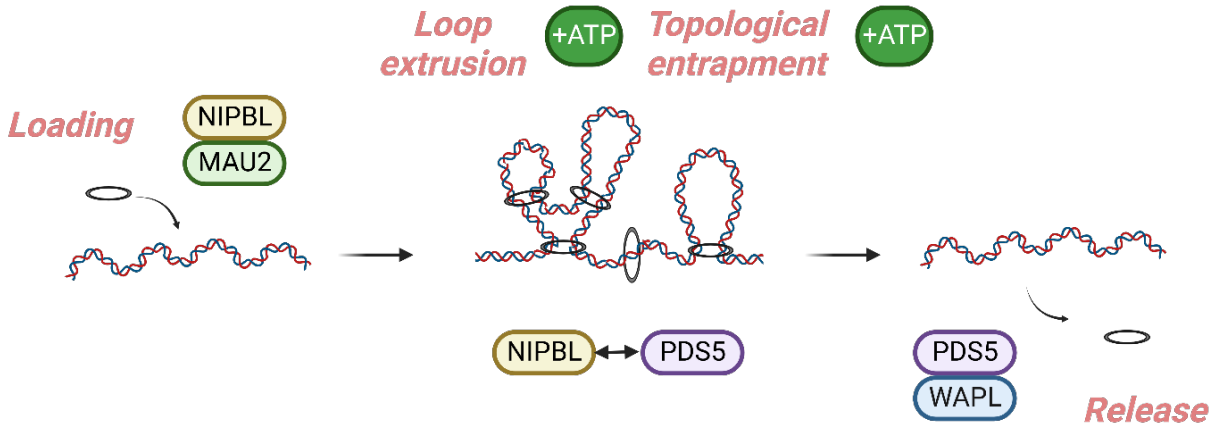

Figure 1-6. Regulation of cohesin during G1. NIPBL/Mau2 facilitates loading of both topological (+ATP) and non-topological DNA association. NIPBL promotes loop extrusion (+ATP) and is replaced by PDS5. PDS5 recruits WAPL which facilitates release.

onto DNA (Bermudez et al., 2003). Fascinatingly, whilst these proteins are non-essential, they are highly conserved with depletion in mammalian systems leading to cohesion defects (Cortone et al., 2018; Zheng et al., 2018).

Based on the synthetic lethality of these two groups, it was suggested that cohesin might have a redundancy in its mechanism of cohesion establishment. This lead to the proposal of two alternative models for cohesion establishment. The first model proposes that cohesin that is loaded onto DNA prior to DNA replication can be "converted" to cohesive cohesin. This could be accomplished through a temporary dissociation in front of the replication fork and reassembly after the replication fork, much like histones (Petryk et al., 2018; Yu et al., 2018). Alternatively, this could be accomplished by the entire replication machinery passing through the cohesin ring. An alternative model for cohesion establishment is that soon after DNA replication has taken place, NIPBL is able to load cohesin directly onto newly replicated sister DNAs via a *de novo* establishment pathway (**Fig. 1-7**).

Evidence for both models exist. In yeast, initial indications of a conversion pathway came from observations that cohesion could still be built if Scc2 was depleted in early S phase (Lengronne et al., 2006). Later work demonstrated that topologically bound cohesin rings that were separase resistant could be onto loaded to chromosomes in G2 and build cohesion in the subsequent cell cycle, even in the absence of Scc2 (Srinivasan et al., 2019). In humans, microscopy studies showed that cohesin that was associated with DNA prior to replication remained bound to DNA with the passage of the replication fork, albeit in a background where WAPL was depleted to prevent cohesin turnover (Rhodes et al., 2017). Whilst cohesin remained associated it could not however be determined whether the cohesin remaining has become cohesive. Meanwhile evidence for a *de novo* loading pathway has come from *in vitro* work which demonstrated cohesin can entrap a first strand of DNA, followed by a second strand

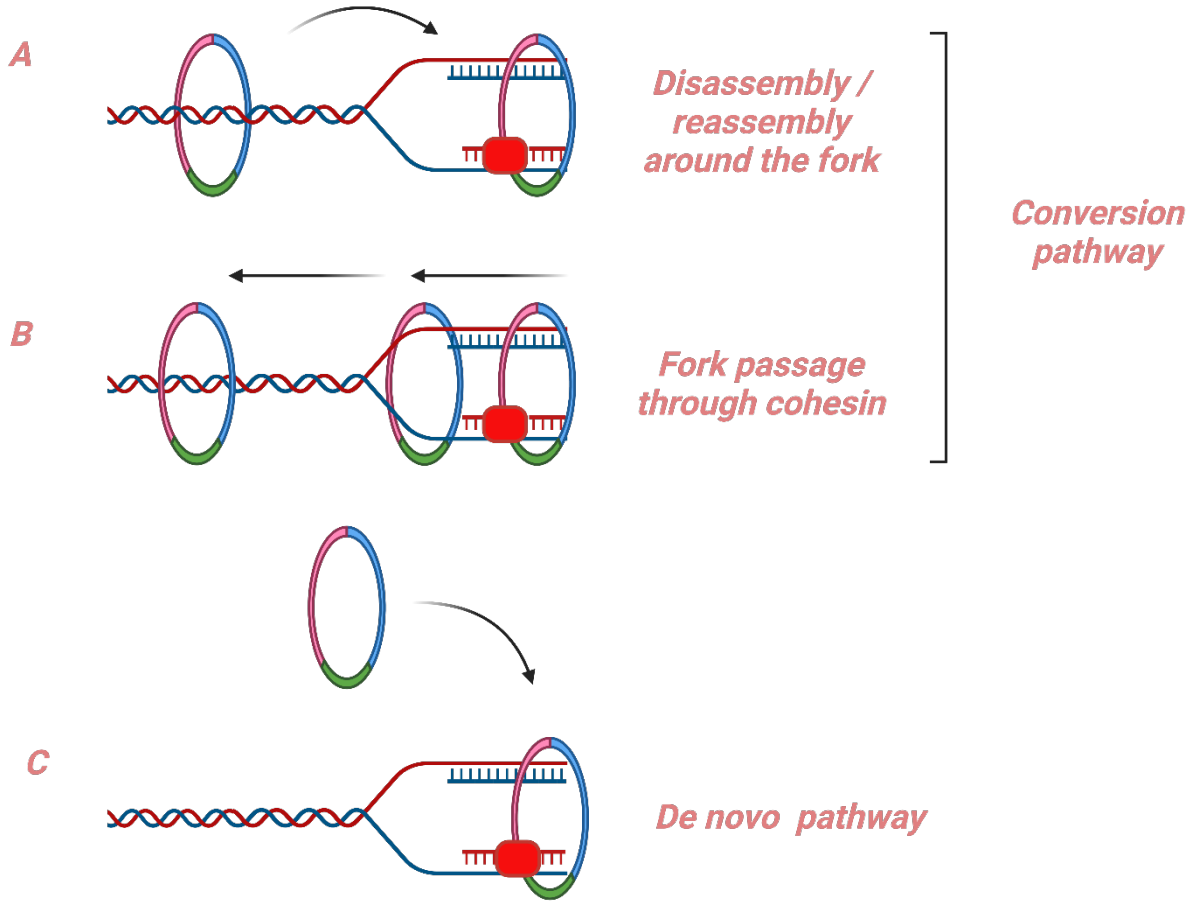

Figure 1-7: Models for cohesion establishment. (A) Conversion pathway: Cohesin disassembles in front of replication fork and reassembles onto sister DNAs. **(B)** Conversion pathway: Replication fork goes through the cohesin ring. **(C)** *De* novo pathway: Cohesin is loaded onto sister DNAs directly.

of single-stranded DNA (ssDNA) which could then be converted to double-stranded DNA (dsDNA) with replication (Murayama et al., 2018). Critically, the entrapment of both the first and the second ssDNA strand were Scc2 and ATP hydrolysis dependent.

Most compellingly, both cohesion models were assessed in the context of the replisome associated proteins described above using a conversion system established in yeast (Srinivisan et al., 2020). Here, loaded and trapped cohesin molecules could clearly build cohesin with the dependency of the first group of proteins (Chl1, Ctf4, Csm3 and Tof1), but no the second (Ctf18-RFC), completely in the absence of Scc2. Depletion of the replisome components in the first group however disrupted cohesin's ability to convert. Likewise, a *de novo* loading pathway was tested to be dependent on the second group of proteins (Ctf18-RFC) through a modest overexpression of Scc2.

Taken together, the work in yeast makes a compelling argument for the existence of two methods of cohesion establishment which could operate through parallel but independent pathways. Thus far, work on understanding the mechanism of cohesion establishment in higher eukaryotes and also on full chromosomes has been very limited and will be required to understand this system fully.

3. Cohesion maintenance – Eco1 and sororin

Whilst the mechanism of cohesion establishment is still largely unknown, the mechanism of how cohesive cohesin is maintained is better understood. Essential to cohesion maintenance is the replication-fork associated acetyltransferase Esco1/2^{Eco1} (Ivanov et al., 2002; Lengronne et al., 2006; Skibbens et al., 1999; Tóth et al., 1999). As cohesion is built, Eco1 acetylates two highly conserved lysine residues on the ATPase head of SMC3 (K112 and K113 in yeast) (Ben-

Shahar et al., 2008; Ünal et al., 2008; Zhang et al., 2008). The acetylation of these residues prevents WAPL from disengaging the SMC3/SCC1 interface and thus protects cohesive cohesin from WAPL release (Beckouët et al., 2016; Chan et al., 2012; Rowland et al., 2009). In yeast, acetylation of K112 and K113 is sufficient to prevent WAPL release (Beckouët et al., 2010). In fact Eco1's role in blocking WAPL release appears to be its main contribution to sister chromatid cohesion, as cohesion can still be built and maintained in cells where both Eco1 and WAPL are co-depleted (Rowland et al., 2009). In vertebrates, the acetylation of cohesin by Esco1 and Esco2 recruits a protein called Sororin which displaces WAPL binding to PDS5 which is thought to inhibit the release complex from forming (Lafont et al., 2010; Nishiyama et al., 2010; Rankin et al., 2005).

Thus PDS5 is able to have both a stabilising and destabilising effect on cohesin. Once it has displaced NIPBL, PDS5 can form the release complex with WAPL or if it is replaced with Sororin, it maintains sister chromatid cohesin (Ouyang et al., 2016). This duality of PDS5 explains the early observations that PDS5 is required to establish and maintain sister chromatid cohesion (Hartman et al., 2000; Panizza et al., 2000).

4. G2

As cells exit S phase and move to G2 phase, the cell has two populations of cohesin. That which is cohesive, entrapping two sister DNAs in *trans*, and that which is loop extruding, entrapping two pieces of the same strand of DNA in *cis* to make a loop. Cohesive cohesin is passive, as it is bound to PDS5 will not hydrolyse ATP. Cohesive cohesin is also prevented from turning over as it cannot bind WAPL. The loop extruding cohesin operates alongside cohesive cohesin and is thought to push cohesive cohesin sites to the edge of CTCF loops

(Mitter et al., 2020). Furthermore, *in vivo* the knock down of NIPBL was shown to disrupt interactions specifically in *cis* (loop extruding) but not in *cis* (cohesive).

5. Prophase pathway

Cells move past a second checkpoint G2/M where DNA replication is checked and the cells ensure that they are now ready for mitosis. First, sister chromatids condense into manoeuvrable chromosomes by the action of condensin. Whilst the cells are still in prophase, higher eukaryotes (but not yeast), undergo the prophase pathway (Waizenegger et al., 2000). During prophase, mitotic kinases CDK1, Polo-like kinase 1 (Plk1) and Aurora-B phosphorylate sororin and SA2 which induces its dissociation from cohesive complexes (Dreier et al., 2011; Hauf et al., 2005; Nishiyama et al., 2010). WAPL subsequently removes all cohesin from the sister chromatid arms, with the exception of a small amount of cohesin found at the centromere (Gandhi et al., 2006; Kueng et al., 2006). Here, a protective complex Shugoshin - protein phosphatase 2A (SGO1-PP2S) binds and actively dephosphorylates sororin-bound cohesive complexes (Kitajima et al., 2006; Liu et al., 2013). Furthermore, SGO1 actively competes with WAPL for binding to a conserved site on SA2-SCC1 to protect cohesin from WAPL release (Hara et al., 2014). A result of the prophase pathway is sister chromatid resolution which generates the characteristic "X" shape of chromosome pairs, where they are resolved other than the region at the centromere where they remain cohesed by cohesin.

6. Spindle assembly checkpoint

As discussed earlier in this chapter, after sister chromatid resolution in prophase, the cells enter prometaphase where sister chromatids must biorient to ensure equal segregation to daughter

cells. We now know that cohesin is the protein which ensures sister chromatid cohesion and holds sister chromatids together against the forces of opposing spindle microtubules at the centromere. Before cells undergo the very high risk stage of anaphase, there is a critical checkpoint which ensures that every sister chromatid pair properly bioriented called the spindle assembly checkpoint (SAC) (**Fig. 1-8**). This checkpoint operates using a remarkable mechanical and chemical system to detect biorientation (Reviewed in Musacchio, 2015). The mitotic kinase Aurora B is greatly enriched in the region between kinetochores where it phosphorylates substrates in the inner and outer kinetochore (Carmena et al., 2012). When opposing microtubules attach to a pair of sister chromatids, one from each side achieving biorientation, the opposing forces which are resisted by cohesin create tension across the kinetochore. This tension lifts the outer layer of the kinetochore protein assembly away from the inner layer which reduces Aurora B phosphorylation as the spatial distance increases (Liu et al., 2009). The reduction in phosphorylation regulates kinetochore attachment, allowing stable binding (Tanaka et al., 2002). When chromatids experience mono-orientation, no such tension across from the kinetochore exists and substrates remain phosphorylated by Aurora B which destabilises microtubule attachments, promoting turnover of the spindle pole body attachments until the correct attachment is achieved. Not only does this mechanism ensure trial and error testing of proper attachment in the mechanical sense, but it further holds a regulatory function. The protease that will eventually target cohesin for destruction in anaphase is called Separase. Separase cleaves the SCC1 subunit of cohesin and thus releases the sister chromatids allowing sister chromatid disjunction (Uhlmann et al., 1999). Until all the sister chromatids are correctly bioriented, it is essential that separase is inhibited. The SAC achieves this through one of Aurora B's other targets for phosphorylation called the mitotic checkpoint complex (MCC). The MCC forms on unbound kinetochores and binds to and inhibits a ubiquitin ligase

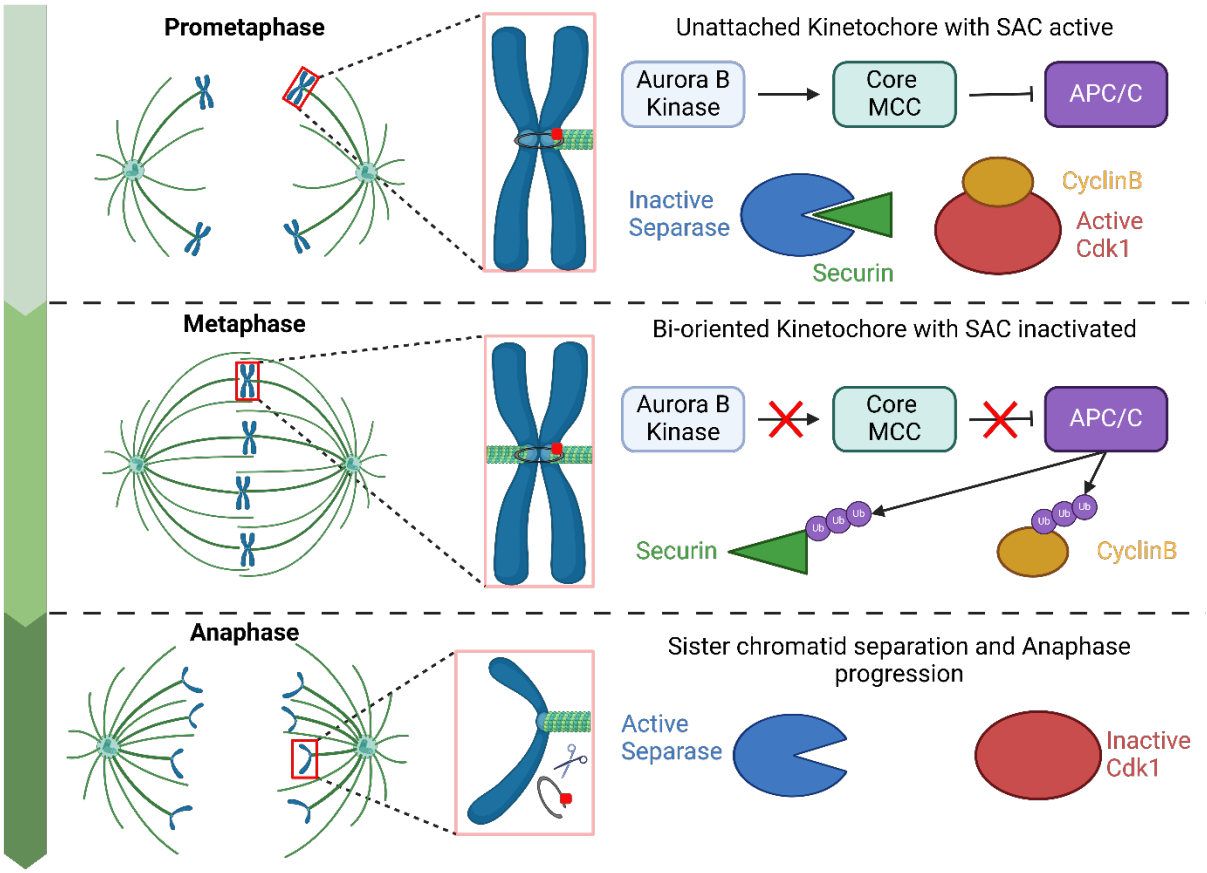

Figure 1-8. The spindle assembly checkpoint. Spindle microtubules prepare to biorient during prometaphase which keeps the APC/C inhibited and separase inactive. Upon full biorientation in metaphase, the spindle assembly checkpoint is relieved, releasing APC/C which polyubiquitinates securin and cyclin B targeting them for destruction by the proteasome. Separase is active and cleaves cohesin.

called the anaphase-promoting complex / cyclosome associated with Cdc20 (APC/C^{Cdc20}). This ubiquitin ligase triggers mitotic exit through targeting two critical substrates for degradation, Securin and Cyclin B (King et al., 1995; Shirayama et al., 1999). Securin stoichiometrically inhibits the active site of Separase, preventing it from cleaving, and cyclin B/CDK1 further inhibits separase through phosphorylation (Stemmann et al., 2001). Upon successful biorientation of all sister chromatids, inhibition of the APC/C is relieved and Separase can trigger anaphase through the cleavage of the SCC1 subunit of cohesin at two sites, allowing the spindle microtubules to draw one sister chromatid to each end of the cell (Ciosk et al., 1998; Oliveira et al., 2010; Uhlmann et al., 1999, 2000). Thus, sister chromatids are faithfully segregated and each daughter cell receive an identical and complete copy of the genome.

7. Resetting the system

Cyclin-B degradation activates the mitotic progression phosphatases PP1 and PP2A which progress the cell cycle toward mitotic exit (Cundell et al., 2016; Dohadwala et al., 1994). After sister chromatid disjunction, the Esco1/2 antagonist, a histone deacetylase called HDAC8 ^{Hos1}, deacetylates the lysine residues of all cleaved cohesin complexes which are no longer DNA bound. This allows the release of the cleaved SCC1 subunit from the complex and the recycling of the SMC proteins for fresh reloading in telophase (Beckouët et al., 2010; Borges et al., 2010). Furthermore, to ensure that proteins specific to cohesion remain inactive until they are needed again, a form of the APC/C^{Chdl} remains active during mitotic exit and G1 and continues to target Sororin and Esco2 for degradation, ensuring that they does not reactivate until S phase (Lafont et al., 2010; Rankin et al., 2005). Thus, cohesin can re-load onto DNA once again and the cohesin cycle restarts.

The process of cohesion is essential during mitosis to ensure that one copy of each sister is received by each daughter, and any failure in cohesion will lead to an inability to properly biorient the sisters and a failure to segregate equally. The unequal segregation of chromosomes is known as aneuploidy and has dire consequences for the cell, including cell death, DNA damage and incorrect copy numbers of genes which is often a hallmark of cancers (Santaguida & Amon, 2015). Given the number of cellular divisions an organism like a human undergoes every day, the importance and fidelity of the system is remarkable.

Mammalian cell lines as an experimental model

Whilst many key discoveries about cohesin have come from yeast, yeast models ultimately explore cohesin in a simpler living system. The "cohesion cycle" demonstrates the increased complexity of mammalian systems, with additional regulatory mechanisms around cohesion including the protective proteins, sororin and SGO1. DNA organisation is also more complex in mammalian systems, with greater genome sizes and regulatory elements such CTCF proteins which border TADS and are absent in yeast. In order to fully understand cohesin behaviour in higher eukaryotes it is therefore essential to study cohesin regulation in mammalian systems.

The ideal model systems for the study of cell biology in higher eukaryotes are immortalised mammalian cell lines. These cell lines have escaped the various mechanisms which prevent cell division and gained the ability to replicate indefinitely, often deriving naturally from human cancer cells. Various cancer cell line models exist, and have the advantage that they grow quickly and are generally robust to cellular manipulations such as CRISPR-Cas9 gene editing, RNA interference, or overexpression systems. Additionally, due to their size and growing conditions (often growing as a monolayer) they provide an invaluable system for

microscopy studies, a factor which has allowed the visualisation of chromosome dynamics and protein localization in live cells, providing valuable insights into the spatial and temporal dynamics of cohesin (Mach et al., 2022). Although immortal cell lines do not fully behave as somatic cells, they often possess sufficient unaltered fundamental systems to make them an analogous system. It is therefore essential to know the limitations of the particular cell line being worked with, in case they miss key cell cycle controls which could interfere with the system being studied. As well as cell cycle dysregulation, cancer cells also have genome instabilities leading to the differential dosage of some proteins, thus the study of chromosome biology in immortal cell lines necessitates properly controlled experiments to ensure any discoveries are applicable outside of these models.

Thesis objective

Sister chromatid cohesion is essential for life, as it is found in every living organism on earth. Understanding the mechanism of how cohesion is regulated is key to understanding how the process might sometimes go wrong. A large unknown in the field is currently how cohesion is established and which proteins regulated this process. An unexplored area of study for this has been the role of NIPBL in establishing cohesion. NIPBL is arguably cohesin's most important regulator. We know that NIPBL is the cohesin loader, therefore it ultimately underpins all activities of cohesin's activities on DNA. Recently, there has been a dramatic rise in interest regarding NIPBL's role in chromatin organisation by loop extrusion. The field however has thus far lacked the tools to explore NIPBL's role in cohesion, as there has been to date no complete way to degrade the protein in mammalian cells. If cohesion is a sensitive and essential process, even small amount of cohesin will be able to build cohesion (REF from chapter 1). In order to explore NIPBL's contribution to regulating cohesion therefore, we sought to develop a degron that could deplete NIPBL in a complete and rapid manner. Using this tool, we were able to ask a series of questions which explored cohesin's dependency on NIPBL throughout the cell cycle to build and maintain cohesion. Through this body of work, we have been able to identify a clear way in which NIPBL is required to establish cohesion, and furthermore, identify the time in the cohesion cycle where NIPBL is absolutely essential.

Chapter II: Generation and validation of a NIPBL degron

Introduction

In order to understand NIPBL's role in regulating cohesin behaviour, it is important to develop a system whereby the protein can be depleted and the consequences of depletion studied.

Early work in yeast used temperature sensitive mutants of Scc2 which could inactive the protein when strains were moved to non-permissible temperatures. This conditional knockout allowed the study of an otherwise essential gene, and was how it was first demonstrated that Scc2 along with its partner Scc4 is required for the association of cohesin complexes to chromatin (Ciosk et al., 2000; Tóth et al., 1999). By inactivating Scc2 in various stages of the cell cycle, it was further demonstrated that Scc2 is essential for sister chromatid cohesion, with its inactivation in G1 causing cohesion defects during S phase (Ciosk et al., 2000; Michaelis et al., 1997). Scc2 was required for the establishment of cohesion prior to S phase, but not after S phase, suggesting that its primary role in cohesion establishment occurs around the time of DNA replication and not required to maintain sister chromatid cohesion once established.

Studying NIPBL's role in mammalian systems is more challenging as the model organisms require carefully controlled growth conditions, so different methods must be employed to knock out essential genes. By the nature of an essential gene, it cannot be removed from the genome. Therefore, tools which target either the protein or the mRNA for destruction are used.

One such tool harnesses RNA interference using small interfering RNAs (siRNA). Here, mRNAs of the protein of interest are cleaved by the siRNA/ RNA-induced silencing complex (RISC) complex prior to translation so can largely knock down the expression of a protein. Whilst siRNAs are useful as they do not require genomic manipulations, they have knock-down rather than knock-out effects and can take several days to deplete, meaning that the effects of protein degradation cannot be acutely measured. SiRNA knock downs of NIPBL

over a number of days revealed effects on cohesin loading and loop extrusion (Alonso-Gil et al., 2023). From this study, NIPBL had a clear role in promoting loop extrusion and the accumulation of cohesin at CTCF sites. The conclusions of whether NIPBL was the cohesin loader however remained controversial, as experiments showed a modest reduction in SMC1 levels on DNA, leading to the suggestion that NIPBL may not be the only method of associating cohesin with DNA. Alternatively, it was proposed that cohesin can associate with DNA alone (using SA1/2), and rather than loading cohesin onto DNA, NIPBL could instead is simply a processivity factor allowing translocation through loop extrusion. Thus, NIPBL's role as the cohesin loader in mammalian systems came under question.

Other methods targeted the NIPBL gene in order to achieve a conditional knock out. In work by Schwarzer et al., a tamoxifen-inducible Cre-recombinant NIPBL was engineered in a mouse model to specifically deplete NIPBL from non-dividing hepatocytes (Schwarzer et al., 2017). This system circumvents the essential nature of NIPBL, as it could be targeted specifically to the liver, and could be induced. Using this system, SMC1 levels were mostly displaced from chromatin and virtually all loops were lost in Hi-C maps, providing a much stronger case for NIPBL as the cohesin loader, and its requirement for loop extrusion. Interestingly, hepatocytes did not die or show proliferation defects with NIPBL depletion. The disadvantage of this system however is that it required at least 10 days between tamoxifen injection and analysis to knock down NIPBL to significant levels, therefore the immediate effects of NIPBL depletion could not be studied. Furthermore, whilst this system disrupts the gene, its application to the whole tissue over a number of days collectively achieved a knock down rather than a knock out effect, with low expression levels of NIPBL remaining potentially due to the lack of penetrance of the drug through the tissue.

The most effective method to achieve complete and rapid depletion of a protein is through the use of protein degron technologies (de Wit & Nora, 2023). Here, genome editing is used to attach a degron sequence to the protein of interest, which can target the protein to an E3 ligase for destruction by the cells proteasome upon induction with a drug. The most widely used inducible degron is the auxin-inducible degron (AID) system, based on a naturally occurring system in plants where the hormone auxin triggers the rapid degradation of a family of transcription factors via the SCF ubiquitin ligase complex (Nishimura et al., 2009). Here, the auxin degron sequence can be added to the protein of interest, in a background where a TIR1 transgene is also exogenously expressed, to create a system whereby the protein can be rapidly degraded upon treatment with an auxin drug. Other degron technologies have since been developed such as the dTAG system, which works by a similar principle of E3 ubiquitin ligase targeting (Nabet et al., 2018). The major advantage of degron systems is the speed at which they can acutely degrade a target protein to levels of near complete knock-out, usually within 30 minutes – 2hrs. Degrons are therefore extremely useful for studying proteins that operate in small temporal windows. They are also reversible and can be finely tuned using concentration, making them a very flexible tool for studying the acute loss of a protein (Verma et al., 2020).

Using a smaller version of the AID, the Peters lab generated an N-terminally tagged miniAID (mAID) degron of NIPBL (Kubota et al., 2013; Natsume et al., 2016; Nishimura & Kanemaki, 2014). Using this degron, NIPBL was shown to have dramatic effects on chromatin architecture and the ability to form loops in *cis* using sister-chromatid-sensitive Hi-C (scs-Hi-C) (Mitter et al., 2020). From what we know from yeast and from *in vitro* studies, we would also expect that NIPBL is essential, and that it is needed to load cohesin onto DNA and build cohesion. Contrary to what is known in yeast however, depletion of NIBPL using this degron found that sister

chromatid cohesion remained unaffected and cells were able to survive in the absence of NIPBL (Jan-Michel Peters – Personal communication).

In a final example of NIPBL depletion, Scc2 becomes highly unstable in the absence of its binding partner in Scc4 knock-out cells, and expression levels of Scc2 are dramatically reduced. These cells are however also viable, albeit with impaired growth, and are able to form normal cohesion (Haarhuis et al., 2017).

The consistent finding that NIPBL depletion lead to dramatic losses of chromatin architecture, but still displayed WT cohesion and cell viability, led to the proposal that NIPBL might not have the same essential functions of loading cohesin and building cohesion, as in yeast. An alternative explanation for the results was that the degradation methods used thus far which achieve significant knock down are still not complete enough to remove all NIPBL from the cell, with enough remaining to support life.

It is known that Scc2 is a substoichiometric protein to cohesin, and indications from microscopy studies show that NIPBL can function in a highly sub stoichiometric manner, associating briefly with multiple cohesin molecules (Rhodes et al., 2017; Tóth et al., 1999). Here, NIPBL associates with chromatin with a residency time of 51s, as opposed to the residence time of cohesin which is known to be 15-30 minutes, suggesting that the loading of cohesin is a singular event (Hansen et al., 2017; Rhodes et al., 2017). Furthermore, NIPBL is known to operate at a haploinsufficiency in the case of patients with CdLS, where patients have normal cohesion pathways but affected transcriptomes (Krantz et al., 2004). *In vitro* studies have indicated that NIPBL, the ATPase activator, must be bound to cohesin in order to extrude a loop, which would make sense in loop extrusion being the primary function affected (Davidson et al., 2019). It is therefore possible that unless NIPBL is depleted in a complete manner, the small amount remaining in the cell might be able to sustain the loading of enough

cohesin to support life and sister chromatid cohesion. A corollary of this notion is the possibility that a small amount of cohesin is sufficient to support life and ensure accurate chromosome segregation. Indeed, in support of this, a study in budding yeast it was demonstrated that only a small amount of DNA-associated cohesin is required to support sister chromatid cohesion (Heidinger-Pauli et al., 2010).

Thus far, there has been no sufficient tool developed to study the effects of NIPBL depletion in a complete and rapid manner. This has prevented the field thus far from studying NIPBL's contribution to cohesion establishment which requires the ability to acutely deplete the protein in controlled cell cycle stages. The first objective of my thesis was therefore to develop a NIPBL degron which could achieve a complete knock-out of NIPBL rather than a knock-down, and could deplete rapidly so that NIPBL's role in cohesion could be studied throughout the cell cycle. Using this system, I would be able to address whether mammalian systems do operate differently from what we know *in vitro* and in yeast and ask whether NIPBL, like Scc2, is essential, required for cohesin loading and needed to build cohesion.

Designing a NIPBL degron

In order to develop a degron, it was first important to understand NIPBL's domain structure and conservation so that the best position for a tag could be identified.

NIPBL is a large protein of over 2500bp, with a canonical A isoform (316KDa) and shorter B isoform (304KDa) which differ in their C-terminus. The very N-terminus of NIPBL is disordered and binds to its cohesin loading partner, MAU2^{Scc4}, in a manner that appears to stabilise NIPBL (Chao et al., 2015; Haarhuis et al., 2017; Hinshaw et al., 2015; Seitan et al., 2006). The remaining N-terminal half of NIPBL is largely disordered and contains a series of

binding motifs including an HP1 binding region which allows the recruitment of NIPBL and cohesin to sites of double strand break by HP1γ (Bot et al., 2017; Lechner et al., 2005; Oka et al., 2011). The N-terminal portion of the protein has also been shown to interact with a variety of transcription factors including BRD4 and Mediator (Kagey et al., 2010; Luna-Peláez et al., 2019; Mattingly et al., 2022; Olley et al., 2018). The C-terminal portion of the protein consists of an array of 24 HEAT repeats, forming the distinctive "hook" shape characteristic to the HAWK proteins (Kikuchi et al., 2016). This region also includes a HDAC Interacting Domain (HID) which facilitates chromatin remodelling of the surrounding region of DNA (Jahnke et al., 2008). Whilst NIPBL may be able to interact with chromatin directly, it can be seen from its structure that it also possesses a large variety of binding partners for DNA recruitment (**Fig. 2-1**).

NIPBL is often tagged at its N-terminus despite its MAU2 binding region, as the C-terminus of NIPBL varies between its two major isoforms $NIPBL^{A}$ and $NIPBL^{B}$. Along with NIPBL's major isoforms, it is likely that other functional isoforms exist as it has been shown that mutations disrupting the reading frame of Scc2 can lead to viable truncated versions of Scc2, either by experimental design or seen naturally occurring in some patients with CdLS (Braunholz et al., 2012; Haarhuis et al., 2017). In order to assess the optimal position for a tag, I aligned all the known and predicted isoforms of NIPBL using alternative mRNA splicing transcripts from NCBI as well as their translated protein FASTA sequences. Protein sequences were aligned using EMBL's Clustal Omega Multiple Sequence Alignment tool which was provided a more reliable alignment than EMBL's T-Coffee software when later including species from yeast. Alignments were then mapped back to the gene to create a map of the exons included in the known and predicted version of the protein (**Fig. 2-2**).

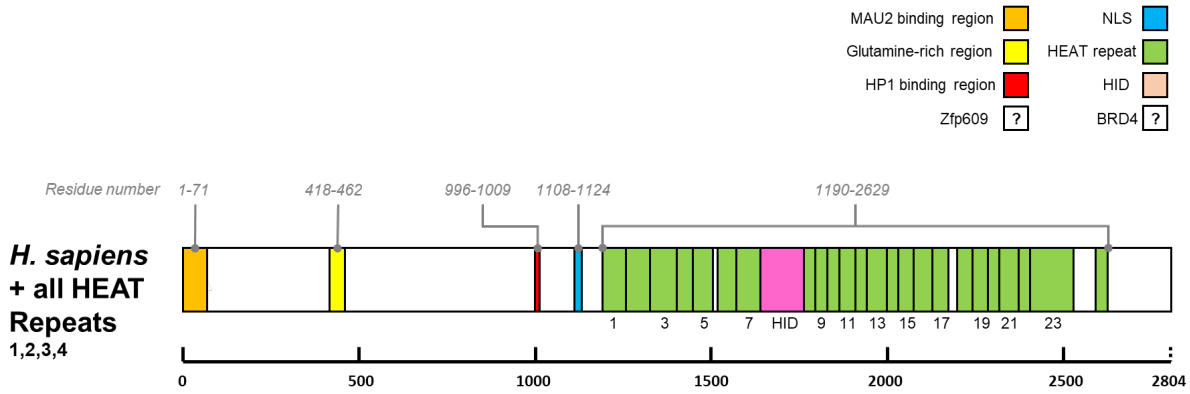

Figure 2 – 1. NIPBL domain structure. Domain structure of Human NIPBL with residue numbers based on alignments from known regions in yeast and mammals (Braunholz et al., 2012; Jahnke et al., 2008; Kikuchi et al., 2016; Lechner et al., 2005)[1-4]. Key domains marked; MAU2/Scc4 binding site (orange), Glutamine-rich region (yellow), HP1 binding region (red), NLS (blue), HEAT repeats (green), HID binding domain (pink). Domain sizes and positions are proportionally to size.

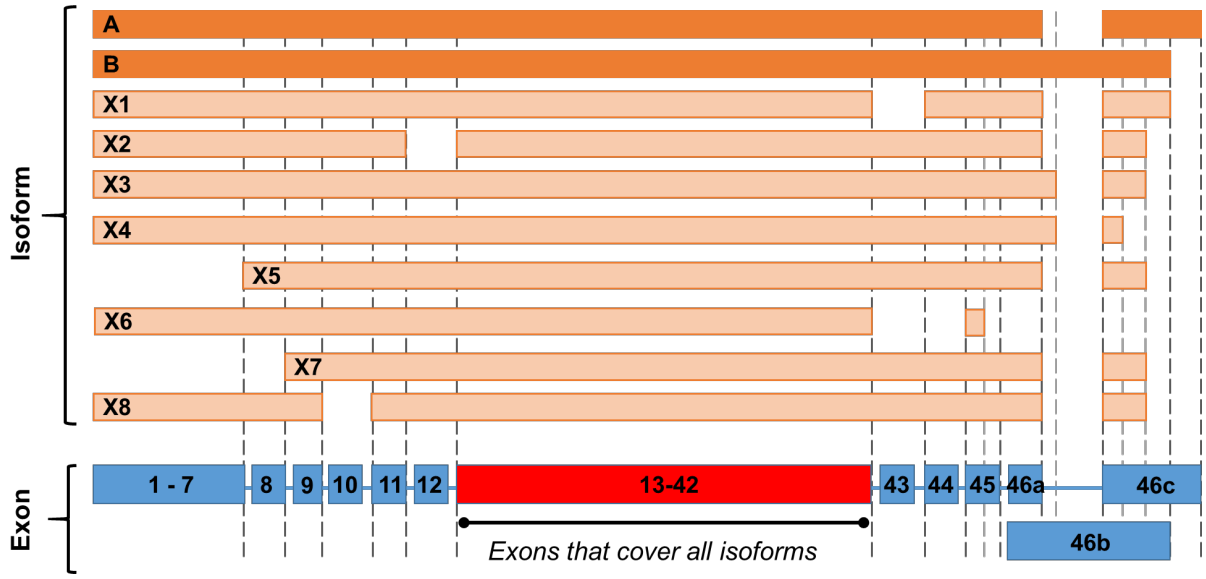

Figure 2-2. Homology alignments of known and predicted isoforms of NIPBL. Representative map of known (block orange) and predicted (light orange) transcripts of NIPBL isoforms mapped against corresponding exons (not to scale). Dark grey dashed lines indicate exon 3'/5' ends and light grey indicates the exon middle. Exon 13-42 are covered by all known and predicted isoforms. Exon alignments generated from predicted mRNA transcripts available on NCBI and aligned using Clustal Omega. Exons listed in Appendix Figure 1-1 sup.

The first observation from this mapping was that both the N and the C-terminus of the protein are not covered by all of the predicted isoforms. This means that an N-terminal degron would not deplete all versions of the protein. Interestingly, besides exons 11 and 45, the stretch of the protein that was conserved across all known and predicted isoforms was encoded by exon 13 to 42 (amino acids 1169 – 2422) of the protein. In terms of structure, this correlates to the C-terminal HEAT repeat hook region of NIPBL.

Evidence suggests that this is the most critical functional region of the protein. The C-terminal portion of NIPBL appears to be the oldest region evolutionarily, and the most highly conserved between species. Alignments created using Clustal Omega of metazoan NIPBL with lower eukaryotes of the fungi family showed that yeast and other fungi only possess the C-terminal portion of the protein, but entirely lack the unstructured N-terminal half of the protein, aside from the very N-terminal Scc4 / MAU2 binding site which was conserved (**Fig. 2-3c**). The C-terminal portion of NIPBL had a 50% conservation score with lower eukaryotes, assessed using the Boxshade tool, and over 80% with higher eukaryotes, showing that this portion of the protein is the oldest genetically and therefore likely to carry its critical functions.

Indeed, the C-terminal HEAT repeat portion of NIPBL alone has been shown to be sufficient to activate cohesin's ATPase activity and promote loop extrusion *in vitro* (Kim et al., 2019; Petela et al., 2018). Purified Scc2 from *S. pombe* was also sufficient to catalyse the cohesin loading reaction of cohesin onto circular DNA *in vitro*, even without Scc4 (Murayama & Uhlmann, 2014). Loading *in vitro* was further demonstrated using only the truncated C-terminal HEAT repeat portion of Scc2 (Chao et al., 2015). Most compellingly, in human cancer cells it was found that NIPBL could tolerate disruptive insertions up to exon 10 of the gene but absolutely not within the C-terminal region of the protein from exon 11-47, which was essential (Haarhuis et al., 2017). Critically, a truncated version of NIPBL, lacking the first 10 exons and

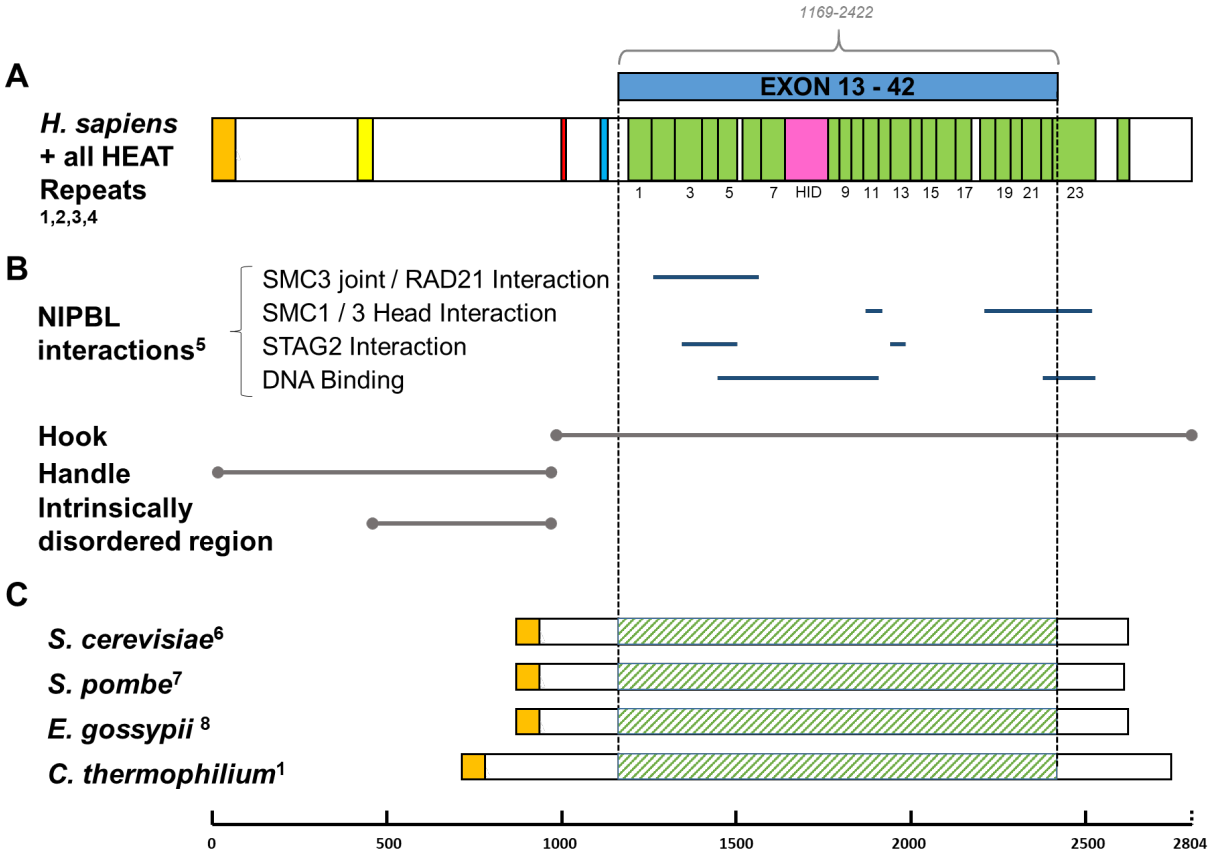

Figure 2-3. Importance of region exon 13-42, covered by all isoforms. **(A)** Domain structure of NIPBL as in Fig. 2-1, with exon 13-42 covered by all isoforms marked with amino acid residues to scale. **(B)** Positions of major cohesin complex interactions marked on schematic according to the crystal structure (Shi et al., 2020)[5]. Amino acid residues to scale. **(C)** Alignment of human NIPBL to equivalent regions in fungal Scc2. Sequences obtained from NCBI and aligned to H. sapiens using Clustal Omega and visualised using BoxShade Server conservation: set to >80% conservation. Actual amino acid sequences are shorter due to regions misalignment not shown. Amino acid positions obtained from (Kikuchi et al., 2016)[1]; (Hinshaw et al., 2015, 2017)[6]; (Higashi et al., 2020)[7]; (Chao et al., 2015, 2017)[8]

uncoupled from MAU2, was sufficient to support cohesin loading, enable robust sister chromatid cohesion and catalyse cohesin's ATPase as shown by vermicelli formation (Haarhuis et al., 2017).

Structural studies in both human and yeast have shown that the C-terminal hook region of NIPBLC (residues 1163 to 2804) interacts with both DNA and the cohesin complex (Collier et al., 2020; Higashi et al., 2020; Shi et al., 2020) (**Fig. 2-3b**). Furthermore, mutation analysis using missense mutations from CdLS patients were also shown to form two clusters within the hook region of Scc2 (Kikuchi et al., 2016).

As both the N and the C-terminus do not cover all isoforms of NIPBL, they were non-viable options for targeting with a degron. I therefore designed a degron that would sit internally within the protein within the conserved C-terminal region of NIPBL. The risk of designing an internal degron was that it would disrupt the protein structure. To best mitigate this possibility, I used conversation alignments between metazoans to see where other species had tolerated insertions in the protein, and further looked for unstructured loops according to the human structure of NIPBL which would be less likely to disrupt the HEAT repeat structure (**Fig. 2-4c**). I was also able to reference prior work which had found a series of sites that tolerated a TEV insertion site in both mouse NIPBL (Nasmyth lab – personal communication) and yeast (Bin Hu – personal communication). Using the species alignments, I mapped these sites back to Human NIPBL and remarkably, some of these mouse and yeast sites overlapped (**Fig. 2-4a**). Finally, using the crystal structure published of human NIPBL interacting with DNA and the cohesin complex, I looked for loops that were outward facing away from the side that NIPBL interacts with DNA and the cohesin subunits (**Fig.2-4d**). Under these criteria, one site at residue V1641 was the best candidate as it tolerated TEV insertions in both yeast and mice, was within

an outward facing loop on the opposite site to the cohesin interacting region, and had tolerated insertions in other higher eukaryotes (**Fig. 2-4b**).

The miniAID (mAID) degron system was chosen over other degron systems such as dTAG due to its small size of 68aa, which was important to minimise the size of the insertion for the internal tag to minimise disruption. The mAID is itself a minimum region from the original AID construct (Kubota et al., 2013; Nishimura & Kanemaki, 2014). A small inert 12aa Spot-Tag® epitope tag was also added which is able to bind various Spot-nanobodies to assist with the pull down and detection of the construct. The initial rationale for Spot-Tag inclusion was that NIPBL antibodies were not very good, however as the project developed, a good system for NIPBL detection was developed, so I did not end up using this tag during my project despite its presence in my construct. As this was an internal tag, I flanked the insert with two 7aa Glycine / Serine linkers (GGGSGGG) on either side to provide flexibility to the construct (**Fig. 2-4e**).

Targeting the internal NIBPL degron

Human U2OS osteosarcoma cells were used to build this cell line as they are a well characterised cell model and grow as a monolayer tissue which are easy to image as they are relatively flat. As a human cancer cell line, U2OS can be cultured for extended periods of time but are WT for P53 and Rb (Diller et al., 1990; Isfort et al., 1995), and respond well to cell synchronisation protocols. U2OS are aneuploid and have 4 copies of chromosome 5 where the *NIPBL* gene is found, however this is fewer than other fast growing cancer cell lines such as HeLa which have 8, making it easier to homozygously tag the gene (Janssen & Medema, 2013).

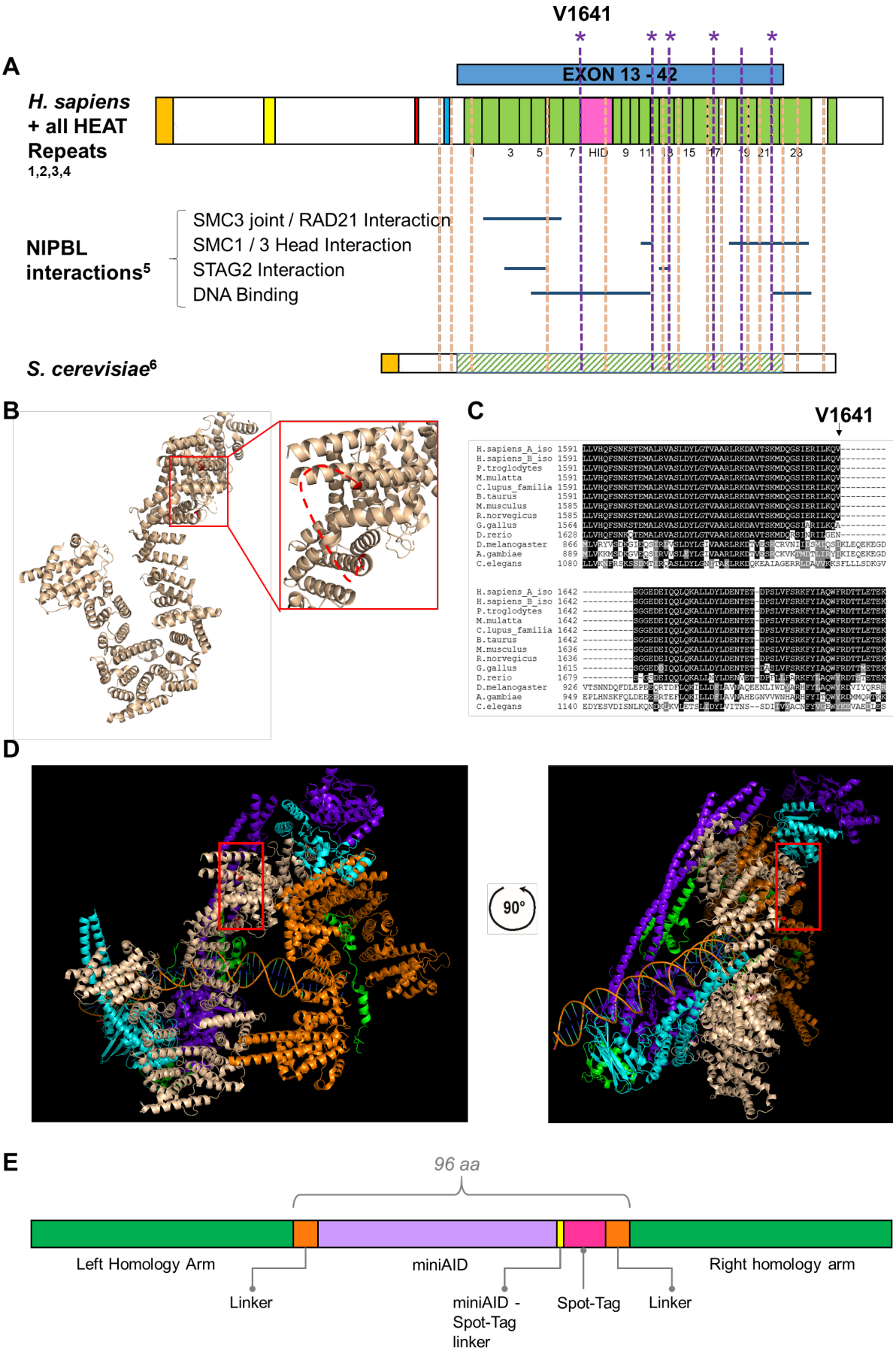
A
V1641
EXON 13 - 42
H. sapiens
+ all HEAT
Repeats
1,2,3,4
1 3 5 7 HID 9 11 13 15 17 19 21 23
NIPBL
interactions5
SMC3 joint / RAD21 Interaction
SMC1 / 3 Head Interaction
STAG2 Interaction
DNA Binding
S. cerevisiae6
B
C
V1641
H.sapiens_A_iso 1591 LLVHQFSNKSTEMALRVASLDYLGTVAARLRKDAVTSKMDQGSIERILKQV
H.sapiens_B_iso 1591 LLVHQFSNKSTEMALRVASLDYLGTVAARLRKDAVTSKMDQGSIERILKQV
P.troglodytes 1591 LLVHQFSNKSTEMALRVASLDYLGTVAARLRKDAVTSKMDQGSIERILKQV
M.mulatta 1591 LLVHQFSNKSTEMALRVASLDYLGTVAARLRKDAVTSKMDQGSIERILKQV
C.lupus_familia 1591 LLVHQFSNKSTEMALRVASLDYLGTVAARLRKDAVTSKMDQGSIERILKQV
B.taurus 1591 LLVHQFSNKSTEMALRVASLDYLGTVAARLRKDAVTSKMDQGSIERILKQV
M.musculus 1585 LLVHQFSNKSTEMALRVASLDYLGTVAARLRKDAVTSKMDQGSIERILKQV
R.norvegicus 1585 LLVHQFSNKSTEMALRVASLDYLGTVAARLRKDAVTSKMDQGSIERILKQV
G.gallus 1564 LLVHQFSNKSTEMALRVASLDYLGTVAARLRKDAVTSKMDQGSIERILKQA
D.rerio 1628 LLVHQFSNKSTEMALRVASLDYLGTVAARLRKDAVTSKMDQGSIERILGEN
D.melanogaster 866 MLVKYSPKSIESSRDVLSLDYLGTVAARLRKDTVSSKCRVNILESMLQSKLEQEKEGD
A.gambiae 889 MLVKKMSPKSVESSRDVLSLEYLGTVAARLRKDTVSSKCKVNQMDTMLETYIKIEQEKEGD
C.elegans 1080 LLVQNLRRSKSSDVTIRQASLDYLGNVTAALRKDQKEAIAGERRLLAVWKSFLLLSDKGV
H.sapiens_A_iso 1642 ----------SGGEDEIQQLQKALLDYLDENTET-DPSLVFSRKFYIAQWFRDTTLETEK
H.sapiens_B_iso 1642 ----------SGGEDEIQQLQKALLDYLDENTET-DPSLVFSRKFYIAQWFRDTTLETEK
P.troglodytes 1642 ----------SGGEDEIQQLQKALLDYLDENTET-DPSLVFSRKFYIAQWFRDTTLETEK
M.mulatta 1642 ----------SGGEDEIQQLQKALLDYLDENTET-DPSLVFSRKFYIAQWFRDTTLETEK
C.lupus_familia 1642 ----------SGGEDEIQQLQKALLDYLDENTET-DPSLVFSRKFYIAQWFRDTTLETEK
B.taurus 1642 ----------SGGEDEIQQLQKALLDYLDENTET-DPSLVFSRKFYIAQWFRDTTLETEK
M.musculus 1636 ----------SGGEDEIQQLQKALLDYLDENTET-DPSLVFSRKFYIAQWFRDTTLETEK
R.norvegicus 1636 ----------SGGEDEIQQLQKALLDYLDENTET-DPSLVFSRKFYIAQWFRDTTLETEK
G.gallus 1615 ----------SGGEDEIQQLQKALLDYLDENTET-DPSLVFSRKFYIAQWFRDTTLETEK
D.rerio 1679 ----------SGSDEIQQLQKALPAYLDENTET-DPSLIFSRKFYIAQWFRDTSLETEK
D.melanogaster 926 VTSNNDQFDLEPPEQRTDFLQKILLDLIAVVAQEENLIWDVARHFYIAQWFRDVIYQRRE
A.gambiae 949 EPLHNSKFQLDEEQRTEFLQKILLDLIAVVAHEGNVVWNHARHFYIAQWFRDMMQRRKK
C.elegans 1140 EDYESVDISNLKQNLKQKVLETSLIDYLVITNS--SDILLVVACNFYVEQWMKGVAEDIES
D
90°
E
96 aa
Left Homology Arm
miniAID
Right homology arm
Linker
miniAID - Spot-Tag linker
Spot-Tag
Linker

Figure 2-4: Sites for endogenous tagging. (A) Domain structure of NIPBL as in Fig. 2-1, with alignments of previously targeting regions for TEV insertion in both yeast (orange dashed lines) and mouse (purple dashed lines). Overlapping yeast and mouse sites marked with purple star. Positions are to scale. **(B)** Structure of Human NIPBL hook region with residues surround V1641 (D1646 and M1629) marked in red, as region is an unstructured loop. **(C)** Alignment of metazoan NIPBL sequence around V1641 using an 80% conversation mapping in Boxshade. **(D)** Structure of human NIPBL (cream) interacting with DNA and the cohesin complex; the heads of SMC1 (blue) and SMC3 (purple), the kleisin (green) in the clamped position and Scc3, which is constitutively bound to cohesin (orange). *PDB: 6WG3* (Shi et al., 2020). Position V1641 is marked with a red box and is on the opposite face of NIPBL to its binding regions to cohesin. **(E)** Internal mAID construct design. Left HA (77aa), linker (7 aa), miniAID (68aa), miniAID-Spot-Tag linker (2aa), Spot-Tag (12aa), linker (7 aa), right HA (77aa).

NIPBL was endogenously tagged using CRISPR-Cas9 genetic engineering (Yang et al., 2013). Suitable guide RNA (gRNA) pairs were selected using the CRISPOR.org server by UC Santa Cruz, and inserted into a pX459V2 plasmid which is conjugates the gRNA to the Cas9 enzyme by a scaffold. The guide plasmid was co-transfected with a donor plasmid, designed as in Fig. 2-4e, with 230bp homology arms around the V1641 residue. In order to ensure the gRNA does not continue to cut the new donor once inserted by homologous recombination, the PAM sequence and 3 neighbouring amino acids of the guide RNA binding region were silently mutated in the donor plasmid so that the guide can no longer recognise the sequence but the peptide sequence remained the same.

Cell models respond differently to transfection reagents, therefore in order to optimise the CRISPR protocol specifically for U2OS cells, a non-site specific GFP plasmid was transfected into U2OS with different transfection reagents and tested for positive GFP signal (**Fig. 2-5**). FuGENE® HD had the highest transfection efficiency of 32% so was used to transfect WT U2OS from ATCC. Post transfection, cells were puromycin selected for 2 days with a puromycin resistance marker selected on the guide plasmid but not for so long that the Cas9

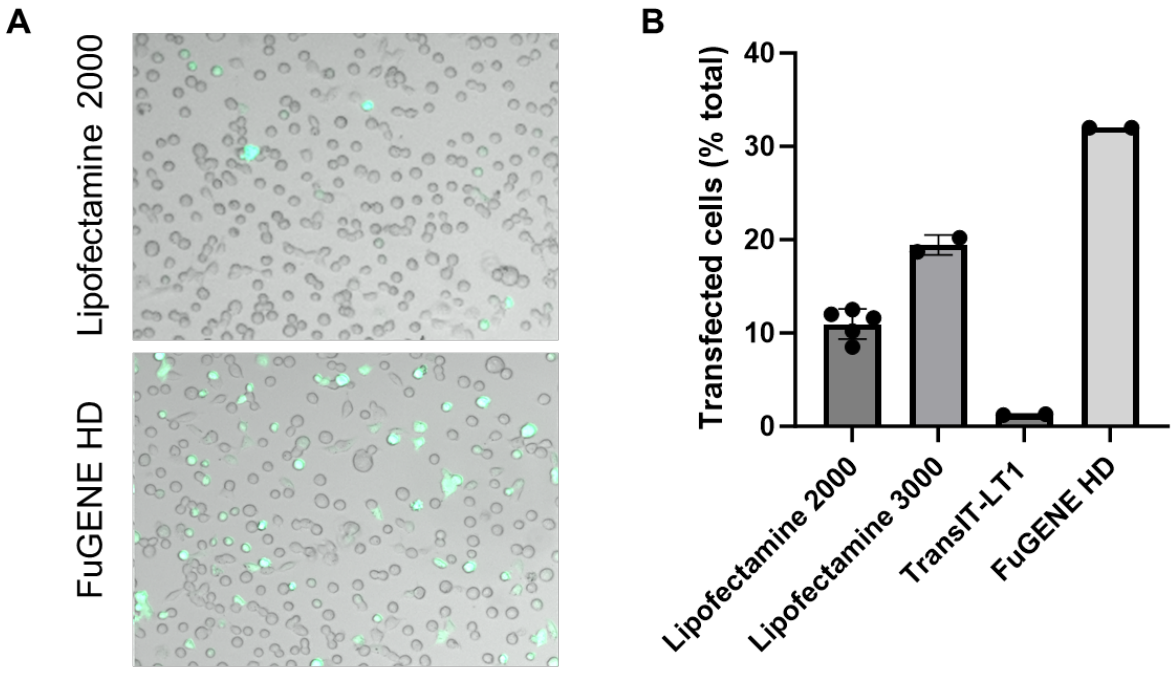

Figure 2-5. Transfection efficiency test in U2OS. Live cells imaged under bright field 24 hours after transfection with a GFP plasmid using different reagents and measured for positive GFP signal **(A)** Representative images from FuGENE and Lipofectamine 2000 transfections under bright field with GFP fluroesence **(B)** Transfection rate across transfection reagents.

enzyme integrates into the genome. Cells were then plated for single cells and colony picked for individual clones.

Genotyping primers were designed using a NCBI primer BLAST search in order to find pair that were specific to the NIPBL loci of the genome. Clones were validated for homozygosity using 3 sets of primers covering the insertion site, the left homology arm and the right homology arm (**Fig. 2-6a**). Fragment sizes were purposefully kept small for ease doing PCR from genomic DNA. The junctions at the ends of the left and right homology arm were checked as these regions are prone to error during homologous recombination. PCR genotyping identified one homozygous clone (clone 15), which was positive for the construct insertion as checked by Sanger sequencing. It can be noted that the insertion PCR appears to have a shadow around the molecular weight of the WT band in the homozygous clone. The band was sequenced and did not match the genomic loci, and furthermore was gone with both junction PCRs suggesting that it was caused by a nonspecific locus in the genome by the primer pair. In a second round of CRISPR targeting to obtain more mAID-Spot-NIPBL clones, I achieved a 2.2% homozygosity rate and 6 more homozygous clones.

Clone 15 was verified by western blot. Western blots of WT NIPBL vs mAID-Spot-NIPBL show that NIPBL is tagged and furthermore that all the isoforms below the expected protein weight are also tagged as they shift to a higher molecular weight (**Fig. 2-6b**).

Using the mAID2 system

To complete the mAID degron, TIR1 must be inserted exogenously into the genome. The mAID degron system had reports of "leaking" where naturally occurring analogues of the auxin compound could activate the destruction of the protein, causing lower basal expression levels.

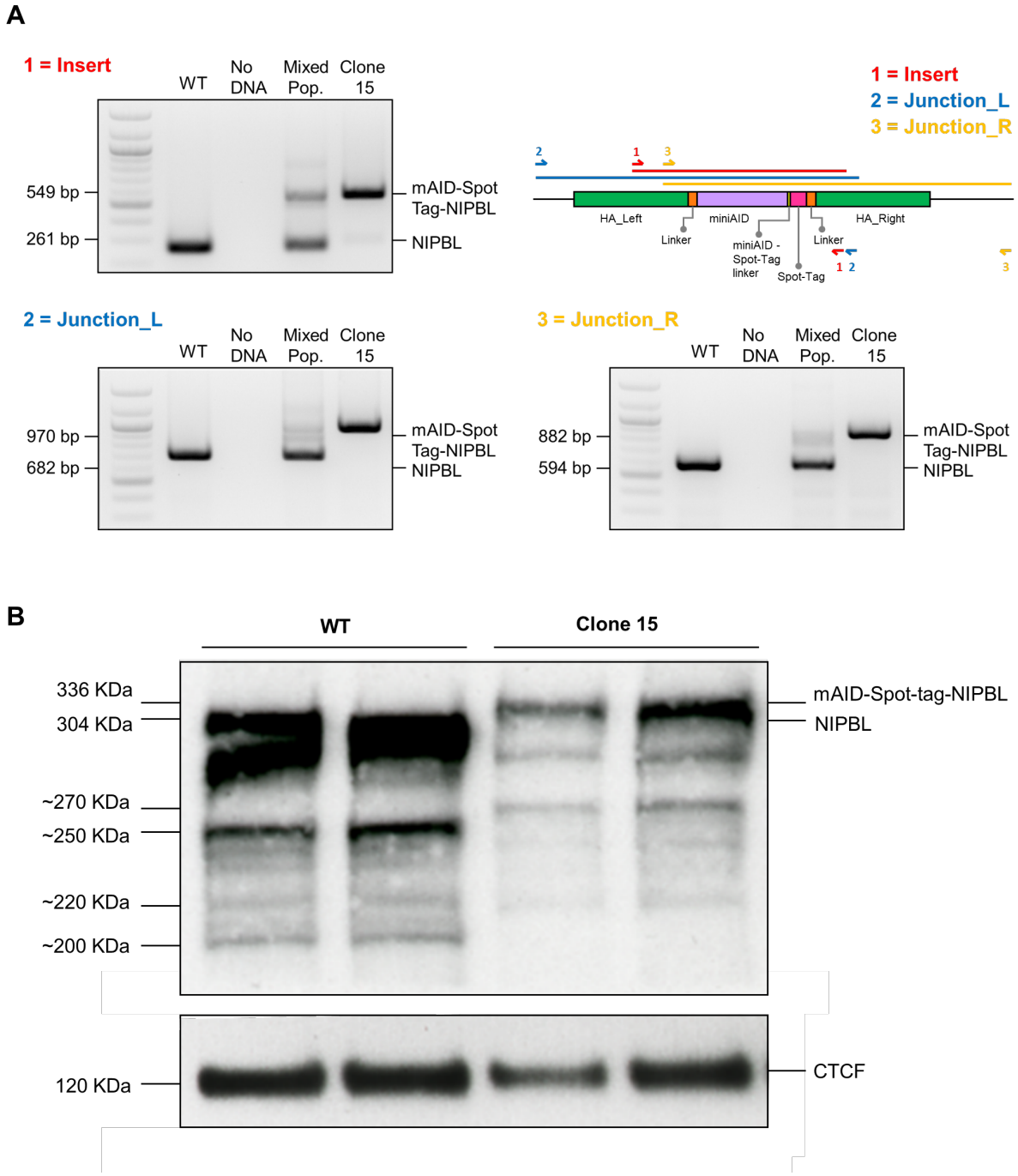

Figure 2- 6. Homozygous tagging of mAID-Spot-NIPBL at site V1641. **(A)** PCR genotyping of homozygous clone 15 using primers that target the insertion region, the left homology arm junction and the right homology arm junction. **(B)** Immunoblot of homozygous clone 15 using antibody against NIPBL showing tagging of all NIPBL isoforms. CTCF was used as a loading control.

This issue was largely resolved with the development of the mAID2 degron system, which mildly adapted the TIR1 protein and the auxin drug used, by removing a phenylalanine in the active site of the TIR1 protein creating a "hole", and by adding a phenyl group to the auxin drug compound, creating a "Bump" (Yesbolatova et al., 2020). This "Bump and hole" method increased the specificity of the drug 100 fold, reducing the recommended concentration of auxin from 500μM to 5μM. It also reduced the issue of "leakage" through the added specificity. The adapted TIR1 (F47G) protein was therefore used to upgrade to the mAID2 system. Another issue that can occur when tagging essential proteins is that the TIR1 protein can become silenced and be selected for on a population level over time due to the added fitness of the cells. In order to provide stable expression of the transgene, TIR1 was targeted to the AAVS1 safe harbour locus and further selected for the expression of the gene using a blasticidin resistance marker (Natsume et al., 2016; Smith et al., 2008). To ensure that TIR1 was not inhibited by the blasticidin resistance marker, I used a porcine teschovirus-1 2A (P2A) self-cleaving peptide between TIR1 and blasticidin gene, which allows the co-expression of TIR1 and Blasticidin transcripts but cleaves in order to create two separate proteins (**Fig. 2-7a**) (Wang et al., 2015). This system has the advantage allowing the resistance marker to be expressed under the same promoter as the gene of interest so that their expression or silencing are linked, however does not labour the protein of interest with an extra marker.

A second round of CRISPR/Cas9 was used to target TIR1-P2A-BSD to the AAVS1 locus in the mAID-Spot-NIPBL clone 15 parent. Genotyping identified six homozygous clones with the TIR1 insert as confirmed by sanger sequencing (**Fig. 2-7b**). The V1641 mAID-Spot-NIPBL AAVS1-TIR1(F74G)-P2A-BSD clones will herein be referred to as mAID^{int}-NIPBL.

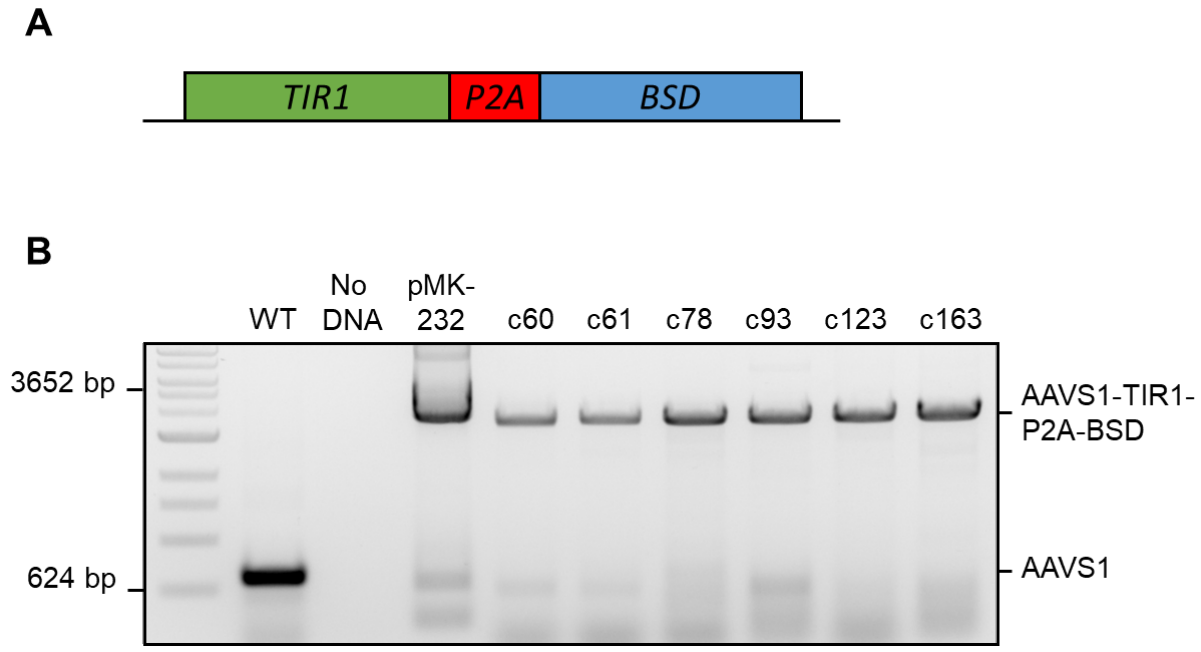

Figure 2-7. Targeting for the mAID2 system. (A) plasmid design with mutated TIR1(F74G), P2A self-cleaving peptide and a blasticidin resistance marker. **(B)** PCR genotyping of homozygous clones for AAVS1-TIR1-P2A-BSD insertion

NIPBL and all its isoforms can be depleted fully within 6 hours

The six homozygous clones were tested for NIPBL depletion to see whether they could form the correct degradation complex, even with the degron placed internally within a protein where there is greater steric hindrance. All clones were incubated with 5μM of the adapted mAID2 auxin drug 5'Ph-IAA, herein referred to as a just IAA, for a timecourse of 6 hours and a sample was taken periodically for western blotting. Immunoblotting revealed that within 2 hours of auxin addition, and always by 6 hours, both the major band of NIPBL (336KDa) and its isoforms of NIPBL at lower molecular weights depleted to levels below western blot detection. This demonstrates that the internal degron is functional and that it targets all isoforms of NIPBL that are detectable by this antibody (**Fig. 2-8**). All mAID^{int}-NIPBL clones also showed lower expression levels of NIPBL than WT cells, suggesting that there is either some inherent destabilisation of the protein due to the internal tag or that there is still some basal level of degron leakage. The levels of NIPBL are still sufficient however to support life.

.

NIPBL is an essential protein

Whilst the NIPBL degron cell line is able to deplete NIPBL fully according to western blots, it was important to see whether it would create the function phenotype we would expect from what is known in yeast, namely, to see whether the protein is essential for life and whether NIPBL is required for cohesion. In order to test whether NIPBL is essential, the 6 degron clones were grown in the presence or absence of auxin for 6 days, with cell numbers counted every 24 hours (**Fig 2-9**).

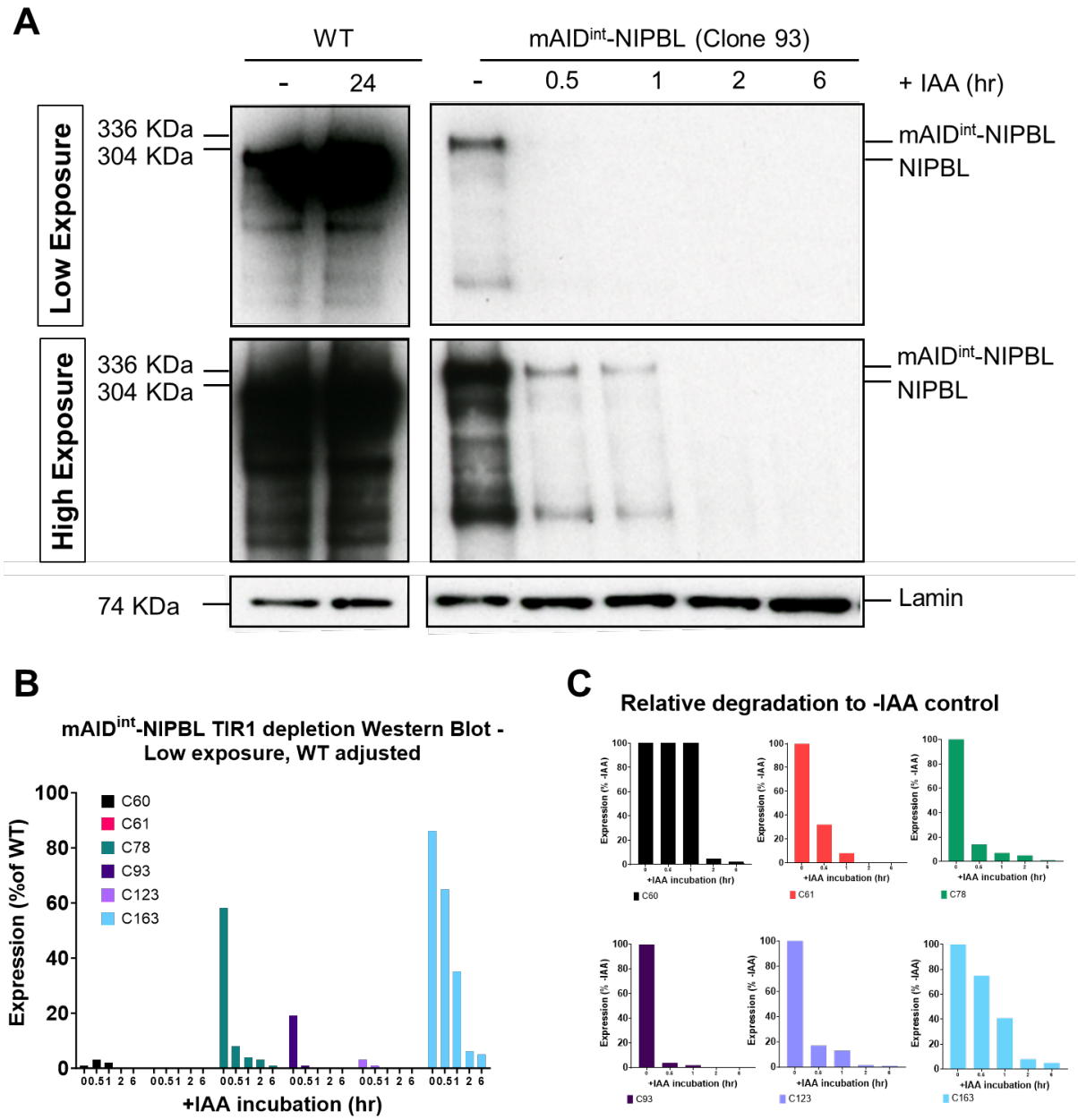

Figure 2-8. NIPBL and detected isoforms deplete fully within 6 hrs. (A) Immunoblot of mAID^{int}-NIPBL depletion with auxin addition over the course of 6 hrs. Clone 93 is shown for illustration **(B)** Quantified expression and depletion levels across all 6 clones against WT levels **(C)** Relative depletion rates of clones according to their non-treated NIPBL expression levels

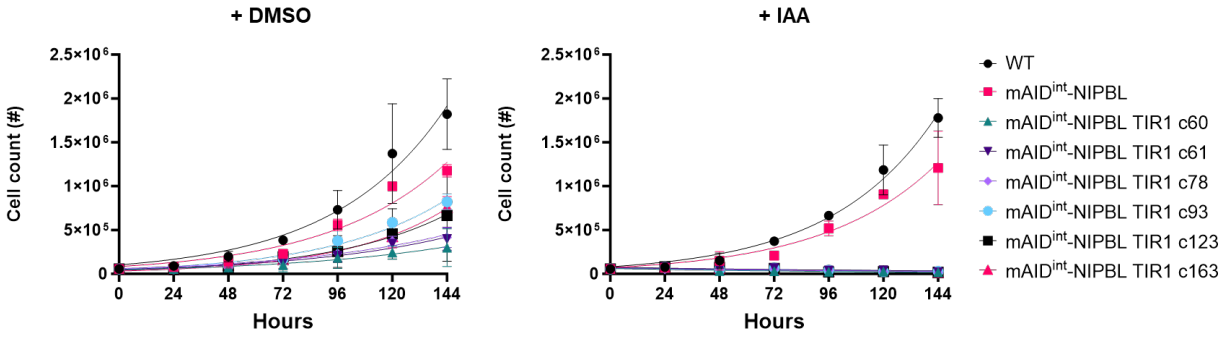

Figure 2-9. NIPBL is essential. Cell proliferation assay of WT cells, the mAID^{int}-NIPBL parent cell line and the 6 mAID^{int}-NIPBL TIR1 clones.

From the cell proliferation curves, it can first be observed that the WT clones have a faster proliferation rate than the parent mAID^{int}-NIPBL cell line and the subsequent 6 mAID^{int}-NIPBL AAVS1 TIR1 clones. This suggests that NIPBL is itself essential, as a hypomorphic expression of this protein causes slower growth rates. Furthermore, the parent mAID^{int}-NIPBL cell line grows more slowly than WT even before TIR1 is added to complete the degron, suggesting that tag insertion alone may cause some destabilisation of the protein, independent of degron leakage. Once the full degron is completed, the clones are able to respond to auxin addition and absolutely cannot grow. This further shows that NIPBL is required for growth and is therefore an essential protein.

Based on the results of growth rate, NIPBL protein levels compared to WT and depletion efficiency, the final two independent clones selected for future experiment were clone 93 and clone 123, herein known as C1 and C2 for ease.

Cells have chromosome segregation defects in the absence of NIPBL

An indication of why cells were failing to proliferate in the absence of NIPBL came from observed higher levels of mitotic cells suggesting cell cycle arrest by the spindle assembly checkpoint due to issues with chromosome segregation. To investigate this further, I used both FACS and microscopy to assess the number of mitotic cells using H3PS10 staining which specifically marks mitotic cells. Microscopy was used to assess mitotic cell staining as this method also enables the visualisation of other nucleic defects. During coverslip preparation however, mitotic cells are more likely to be lost from the sample as cells round up during

mitosis and can be knocked off the sample. As an orthogonal approach to look at total mitotic cell numbers, FACS was used along with H3PS10 staining as this processes cells in suspension.

The results from both experiments and repeats were in line, showing that within 24 hours, the mitotic index of clones incubated in auxin increased roughly 4 fold from ~1.5% to ~7% mitotic cells and other chromosomal defects could start to be observed such as aneuploid cells which have a much greater volume than a typical G2 cell (highlighted by blue arrow) (**Fig. 2-10**). Cells were eventually able to escape the arrest and by 48hrs, the mitotic index reduced to ~4%, however the incidence of micronuclei formation and chromosomal disaster was much greater (highlighted by red arrow) caused by the missegregation of chromosomes.

NIPBL is required for cohesion

I next wanted to see whether the increased rate of chromosome missegregation was a result of cohesion defects in the absence of NIPBL. To assess this, I repeated this timecourse of auxin addition for 24hrs and 48hrs in an asynchronous culture and took samples for chromosome spreads (**Fig. 2-11**). Chromosome spreads visualise mitotic chromosomes and can identify cohesion between sister chromatids at the centromere forming the characteristic "X" shape in a WT scenario. If sister chromatids experience a loss of cohesion, they can present as a "Railroad" phenotype, whereby the sister chromatids appear parallel, but lack centromeric joining. The most extreme phenotype of loss of cohesion is premature chromatid separation (PCS), whereby the two sister chromatids are fully detached. When incubated with auxin the results of NIPBL depletion were evident with ~ 90% of cells having loss of cohesion by 24 hrs and 95% of cells by 48hrs, across both clones. This shows that NIPBL is required for cohesion.

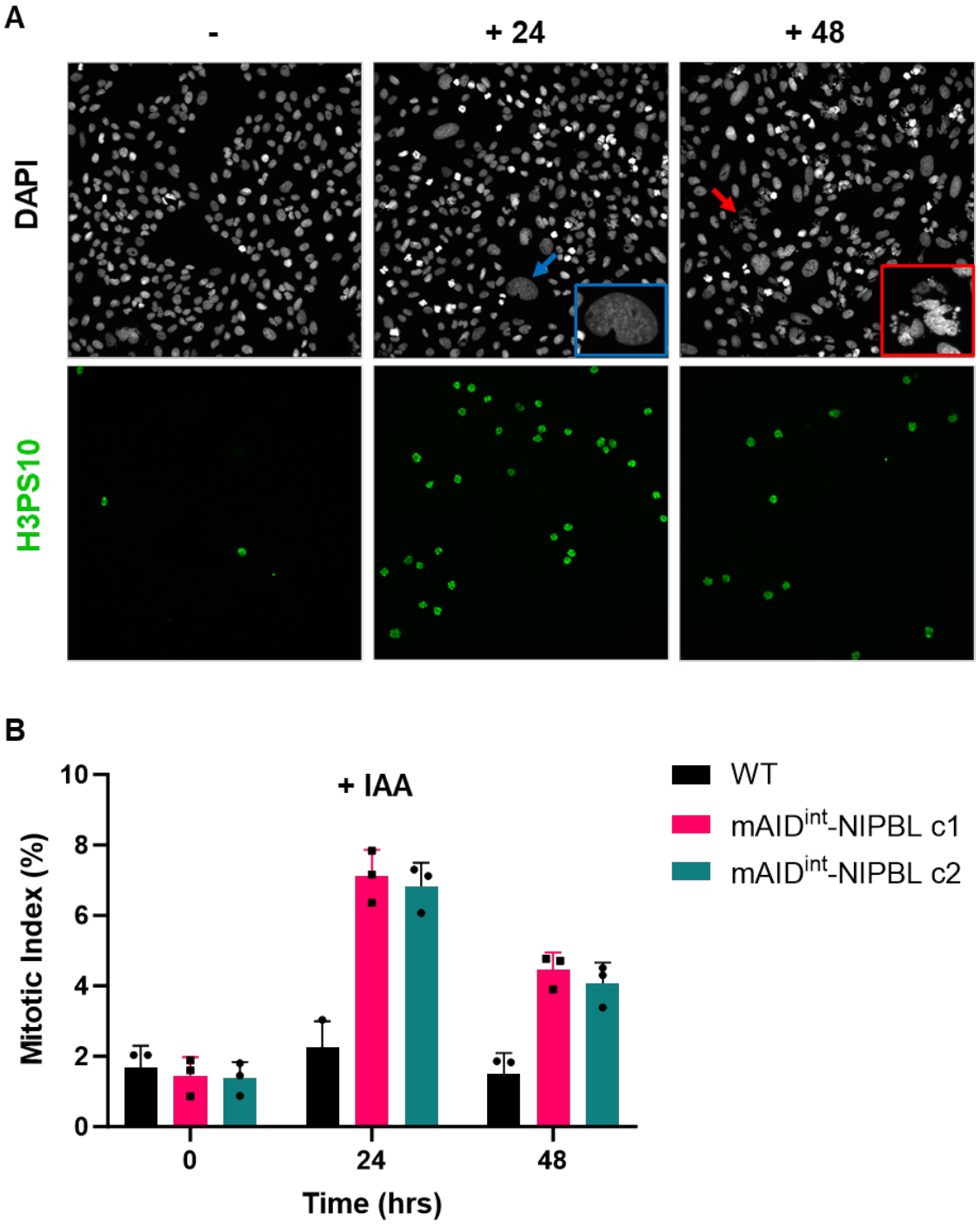

Figure 2-10. Mitotic Index increases with NIPBL depletion. Mitotic Index with mitotic cells stained by H3PS10 compared to the total population stained with DAPI. **(A)** Representative images of timepoints + IAA. Aneuploid cells can be seen by 24hrs (blue arrow) and severe chromosomal defects with micronuclei formation by 48hrs (red arrow). **(B)** Graph of mitotic index levels across timecourse +IAA as measured by microscopy image analysis and FACS.

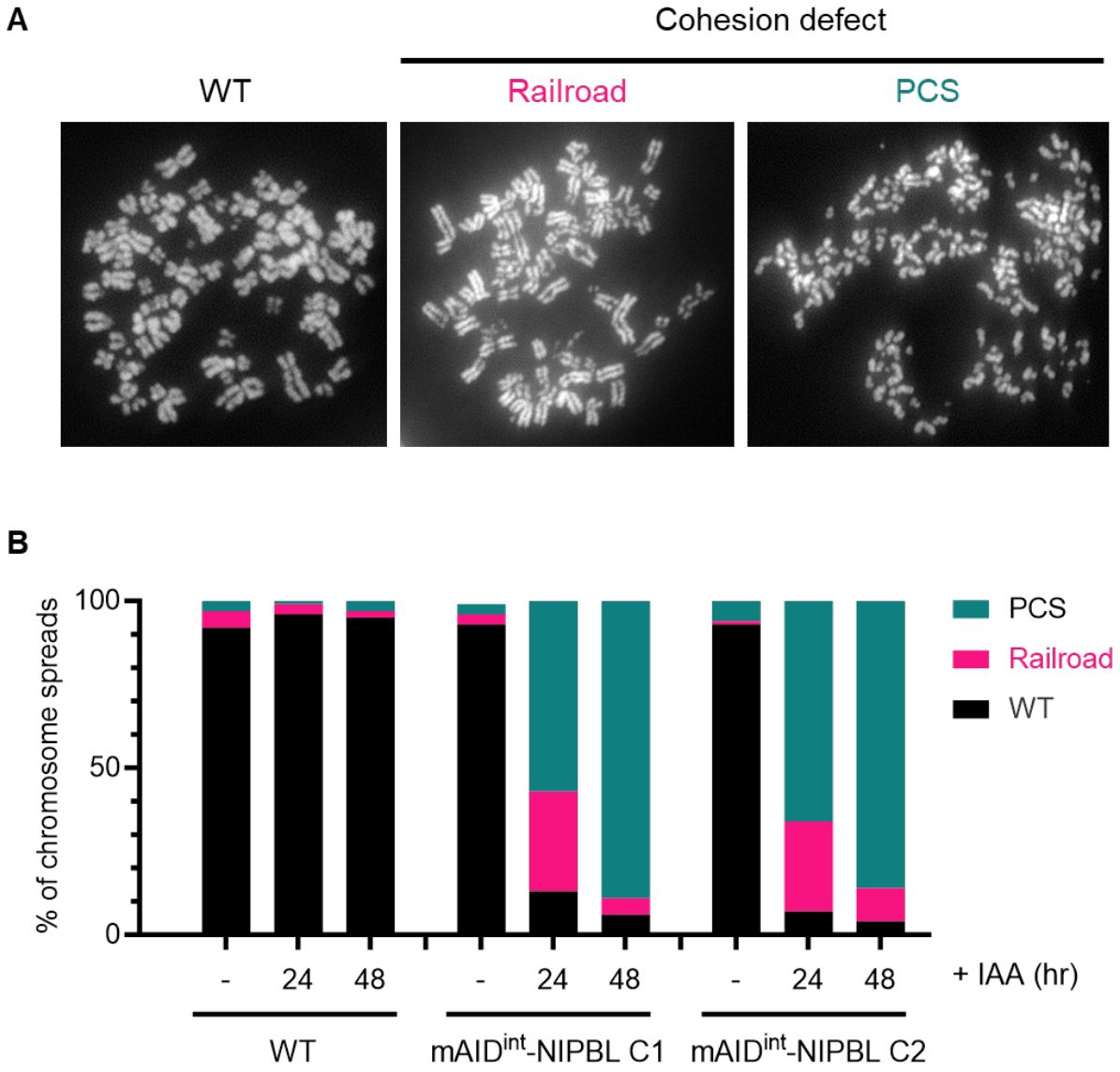

Figure 2-11. NIPBL is required for cohesion. (A) Representative images of cohesion phenotypes of cohered chromosomes or loss of cohesion phenotypes including railroad and premature chromatid separation. **(B)** Analysis of NIPBL depletion over 48 hrs, showing 90-95% loss of cohesion in mAID^{int}-NIPBL cell lines compared to WT. Chromosome spreads analysed are marked on graph.

Cells die without NIPBL

In the absence of NIPBL, cells were unable to build cohesion, leading to chromosome segregation defects such as aneuploidy and micronuclei formation, therefore it would be expected that cells eventually die as nuclear catastrophes accumulate. To test this, single cells were seeded a set density and allowed to grow for 2 weeks until colonies could be seen, in either the presence or absence of auxin, in a colony formation assay. Once colonies were of a sufficient size, plates were washed and stained with coomassie blue so that cell colonies could be visualised. From these plates, it can be seen that mAID^{int}-NIPBL cells treated with auxin die compared to untreated cells, across both clones (**Fig. 2-12**). As seen previously in the cell proliferation assay, mAID^{int}-NIPBL clones grow at a slower rate than WT cells so the colony sizes are much smaller, which may be due to the reduced expression of NIPBL in these cell lines.

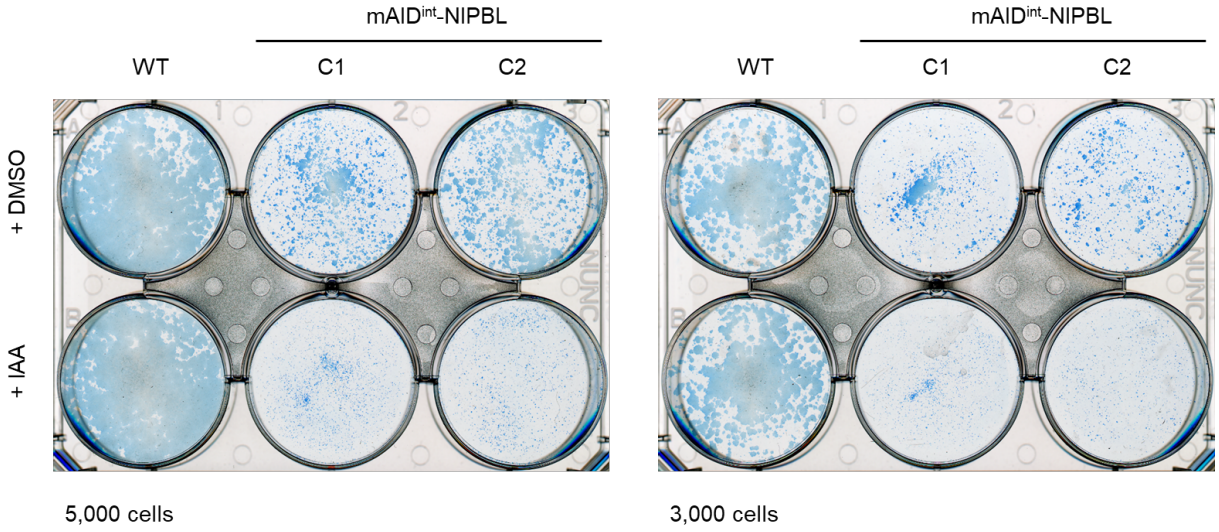

Figure 2-12. Cells die without NIPBL. Cell survival assay of WT and mAID^{int}-NIPBL clones, grown in the presence or absence of NIPBL. Plates were seeded at 5,000 starting cells or 3,000 and left to grow for 2 weeks, with media being changed every 2-3 days. WT cells grow at a faster rate than the clones, hence the higher cell coverage density.

Discussion

The aim of this results chapter was to address whether NIPBL is essential for life. To do this we set out to generate a NIPBL degron that could deplete the protein rapidly and fully. To test whether depletion was complete, we would assess whether NIPBL is essential, as Scc2 is in yeast, and whether it is required to build cohesion. There had been much debate in the field as to whether NIPBL was essential as other labs had knocked-down NIPBL and seen WT cohesion and cell survival. The question therefore remained whether mammalian systems had developed redundancy in their system, perhaps having multiple cohesin loaders compared to yeast, or whether knock-down of this protein was not sufficient, and rather a full knock-out of the protein would be required due to its substoichiometric nature.

By aligning all known and predicted isoforms of NIPBL, it could be seen that the only portion of the protein that was conserved among all isoforms, was the critical "Hook" shape C terminal portion of the protein, which is also oldest as it is found in lower eukaryotes, and the region which is known to interact with the cohesin complex. In order to therefore deplete all isoforms of NIPBL, I designed an internal degron tag in an outward facing loop in a region of the gene which had tolerated insertions in other species and faced away from the cohesin / DNA binding portion of the protein as seen in crystal structures. I selected the mAID tag for its small size and later, expressed the other half of the degron complex in a safe harbour locus of the genome which could be selected for under antibiotics to ensure continued expression. According to western blots, the internal degron appears to have tagged all isoforms of NIPBL as seen by a band shift of the correct corresponding size, and further depletes the expected band of NIPBL, along with these lower molecular isoform bands with auxin addition.

Having made a degron that depletes according to western blotting detection levels, I next aimed to address whether NIPBL was essential and required for cohesion. Unlike the results of other

labs, depletion of NIPBL inhibited cell proliferation showing that it is essential for life. Furthermore, cells lose cohesion within 24 hours of depletion, arrest in mitosis and acquire severe chromosome segregation defects that lead to cell death. From these results it can be inferred that knocking down NIPBL is insufficient to disrupt its most essential functions of supporting cohesion, and that only a conditional knock out of the protein can induce these reactions. Human NIPBL therefore displays similar behaviour to that of yeast and what is seen from *in vitro* work.

Whilst showing that NIPBL is required for cohesion, the next question was to determine how NIPBL is required in the process of building cohesion. The next aim of my project was therefore to determine in what stage of the cell cycle NIPBL activity is required for cohesion to be established and maintained.

Chapter III: NIPBL is not required to build cohesion during S phase

Introduction

In the previous chapter, we observed severe cohesion defects within 24 hours of NIPBL depletion. Whilst this shows that NIPBL is essential for cohesion, it does not reveal in what capacity NIPBL is required; whether NIPBL is required for cohesion establishment, or required for cohesion maintenance once established.

NIPBL, as the cohesin loading factor, associates cohesin with DNA during G1. Cohesion is then built during S phase and maintained throughout G2 until its dissolution in mitosis. The actual mechanism of cohesion establishment during S phase is however unknown. Three models have been proposed in this light. The first two models assume cohesin association with DNA in G1 is a pre-requisite to establishing cohesion, prior to DNA replication in S phase. These models are called "conversion" models, and propose that cohesin is either temporarily unloaded and re-loaded around the replication fork, much like histones, or, the entire replication machinery passes directly through the cohesin ring lumen (Srinivisan et al., 2020). Microscopy studies have confirmed that the passage of the replication fork does not displace cohesin from DNA in cells where the cohesin release pathway is inactive, although it could not be confirmed whether this cohesin was cohesive (Rhodes et al., 2017). The third model instead proposes that after DNA replication takes place, NIPBL loads cohesin directly across the two sister chromatids to actively build cohesion during S phase, and is referred to as the "*de novo*" pathway (Srinivisan et al., 2020) - an idea which has been supported biochemically through *in vitro* work (Murayama et al., 2018).

A primary question, therefore, is whether NIPBL is required to establish cohesion either indirectly, through simply associating cohesin with DNA in G1, or whether it is actively required during S phase to directly build cohesion by loading cohesin onto replicated sister chromatids.

Once cohesion is established, it must be maintained from S phase, throughout G2, until mitosis. Whilst it is known that the acetylation of SMC3 in cohesive complexes recruits sororin, which in turn inhibits WAPL and prevents cohesive cohesin from releasing from DNA, it is unknown whether NIPBL has a role is maintaining cohesive complexes also. It is therefore important to establish whether NIPBL is required during G2 to be constantly associated with cohesive complexes in order to maintain cohesion, or whether NIPBL is only required during a certain window of G1/S for cohesion establishment, after which it is so longer required.

In order to investigate precisely how NIPBL is required for cohesion, it was essential to study the depletion of NIPBL is specific stages of the cell cycle. If NIPBL is required for cohesion establishment, then depletion in G1 or S phase will lead to cohesion defects. Furthermore, we can learn about the way in which cohesion is established, differentiating between the "conversion" or "*de novo"* loading models, depending on whether NIPBL is required to build cohesion during S phase. Finally, we are able to assess whether NIPBL is required to maintain cohesion once it is established by seeing if it is required during the maintenance phase of G2.

To do this, U2OS specific cell cycle synchronisation protocols were established to enable conditions where NIPBL could be acutely depleted in either G1, S or G2. The effects of acute NIPBL depletion in during G1, S and G2 on cohesion formation where then studied. Finally, the role of NIPBL during S phase was isolated by the generation of a double degron cell line where WAPL could also be depleted, so that the effects of cohesin turnover did not affect cohesion.

NIPBL is required for cohesion establishment

In order to deplete NIBPL in G1, cell cycle conditions were first optimised for U2OS. In order to analyse cells in a true G1 state, a CDK4/6 inhibitor called Palbociclib was used as this prevents cells from producing the CDKs required to pass the G1/S checkpoint and therefore remain in G1. Conditions testing both the concentration and length of time required for maximal G1 arrest were optimised for WT U2OS cells (**Appendix Fig. 1**). The final concentration and incubation time selected was the minimal amount required to provide a good G1 arrest, so that cells were not irreversibly inhibited and could still be released from Palbociclib to progress with the cell cycle. The intention for this was to establish a protocol of arrest for both G1 and G2 cells where arrest conditions were similar to minimise the variables between the two experiments, with the only difference being the point of NIPBL depletion (described later in Fig. 3-6).

We wished to see whether depletion of NIPBL in G1 would lead to cohesion defects, and thus established an experiment to deplete NIPBL in G1, allow cells to run through S phase and check cohesion defects using chromosome spreads in mitosis. In experiments described in Figure 2-8, it could be seen that NIPBL fully depletes within 2 - 6 hours of auxin addition. Cells were therefore synchronised in G1 using 0.6μM Palbociclib for 18 hours, and NIPBL was depleted within the final 6 hours of G1 arrest. Thus, cells were depleted of NIPBL in G1 before they were released through S phase. In order to keep synchronisation conditions similar between both the G1 and G2 arrest experiments, cells were further synchronised once more at the G2 boundary using a CDK1 inhibitor called RO-3306, before release and arrest in metaphase using a spindle pole poison called Nocodazole. Cell cycle profiles were generated using microscopy with DAPI staining analysis at T_0 to ensure that cells were arrested in G1 (**Fig. 3-1a**). Samples for western blots were also taken comparing cycling cells with G1 arrested

cells at T_{-6} and T_0 for both mock treated and treated cells (**Fig. 3-1b**). From both the cell cycle profiles and immunoblot controls, it can be seen that NIPBL was depleted by T_0 in only the treated condition.

To assess whether depletion of NIPBL in G1 lead to cohesion defects, samples for chromosome spreads were taken in mitosis (**Fig. 3-1c**). Cells that had NIPBL depleted in G1 displayed significant cohesion defects of 73.2 ± 14.3 % which mostly presented as a railroad phenotype, when compared to the untreated cells of 5.9 ± 3.4 %. This result shows that NIPBL is required for cohesion establishment, however it this leaves two possibilities open for how it is required. Either NIPBL is required for cohesin loading during G1, and its depletion reduces cohesin levels on DNA which reduces cohesion, or NIPBL is required to actively build cohesion during S phase.

It is important to also note that although cells had cohesion defects, railroads would be classified as a "mild" phenotype which was surprising given the severe nature of cohesion defects found previously when cells were asynchronously depleted of NIPBL for 24 hours in Figure 2-11b. While we had observed that depletion of NIBPL for 24 hours in asynchronously growing cells resulted in catastrophic cohesion defects, the above experiments show that depletion of NIPBL in G1 cells produced relatively milder cohesion defects when the cells went through S-phase without any NIPBL. This raises a formal possibility that the severity of cohesion defects observed in the two conditions relate to the duration for which NIPBL was depleted. This is discussed in detail in Chapter IV.

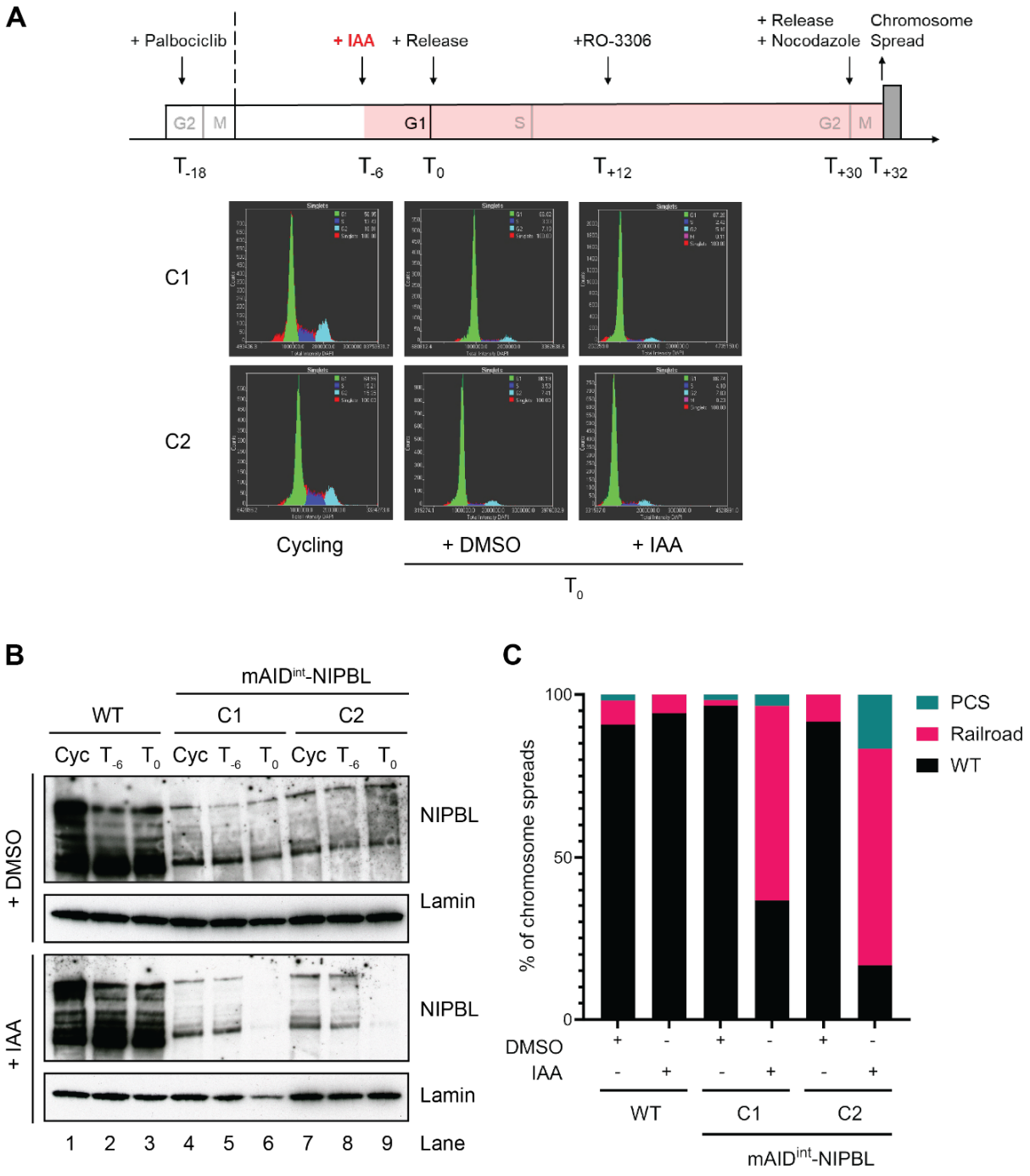

Figure 3-1. NIPBL depletion in G1 leads to cohesion defects. (A) Experiment schematic of cell cycle synchronisation protocol for depletion in G1 and release to chromosome spread collection in mitosis. Cell cycle profiles generated using microscopy with DAPI staining and analysed using the ScanR. **(B)** Immunoblot of the nuclear fraction of cells either cycling or arrested in G1 at T_{-6} and T_0, of experiment outlined in (A). **(C)** Chromosome spreads of experiment outlined in (A), showing quantification of cohesion phenotypes. Scoring was performed as in Figure 2-11, n >50 spreads.

Generating a dTAG-WAPL mAID^{int}-NIPBL double degron

Depleting NIPBL in G1 demonstrated that it is required for cohesion. I could not however answer how NIPBL is required to establish cohesion; whether it is purely in its capacity as a cohesin loader in G1, or whether it is required to actively build cohesion during S phase.

The steady state levels of cohesin on DNA, particularly in G1 cells is regulated by both NIPBL and WAPL. NIPBL loading and WAPL release work in balance to maintain cohesin on DNA with a residence time of 22 - 25 minutes in G1 (Gerlich et al., 2006; Hansen et al., 2017). When WAPL alone is depleted from cells, both the residency time and levels of cohesin on DNA increase (Kueng et al., 2006; Liu et al., 2021; Tedeschi et al., 2013), as NIPBL promotes larger loops as seen by Hi-C maps and a chromosome-like compaction during interphase called "Vermicelli" (Haarhuis et al., 2017; Wutz et al., 2017). Presumably then the inverse is true, and when NIPBL is depleted, with time the WAPL release pathway off-loads the remaining cohesin from DNA. Indeed, a reduction in cohesin levels and chromatin looping in NIPBL knockdown experiments has been observed (Alonso-Gil et al., 2023; Schwarzer et al., 2017).

The difficulty therefore of differentiating between NIPBL's requirements in either G1 or S, is that when NIPBL is depleted and the loading reaction is stopped, the inverse release reaction is still active and with time will off-load cohesin from DNA. This creates a confounding variable, as inevitably low cohesin levels on DNA affect the ability to build cohesion. In order to remove this variable, we therefore had to stabilise cohesin levels on DNA. To do this, we developed a system whereby the cohesin-DNA release reaction could also be abrogated in order to artificially increase the levels of cohesin on DNA and stop cohesin turnover. Thus, cohesin could remain associated with DNA independently of NIPBL and we could ask whether cells need NIPBL during S phase.

To do this we used an orthogonal degron approach, targeting WAPL with a dTAG degron system in the mAID^{int}-NIPBL cell line background. The dTAG system targets proteins fused with a FKBP12^{F36V} tag for degradation via the CBRN E3 ubiquitin ligase pathway upon the addition of a dTAG molecule (Nabet et al., 2018). Thus in this system, we could either acutely degrade NIPBL, or WAPL, or both, with the aim to control cohesin levels on DNA and study the role of the loader in building cohesion in isolation.

WAPL was N-terminally tagged with a FKBP12^{F36V} construct as this had previously been tolerated in other cell lines as described (Nagasaka et al., 2023). PCR genotyping of obtained 7 homozygous clones which were confirmed by sanger sequencing (**Fig. 3-2a**).

To assess whether the degron was functional, clone 6 of FKBP12^{F36V}- WAPL was tested for WAPL depletion using the dTAG-13 drug. Cells were incubated with 100nM dTAG-13 and samples were taken at intervals within a 24 hours timecourse (**Fig. 3-2b**), confirming that WAPL is mostly degraded within 2 hours and fully depleted within 6 hours of dTAG-13 addition.

Critically, it was important to test whether the two degron tags could be used orthogonally, therefore a western blot was run degrading either NIPBL, or WAPL, or both. Clone 5 and clone 6 were incubated with 5µM auxin and / or 100nM dTAG-13 for 6 hours which from previous blots had been determined the time it takes to fully deplete either protein. Immunoblotting revealed that both NIPBL and WAPL could be selectively depleted within 6 hours of drug addition (**Fig. 3-2c**).

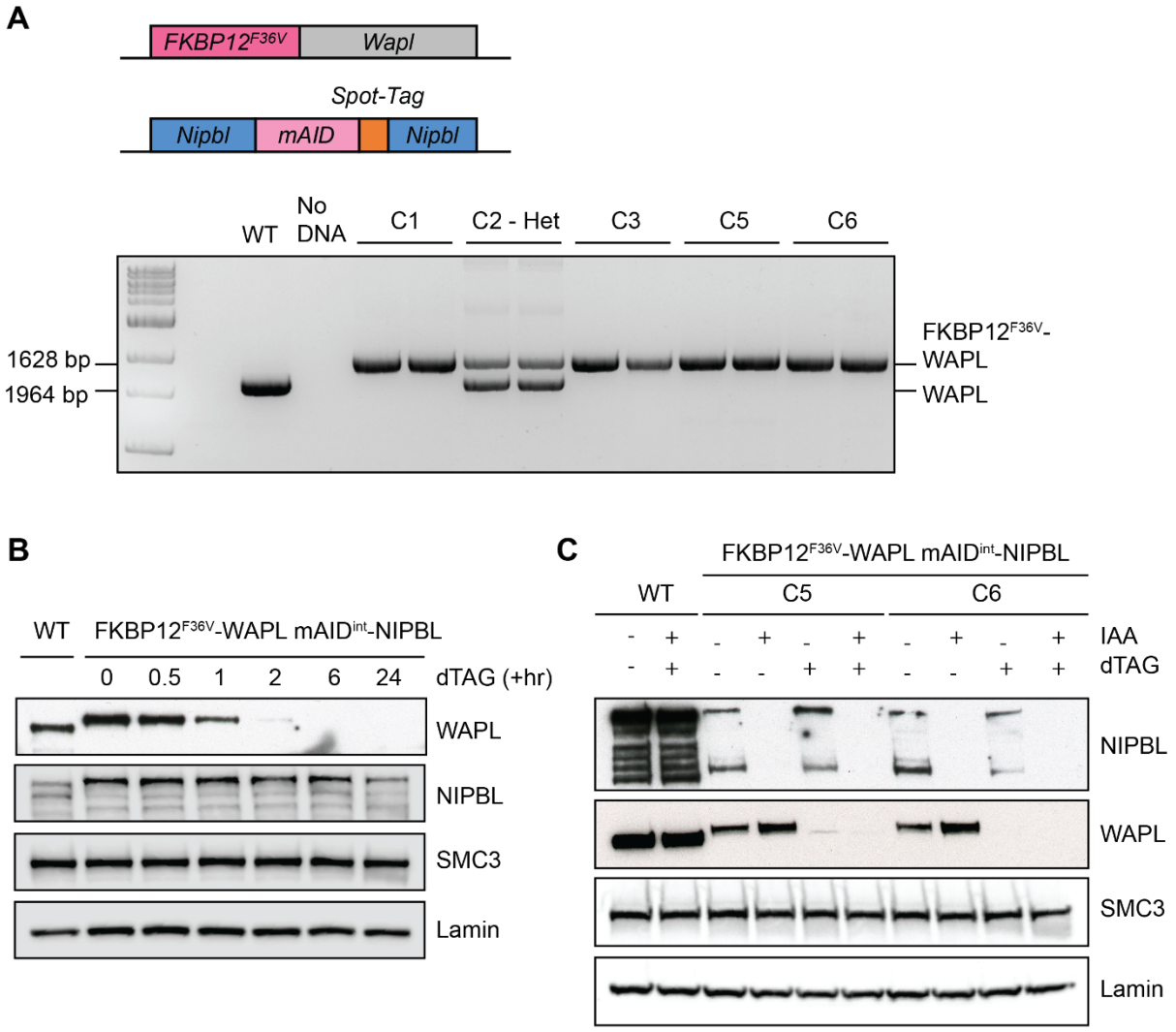

Figure 3-2. Generation of dTAG-WAPL mAID^{int}-NIPBL double degron. **(A)** Representative PCR genotyping of FKBP12^{F36V} insert into the N-terminus of WAPL, showing homozygous and heterozygous insertion. **(B)** Immunoblot of a WAPL depletion timecourse with dTAG-13 addition in the double degron cell line. **(C)** Immunoblot of NIPBL and WAPL depletion using double degron cell line across two clones.

Cohesin remains associated with DNA with the co-depletion of WAPL

With a functional double degron cell line, we wished to see whether cohesin levels on DNA could be altered as expected with either the depletion of NIPBL or WAPL, and critically, whether cohesin levels on DNA could be stabilised with the co-depletion of both NIPBL and WAPL.

In order to allow a larger pool of cohesin to associate with DNA before turnover was stopped, WAPL was depleted first to stop release and allow increased cohesin association with DNA. Only after more cohesin was loaded, was the NIPBL loader then depleted, which would stop cohesin turnover. To this end, cells were synchronised at the G1/S boundary using a double thymidine block rather than palbociclib, in order to improve the release protocol through S phase. 8 hours prior to release from the second thymidine block, cells were depleted of WAPL using dTAG-13, and 2 hours later, cells were depleted of NIPBL using auxin for the remaining 6 hours (**Fig. 3-3a**). Samples were then taken for chromatin fractionation (**Fig. 3-3b**).

In samples depleted of NIPBL alone, roughly a 2-3-fold reduction was observed in chromatin bound cohesin levels compared to the untreated control (**Fig. 3-3c**, lanes 3-4 vs. 5-6.). This is in line with observations from other NIPBL knock down experiments where cohesin association with chromatin is also reduced (Alonso-Gil et al., 2023; Haarhuis et al., 2017; Schwarzer et al., 2017). The reduction in cohesin levels on DNA, however, was less strong than expected with a full knock out NIPBL degron, possibly due to the short length of time for which NIPBL was depleted. Alternatively, this could indicate that the cohesin remaining on DNA by late G1 was no longer sensitive to WAPL release. It has been demonstrated that acetylated cohesin in G1 favours a PDS5-bound state and that PDS5-bound cohesin produces stabilised long-lived loops, which are now refractory to WAPL due to their acetylation (van

Ruiten et al., 2022; Wutz et al., 2020). Follow up experiments co-depleting both PDS5 and NIPBL in G1 could reveal whether the remaining population of cohesin is lost from DNA.

Depletion of WAPL alone lead to a 1.5-2-fold increase of cohesin on DNA compared to untreated cells (**Fig. 3-3c**, lanes 3-4 vs. 7-8), which is in line with observations in other WAPL depletion experiments (Kueng et al., 2006; Liu et al., 2021; Tedeschi et al., 2013).

In the co-depleted sample where WAPL is depleted 2 hours in advance of NIPBL, cohesin is presumably allowed to accumulate on DNA in advance of depleting the loading factor and thus chromatin-bound cohesin levels are mildly elevated compared to the NIPBL depleted cells alone, although the effect is minor (**Fig. 3-3c**, lanes 5-6 vs. 9-10).

It is worth noting that tests depleting both NIPBL and WAPL simultaneously, showed no recovery of cohesin levels beyond that of NIPBL depletion alone. This suggests that NIPBL loading is the main driving force of cohesin loading on DNA in G1, and that the release pathway is superfluous if there is no loading occurring in the first place. WAPL therefore was depleted prior to NIPBL depletion in order to achieve a small increase in the levels of cohesin on DNA before turnover was stopped. A population of cohesin can therefore be loaded onto DNA in G1 before turnover is halted by depleting both NIPBL and WAPL.

NIPBL is not strictly required to build cohesion during S phase

Previously, we were unable to ask whether NIPBL is directly required to build cohesion during S phase, as we always had the compounding factor of WAPL releasing cohesin from DNA. As shown previously in Figure 3-3, if we first deplete WAPL to hyper load cohesin on DNA, and then deplete NIPBL to stop all turnover, this leaves a portion of cohesin bound to DNA prior to S phase. Now we can ask whether NIPBL is required during S phase to actively build

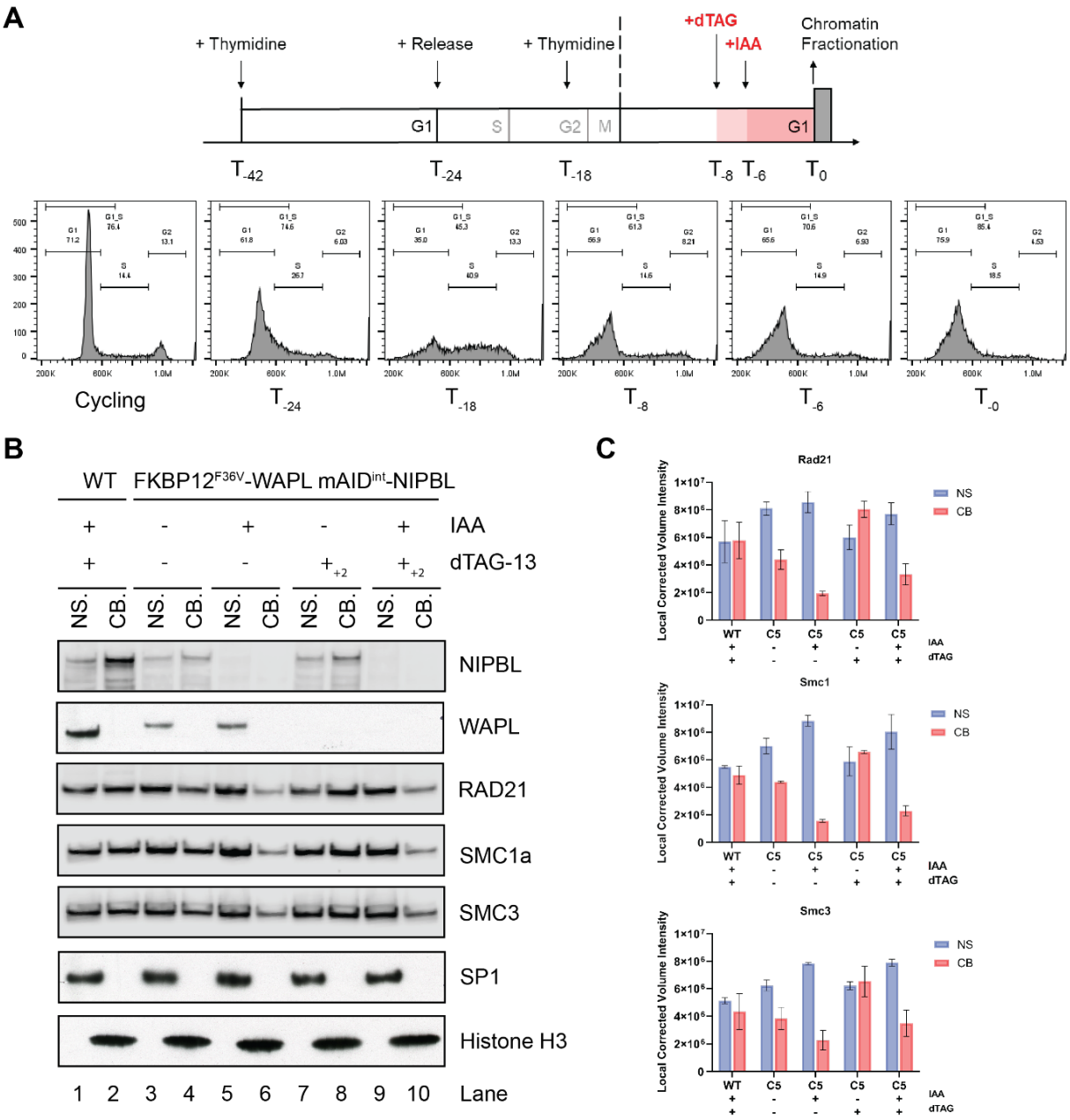

Figure 3-3. Cohesin can be loaded onto chromatin before turnover is paused. (A) Experiment schematic of a double thymidine block with WAPL depletion at T_{-8} ahead of NIPBL depletion at T_{-6}. Cell cycle profile is made using FACS with Propidium iodide staining showing arrest at major experiment time points. **(B)** Representative immunoblot of chromatin fractionation of nuclear soluble (NS) vs. chromatin-bound (CB) fraction. SP1 serves as control for NS fraction and H3 as a control for the CB fraction. **(C)** Quantification of chromatin fractionation using local background corrected band volume normalised against the loading controls for NS and CB fractions, shown for RAD21, SMC1 and SMC3, n=2.

cohesion, or whether the cohesin that has been loaded pre-replication is sufficient, even in the absence of NIPBL, to build cohesion via a "conversion" pathway.

To test this, a similar cohesion experiment was run to the single NIPBL depletion of Figure 3-1, however WAPL was co-depleted to stop turnover. The same cell synchronisation protocol was run as in Figure 3-3 with a double thymidine block and WAPL and NIPBL depleted 8 and 6 hours prior to the end of G1/S, respectively. This time cells were released from the double thymidine block and allowed to pass through S phase in the continued absence of NIPBL and WAPL, and progress to mitosis where they were collected for chromosome spreads where sister chromatid cohesion could be analysed (**Fig. 3-4a**).

Remarkably, when cells were allowed to progress through S phase in the absence of both NIPBL and WAPL (**Fig. 3-4b**), we observed a WT levels of cohesion and no observable difference between the treated and the untreated cells (**Fig. 3-4c**). The progression of cells through S phase in both the absense of NIPBL and WAPL, suggests that cohesin pre-loaded onto chromatin and prevented from turning over, was sufficient to build WT cohesion and could be "converted" into cohesive cohesin during DNA replication. This suggests that "conversion" is a mechanism of cohesion establishment and that NIPBL is not strictly necessary to build cohesion during S phase. It does not however discount the possibility that *de novo* cohesion establishment by NIPBL may happen alongside cohesion establishment by conversion.

A caveat to this experiment is that we presume that the single depletion of NIPBL alone would lead to the mild cohesion defects observed in Figure 3-1, although this experiment was done under a double thymidine block rather than Palbociclib arrest. In order to draw more solid conclusions from this experiment, we would have to repeat the experiment with the single

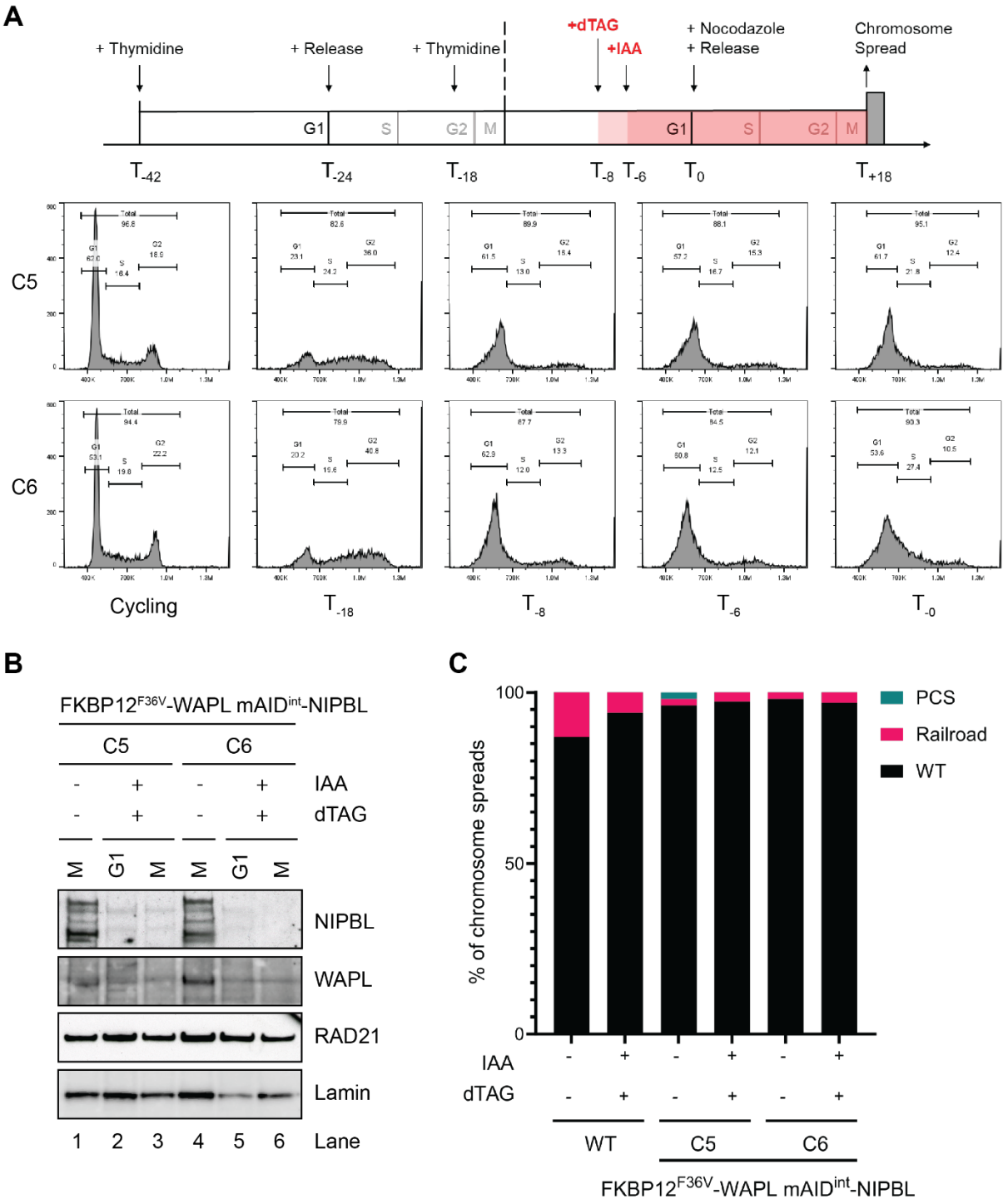

Figure 3-4. Cohesion can be built without NIPBL during S phase. **(A)** Experiment schematic as in Figure 3-3a with release mitosis for chromosome spread collection. Cell cycle profiles generated using FACS with PI staining. **(B)** Immunoblot of the nuclear fraction of cells either in mitosis or at the G1/S arrest at T_0 of experiment outlined in (A). **(C)** Chromosome spreads of experiment outlined in (A), showing quantification of cohesion phenotypes. Scoring was performed as in Figure 2-11, n >50 spreads.

NIPBL depletion as a key control to see cohesion defects observed are rescued with a WAPL co-depletion. The signal of the control immunoblots could also be improved.

Cohesion maintenance is insensitive to NIPBL in G2

Previous experiments have shown that NIPBL is not required to build cohesion in S phase. If NIPBL can be dispensable from S phase onwards, this already suggests that NIPBL is not required for cohesion maintenance once established. To confirm whether this is the case, we arrested cells in G2 and depleted NIPBL in order to see whether cohesion could be disrupted.

The experiment to deplete NIPBL in G2 was performed concurrently with experiment to deplete NIPBL in G1, outlined in in Figure 3-1. Cells were synchronised in G1 with Palbociclib followed by G2 synchronisation using RO-3306, prior to collecting chromosome spreads in mitosis, and the only difference was the stage at which NIPBL was depleted (**Fig. 3-5a**, compared to Figure 3-1a). In this case, NIPBL was depleted 6 hours before the end of G2 which is termed T_0. Immunoblotting showed NIPBL depletion in the auxin treated cells and also intriguingly revealed a difference in the NIPBL isoforms present in G2 arrested cells compared to cycling cells or even G1 cells (**Fig. 3-5b**, compared to Figure 3-1b).

When chromosomes spreads were taken, we could observe no difference in cohesion between cells depleted of NIPBL in G2 vs. untreated cells, unlike the prolific albeit mild defects we observed when NIPBL was depleted in G1 (**Fig. 3-5c**, compared to Figure 3-1c). This confirms that NIPBL is not required as a maintenance factor for G2.

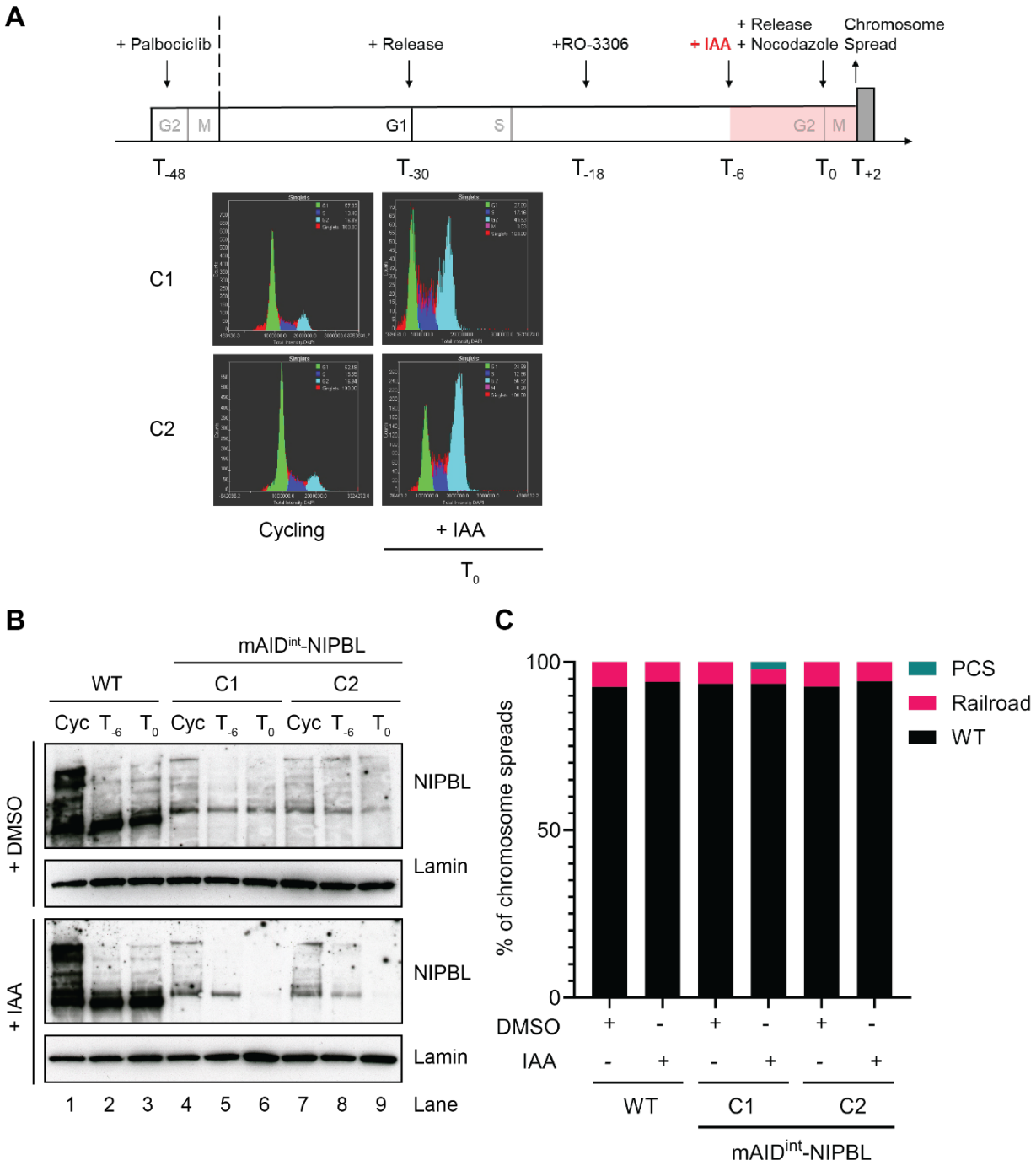

Figure 3-5. NIPBL is not required for cohesion maintenance in G2. (A) Experiment schematic of cell synchronisation in G2 using palbociclib and RO-3306 **(B)** Immunoblot of experiment outlined in (A), blotting for NIPBL and Lamin in cycling cells and cell arrested in G2 at T_{-6} when auxin was added and T_0 at the end of arrest and depletion **(C)** Quantified chromosome spreads of experiment outlined in (A). See Figure 3-1c for comparative NIPBL depletion in G1 control. Scoring performed as in Fig. 2-11, n >40 spreads.

Discussion

Having established that NIPBL was required for cohesion, the aim of this chapter was to determine how NIPBL was required. In this capacity, we asked whether NIPBL was required for cohesion establishment in G1 or S phase. We further asked whether it was required for cohesion maintenance in G2.

Cell cycle synchronisation experiments revealed that NIPBL depletion in G1 lead to significant, albeit mild, cohesion defects in <60% of spreads. This initial observation showed that NIPBL was required in the cohesion establishment process. Early work on the yeast homologue of NIPBL in yeast, had similarly shown that Scc2 inactivation in G1 lead to cohesion defects, as visualised by a GPF split-dot assay where centromere distances could be measured between two sister DNAs (Ciosk et al., 2000).

Although NIPBL is required to establish cohesion, it was unclear whether it was due to its role in cohesin loading in G1 or whether it was actively required during S phase. As cohesin loading is intrinsically linked with cohesin levels on DNA, and cohesin must associate with DNA to build cohesion, we had to uncouple active loading from cohesin levels. To do this we developed a system whereby WAPL, the release factor, could be depleted as well as NIPBL, thereby stopping the release pathway from offloading cohesin.

Indications that WAPL knock down could recover the effects of NIPBL knock down were seen in neurodevelopmental work where there was a modest recovery of developmental defects caused by NIPBL knock down through a lack of genome organisation (Kean et al., 2022; Linares-Saldana et al., 2021). More directly, in a system where SCC2 had been truncated and destabilised, reduced SCC1 levels on DNA could also be partially recovered by the co-

depletion of WAPL (Haarhuis et al., 2017). Together, these findings indicated that WAPL and NIPBL have opposing roles in modulating cohesin dynamics on DNA.

In contrast to these findings however, work in yeast had identified a different relationship between Scc2 and Wapl specifically in G1. Here, even in a Wapl depleted background, Scc2 had to be constitutively active in order to keep cohesin bound to DNA. A Wapl-independent release mechanism was therefore identified which appeared to only be inactivated by the cell cycle transition to S phase by Cdk1 activity (Srinivasan et al., 2019). This finding may also explain the dependency of cohesion establishment on Scc2 during G1 in budding yeast, or Mis4 (an Scc2 homolog) in *S. pombe* (Ciosk et al., 2000; Furuya et al., 1998).

Unlike the behaviour in yeast, co-depletion experiments revealed that we could recover some levels of cohesin on DNA, although we had to deplete WAPL first to abrogate release and allow surplus cohesin association with DNA, before we depleted NIPBL. This recovery was greater than NIPBL depletion alone although not up to the levels found in untreated cells, which suggests that NIPBL is a main driver of cohesin levels on DNA rather than WAPL. The notion that NIPBL's loading rate exceeds WAPL's release rate would be expected if the cohesin levels on DNA must rapidly increase from the exit of mitosis to the end of G1.

The co-depletion of WAPL and NIPBL allowed for cohesin to be loaded onto DNA before turnover was paused. Remarkably, when cells were then allowed to pass through S phase in the continued absence of NIPBL and WAPL, cohesin that had been pre-loaded onto DNA was sufficient to build WT-like cohesion. This work suggests that NIPBL is not strictly required to build cohesion during S phase and provides the first direct evidence in mammalian systems for "conversion" as a method of cohesion establishment on chromosomes. Work in yeast has also demonstrated the ability of a pre-loaded cohesin to build cohesion in the absence of Scc2 during S phase (Srinivasan et al., 2019; Srinivisan et al., 2020). Whilst cohesion can be built in the

absence of NIPBL during S phase, it does not discount the possibility that NIPBL could also build cohesion via a *de novo* pathway.

This results suggests that the co-depletion of WAPL and NIPBL prior to S phase can rescue the cohesion defects observed with NIPBL depletion alone, as in Figure 3-1 when NIPBL was depleted prior to S phase in cells arrested in G1 by Palbociclib. Palbociclib however arrests cells in a true G1 state rather than a G1/S state with a double thymidine block, where it could be argued that some low levels of replication have already occurred. Low levels of replication could lead to low levels of cohesion and might recover cohesion defects alone. Therefore, to make the findings of the co-depletion experiment more robust, it would be critical to repeat this experiment with a single NIPBL depletion control.

If it possible to build cohesion without NIPBL during S phase, this already suggested that NIPBL was not required for the maintenance of cohesin in G2. This was however confirmed with cell cycle synchronisation experiments where depletion in G2 caused no cohesion defects, confirming that once cohesion is established, it is no longer NIPBL dependent. This is in line with what was previously demonstrated in yeast where Scc2 could be depleted during G2 and cohesion was unaffected (Ciosk et al., 2000). It was further observed that synchronisation in G2 vs G1 lead to differences in NIPBL immunoblot bands detected. The same C-terminal NIPBL antibodies have been used in other work to detect minimal NIPBL constructs vs. WT NIPBL (Haarhuis et al., 2017). This suggests that different isoforms of NIPBL may operate between G1 and G2, however further experiments would have to confirm this.

The need for NIPBL during G1 phase but dispensability during S phase suggests that its role in establishing cohesion might be purely based on its role as a cohesin loader. In line with this, whilst depletion of NIPBL in G1 led to prolific cohesion defects, it was observed that the cohesion defects were “mild” in their phenotype, and did not resemble the severe phenotype of

PCS seen in the 24hr asynchronous experiments see in Chapter II Figure 2-11. The mild nature of the defects may be a result of depletion toward the end of G1, which would enable enough cohesin to load prior to NIPBL depletion, that some level of cohesion could be built. This was also seen in the higher than expected levels cohesin on DNA with single NIPBL depletion in Figure 3-3. Cohesin is fully lost from DNA during anaphase, but begins to reload rapidly in telophase as soon as 8 minutes after chromosome segregation once the nuclear envelope starts to reform (Gerlich et al., 2006; Sumara et al., 2000). Therefore, in order to truly see whether NIPBL is required for cohesion establishment purely in its capacity as a cohesin loader during the critical window of Telophase - G1, we had to establish a protocol whereby NIBPL could be depleted before cells exit from mitosis and begin their new cell cycle.

Chapter IV: NIPBL is required for cohesion as cells exit mitosis

Introduction

In previous chapters we saw that NIPBL was essential for cohesion and that its depletion during G1 led to cohesion defects, proving that NIPBL was required for cohesion establishment. The lack of requirement of NIPBL to actively build cohesion during S phase further indicated that NIPBL's main contribution to cohesion establishment was through its role as the cohesin loader during G1.

FRAP studies have previously shown that cohesin reloads onto chromatin before cells have even exited mitosis, with 36% of nuclear cohesin binding chromatin by the time of nuclear reformation in telophase, which is already close to the chromatin bound levels found in G1 (Gerlich et al., 2006). If this is the case, then in order to verify whether NIPBL's role in cohesion establishment is through its role as a cohesin loader, we had to deplete NIPBL prior to mitosis.

Through doing this, we first wanted to assess the levels of cohesin able to bind DNA in the absence of NIPBL when exiting mitosis, and thus determine whether NIPBL is required for cohesin's initial loading onto DNA. Next, we wished to see whether preventing cohesin from loading as cells exit mitosis would recapitulate the severe loss of cohesion we observed in earlier asynchronous experiments. Finally, we wanted to understand how cohesin levels on DNA affected cohesin's ability to build cohesion through observing cohesion defect phenotypes throughout the cell cycle in an unbiased manner. Through these experiment we hoped to identify the critical window in which NIPBL is essential for cohesin loading and ultimately, cohesion establishment.

NIPBL loads cohesin onto DNA from mitotic exit

If NIPBL is the cohesin loading factor, we wanted to verify that depletion prior to the known initial window of loading in telophase would stop cohesin association with DNA. To do this, we used a double thymidine block and depleted NIPBL at the end of the first thymidine block at the G1/S boundary of the previous cell cycle (**Fig. 4-1a**). Previously, we demonstrated that NIPBL fully depletes within 6 hours, therefore we anticipated that depletion at G1/S would be well before the onset of mitosis. Cells were kept in auxin until the end of the second thymidine block at G1/S before they were collected for chromatin fractionation (**Fig. 4-1b**).

Depletion in this manner revealed a dramatic reduction of cohesin on DNA with an average loss of 77.5 ± 5% chromatin-bound cohesin compared to untreated cells (lane 4 vs. 6, lane 8 vs. 10), and 90 ± 1% compared to WT cells (lane 2) (**Fig. 4-1b, c**). The mAID^{int}-NIPBL cell line already has a hypomorphic expression of NIPBL so cohesin levels on DNA are reduced compared to WT. The dramatic reduction demonstrates that NIPBL a key factor required to load cohesin onto DNA, and that its presence as cells exit mitosis is critical.

This experiment cannot however conclude that NIPBL is the sole cohesin loader. Whilst a small population of cohesin remained chromatin-bound in the NIPBL depleted sample, we cannot distinguish whether this was cohesin that was loaded in the absence of NIPBL, or whether this was cohesin that remained on DNA from cells out of phase which were not captured in the cell cycle synchronisation. The latter possibility is likely as a population of cells remained in G1 after the first thymidine release, so may not have cycled through in the appropriate timeframe (**Fig. 4-1a**).

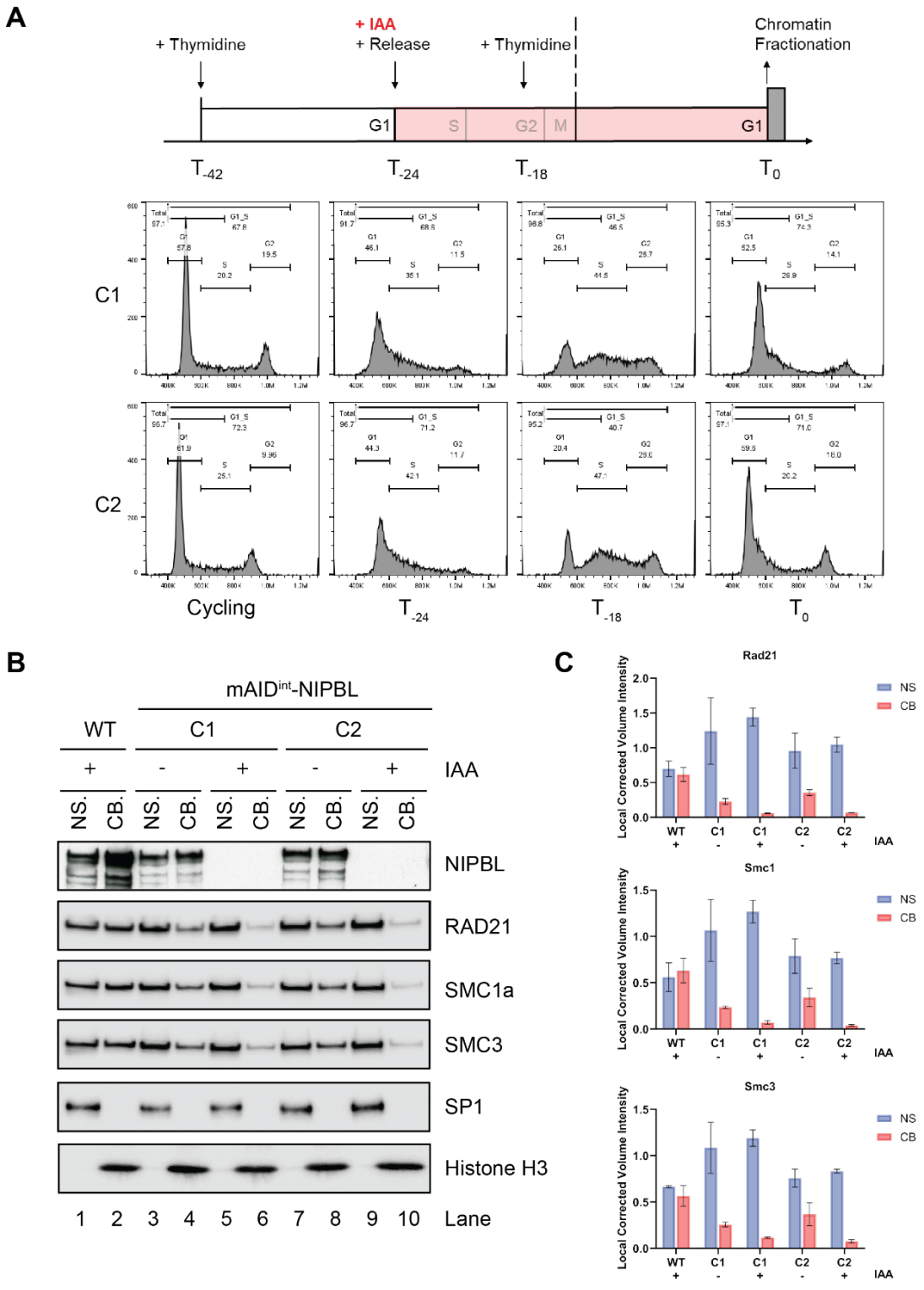

Figure 4-1. NIPBL loads cohesin onto DNA from mitosis. (A) Experiment schematic of NIPBL depletion in G1/S of the prior cell cycle. Cell cycle profile is made using FACS with Propidium iodide. **(B)** Representative immunoblot of chromatin fractionation as in Figure 3-3c, for experiment outline in (A). **(C)** Quantification of chromatin fractionation showing control corrected-local corrected band intensities for NS and CB fractions for major cohesin subunits RAD21, SMC1 and SMC3, n=2.

NIPBL is required for cohesion as cells exit mitosis

If depletion of NIPBL prior to mitosis dramatically reduced cohesin loading onto DNA from the exit of mitosis and onset of G1, we wished to identify whether this loading window was also critical to the cells ability to build cohesion.

Previously, depletion of NIPBL in the final 6 hours of G1 in Figure 3-1 had led to widespread, but mild, cohesion defects. These defects mostly presented themselves as "railroad" phenotypes which were less severe than the "PCS" phenotype largely observed in the 24 hour asynchronous NIPBL depletion of Figure 2-11. In order to reconcile the differences in these phenotypes, we supposed that the milder phenotype might be a result of higher levels of cohesin associated with DNA at the onset of S phase. Indeed, when NIPBL was depleted within the final 6 hours of G1/S, 30% of cohesin remained chromatin bound when compared to WT levels in Figure 3-3.

In order to identify NIPBL's role in cohesion establishment, we therefore wanted to identify the precise cell cycle window in which NIPBL depletion would fully disrupt the cells ability to build cohesion leading to severe cohesion defects. After demonstrating that NIPBL had a profound role in cohesin's initial loading upon the exit from mitosis, we next tested whether NIPBL depletion under these same pre-mitotic conditions would destroy cohesion.

Cells were arrested using a similar protocol as outlined in Figure 4-1. NIPBL was depleted at the G1/S boundary of the first thymidine arrest and depletion was maintained throughout mitosis into the second G1/S boundary using a double thymidine block, before cells were released into Nocodazole to arrest them in mitosis for chromosome spreads (**Fig. 4-2a**).

Depletion of NIPBL prior to mitosis revealed a dramatic loss of cohesion of 88.4 ± 2.8%, with the severe cohesion defect of PCS making up over half of the spreads analysed across both

clones (**Fig. 4-2b**). The severe cohesion defects recapitulated the levels found in the 24hr asynchronous depletion of Figure 2-11. Taken together with the results from the previous chapter, where depletion in G1, S and G2 did not lead to full cohesion loss, this suggests that cohesin loading at the onset of G1 is the critical window in which NIPBL is required to contribute to cohesion establishment.

We acknowledged that whilst depletion over the window prior to mitotic exit did lead to significant cohesion defects, it could be argued that the cause of such defects might be a result of the length of time of NIPBL depletion rather than the cell cycle window. Indeed, here we depleted NIPBL for 24 hours before S phase as opposed to 6 hours previously. This was inherently challenging as the longer you deplete NIPBL for, the earlier in the cell cycle you will be, so the two are inextricably linked. In order to better distinguish between the length of time depleted vs. the cell cycle window, we repeated the experiment but depleted NIPBL only 8 hours later upon the addition of the 2nd thymidine block, so that it would be depleted by early G1 rather than pre-mitosis, but still depleted for an excessive period of time > 18 hours. In these results we found that the rate of PCS reduced dramatically from 60 ± 5% to 31 ± 1 %, even though NIPBL was still depleted for an excessively long time (**Appendix Fig. 2**). This further confirms that NIPBL essential time for building cohesion happens over the period of mitotic exit.

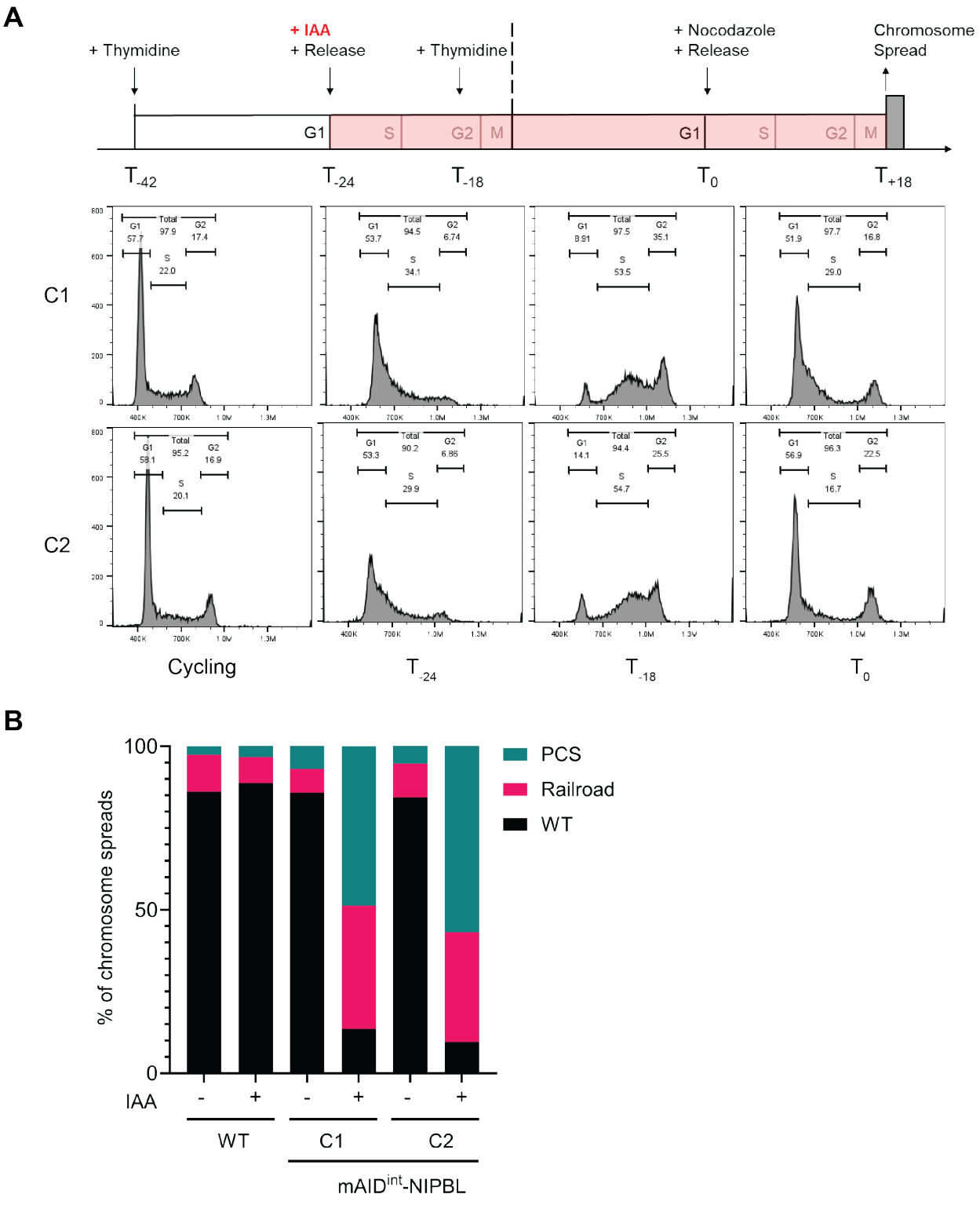

Figure 4-2. NIPBL is essential for cohesion through mitotic exit. (A) Experiment schematic of NIPBL depletion in G1/S of the prior cell cycle as in Fig.4-2a, but allowed to progress to mitosis. Cell cycle profile is made using FACS with Propidium iodide staining **(B)** Quantified cohesion phenotypes of chromosome spreads of experiment outlined in (A). Scoring was performed as in Figure 2-11, n >50 spreads over 2 biological repeats.

NIPBL is essential during a crucial window in the cell cycle to establish cohesion

Through the use of controlled cell cycle synchronisation across one complete cell cycle, we were able to identify a critical window in which NIPBL was essential to load cohesin and build cohesion. Cell cycle synchronisation protocols, however, are inherently stressful to cells, and are also rarely absolute in their synchrony of the whole population. In order to verify our findings of when NIPBL contributes to cohesion establishment and gain a better understanding of the less severe cohesion defect phenotypes, we adapted our approach to use an asynchronous culture in order to minimise the perturbations to cells. By doing this, we wished to see whether we could recapitulate our findings in a system that minimised stress to cells.

In order to circumvent the need for cell cycle synchrony, we developed a new approach to chromosome spreads incorporating EdU staining to mark DNA replication and hence the cell cycle stage of cells in an asynchronous culture. EdU is a thymidine nucleoside analogue which incorporates into the nascently synthesised DNA strand during DNA replication in S phase. EdU is designed with Click-IT chemistry which can be robustly conjugated to a fluorophore and analysed by microscopy (Salic & Mitchison, 2008). EdU is therefore a popular marker for S phase and depending on the staining levels, can differentiate between early, mid and late S phase (Buck et al., 2008). EdU is typically used to pulse label cells 30 minutes prior to fixation to take a snap shot of the population that was in S phase (Flomerfelt & Gress, 2015). We reasoned that if we ran timecourse and instead kept cells continually incubated in EdU, cells in S phase or earlier in the cell cycle (G1 or <M of the previous cell cycle) will eventually be marked positive with EdU as they move through S phase, and cells that are past S phase (G2 or M) upon EdU addition will remain EdU negative.

To test whether EdU Click-IT chemistry could be used as a cellular marker for S phase and combined with chromosome spreads which have been fixed and burst onto glass slides, we added 10μM EdU to asynchronous cells and took chromosome spreads at a short timepoint 2 hours in, and a long timepoint 20 hours in (**Fig. 4-3a**). Even though our bulk sample is asynchronous, through doing chromosome spreads we only observe cells which are mitotic at that timepoint. The cell cycle of U2OS lasts approximately 24 hours, with literature reports anywhere between 22 – 25.6 hrs, with cell to cell variability within a population (Grant et al., 2018; Mahdessian et al., 2021). The length of time in each cycle phase according to phases monitored by the FUCCI imaging system and cell cycle specific proteomic markers demonstrate that G1 is approximately 12 hours, S phase is 8 hours, G2 is 3 hours and Mitosis is 1 hour (Sakaue-Sawano et al., 2008; Zielke & Edgar, 2015). Tests optimising conditions showed that Click-IT chemistry was robust and worked with the chromosome spread fixative. As expected, chromosome spreads at T_2 were negative for EdU signal, as they must have been in M or G2 2 hours prior, thus were past S phase and could not incorporate EdU. Equally, chromosome spreads taken from mitotic cells at T_{20} will have been in S phase or G1 20 hours prior, and thus will have incorporated EdU and were EdU positive (**Fig. 4-3b**).

Observing that chromosome spreads could be EdU labelled, we next wanted to test cohesion over time in cells which are NIPBL depleted. To do this, we used the mAID^{int}-NIPBL cell line and ran a 48 hour timecourse of asynchronous cells depleted of NIPBL, taking chromosome spreads at time points every 6 hours (**Fig. 4-4a**). Auxin was added 4 hours in advance of T_0 to ensure that cells were NIPBL depleted at the start of the experiment (**Fig. 4-4b**). EdU was then added at T_0 to begin marking the cell cycle stage at which cells were depleted of NIPBL.

EdU incorporation over time into chromosome spreads was first assessed to gauge EdU as a marker for cell cycle progression. Cells that had been in late S, mid S, or pre-S (G1/ < M) at

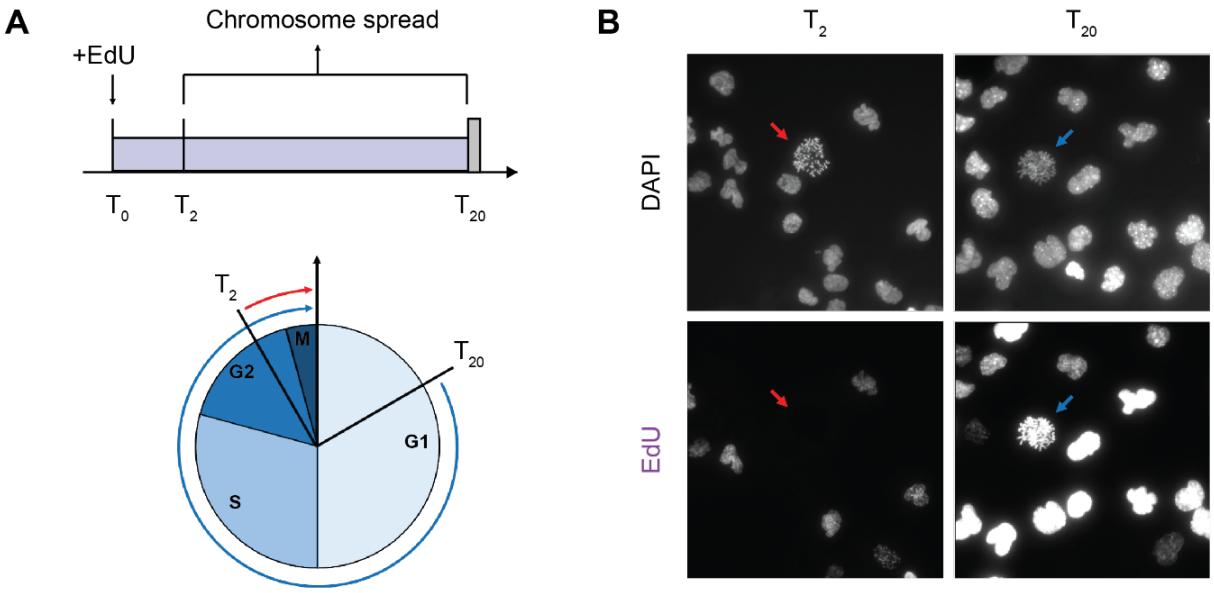

Figure 4-3. Chromosome spreads can be combined with EdU labelling. (A) Experiment schematic of asynchronous timecourse. EdU added at T_0, chromosome spreads taken at T_2 and T_{20}. **(B)** Representative images of chromosome spreads imaged with DAPI and EdU with Alexa 647, showing no EdU signal in chromosome spreads at T_2 (red arrow) and positive EdU signal in chromosome spreads at T_{20} (blue arrow).

T_0 when EdU was added could be clearly differentiated by microscopy depending on the level of EdU incorporation as seen by striation patterns caused by early and late replication regions of the chromosome (**Fig. 4-4c**). EdU incorporation level phenotypes were mapped across the timecourse and appeared to correlate relatively well with the expected cell cycle length of U2OS (**Fig. 4-4d**). It is worth noting there was a slight EdU phenotype delay, namely that late S phase cells peak 6 hours before mitosis, mid S cells peak around 12-18 hours before mitosis and full G1 cells peak around 24 hours before, suggesting that this cell line was taking longer to make its way through one cell cycle.

Next, we analysed chromosome spreads to see whether NIPBL depletion over time in an asynchronous manner would lead to cohesion defects within specific phases of the cell cycle as marked by EdU staining. Interestingly, not only did we observe a clear difference in cohesion defect phenotype but there was a clear emergence of different cohesion defects in different stages of the cell cycle.

Overall, it could be observed that cells treated with auxin had progressively more severe cohesion defects over time compared to the untreated cells (**Fig. 4-4f**). There was a clear switch around the 12-hour mark as cells were in mid S phase where cohesion defects rose from 3.7% to 73% cohesion defect within 6 hours. Cohesion defects become more prevalent as the timecourse progressed until 100% of the spreads analysed had cohesion defects by 48 hours. Furthermore, analysis revealed a previously unobserved cohesion defect phenotype of a "centromeric defect" (**Fig. 4-4e**). Each cohesion defect phenotype appeared to correlate with a particular stage of the cell cycle as marked by EdU (**Fig. 4-4g**). Centromeric defects were the first to appear and peaked around mid-S. This is perhaps why they were previously missed in the G1 cell cycle arrest experiments. Railroads defects appeared next across S and G1 phase, which is in line with the previous observations of G1 depletions in Figure 3-1. Severe cohesion

defects of PCS increased steadily as cells progress through G1 and mitosis into the subsequent cell cycle, which is in line with the observations found in Figure 4-2. These experiments confirm that NIPBL is essential for cohesion establishment, and furthermore, that the cell cycle window in which NIPBL is absolutely required is at the beginning of the cohesion loading cycle around mitosis, after which once cohesin is loaded, NIPBL becomes progressively more dispensable for cohesion, as demonstrated by the reduction in severity of cohesion defects.

Figure 4-4. NIPBL depletion throughout the cell cycle leads to progressively more severe cohesion defects. (A) Experiment schematic of asynchronous timecourse with auxin and EdU addition collecting chromosome spreads every 6 hours. **(B)** Immunoblot of experiment outlined in (A) of WT and mAID^{int}-NIPBL in continuous auxin incubation at specified times. **(C)** Representative images of EdU incorporation level phenotypes which mark the corresponding cell cycle stage. **(D)** Quantification the % of chromosome spreads displaying the EdU incorporation level phenotype over the 48 hour timecourse outlined in (A). Scoring was performed according to (C), n >50. **(E)** Representative images of cohesion defect phenotypes. Centromeric defects are marked by red arrows. WT chromosome phenotype has unresolved arms due to the lack of Nocodazole in the experiment **(F)** Quantified chromosome spreads of cohesion defects with time. Scoring performed according to phenotypes illustrated in (E). EdU positive chromosome spreads levels marked in purple and include late S, mid S and G1/M as in (C), n >50 spreads. **(G)** Cohesion defect phenotype marked against cell cycle stage as defined by EdU incorporation level as shown in (D).

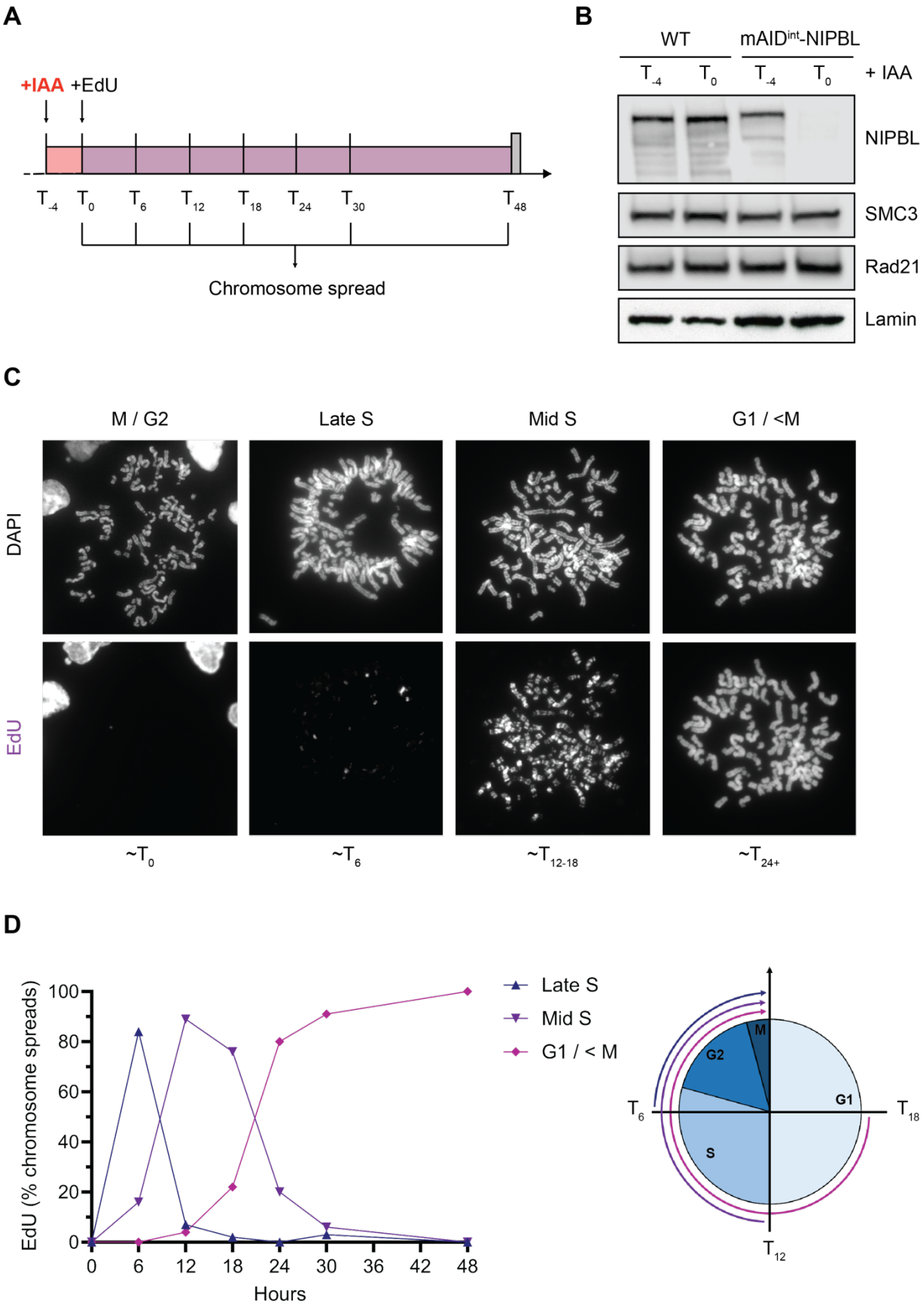
A
+IAA +EdU
T-4 T0 T6 T12 T18 T24 T30 T48
Chromosome spread
B
WT
mAIDint-NIPBL
T-4 T0 T-4 T0 + IAA
NIPBL
SMC3
Rad21
Lamin
C
M / G2
Late S
Mid S
G1 / <M
DAPI
EdU
~T0
~T6
~T12-18
~T24+
D
EdU (% chromosome spreads)
100
80
60
40
20
0
0 6 12 18 24 30 36 42 48
Hours
Late S
Mid S
G1 / < M
M
G2
G1
S
T6
T18
T12

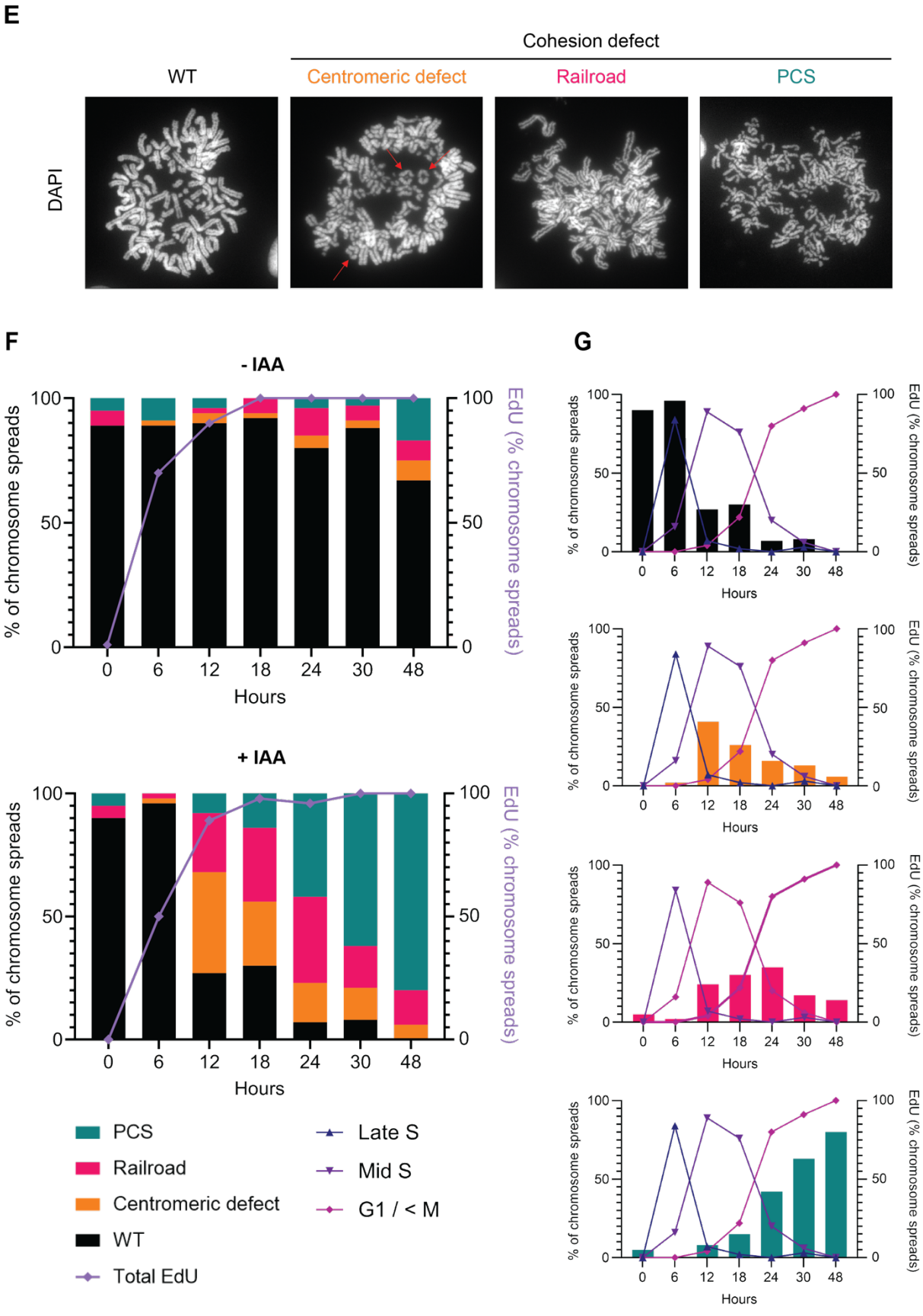
E
Cohesion defect
WT
Centromeric defect
Railroad
PCS
DAPI
F
- IAA
+ IAA
% of chromosome spreads
EdU (% chromosome spreads)
Hours
PCS
Railroad
Centromeric defect
WT
Total EdU
Late S
Mid S
G1 / < M
G

Discussion

In chapter II, we established that cohesion was essential, and in chapter III, we proposed that NIPBL was only required for cohesion establishment, and that its contribution was purely as a cohesin loader. Throughout this chapter we sought to describe the sequence of events that builds cohesion throughout the cell cycle.

Cohesion is established during S phase, and maintained throughout G2 until mitosis. We demonstrated in chapter III that NIPBL was not required to maintain cohesion over this time. Cohesin is destroyed by separase in mitosis during anaphase and chromosomes are segregated equally to two daughter cells. APC/C levels drop rapidly after anaphase and separase becomes inactive, hence new cohesin is loaded onto DNA upon the reformation of the nuclear envelope during telophase. We therefore wanted to see whether this window toward the end of mitosis was when NIPBL was critical for cohesin loading and cohesion establishment.

Experiments depleting NIPBL prior to exit from mitosis showed a dramatic dependency on NIPBL for cohesin loading over this time. More significantly, depletion over this time also lead to catastrophic cohesion defects in the majority of cells analysed, demonstrating that the low cohesin levels directly lead to an inability to build cohesion. Depletion of NIPBL just after this window post-mitosis still led to cohesion defects, however not as severely as prior to mitosis, presumably as a population of cohesin had already been loaded and we have demonstrated in prior experiments that cohesin loaded onto DNA can be converted into cohesion. This confirmed that telophase is the critical window in which NIPBL is required to build cohesion.

These findings were finally corroborated with a parallel approach using asynchronous cells where the cell cycle was not perturbed. Here, we found a clear trend that cohesion defects were more severe the earlier in the cell cycle that NIPBL was depleted .

It has previously been unknown whether phenotypes of cohesion defects were a product of cohesin levels on DNA. Interestingly, an insight into cohesion deposition could be gained here, as we first saw the emergence of a centromere specific defect in cells were NIPBL was depleted around S phase. The centromere is where spindle attachment occurs and it this is where the greatest biorientation forces will be applied to the chromosomes. One possibility is that depletion of NIPBL during S phase was late enough that a low level of cohesion globally was enough to withstands opposing forces along the chromosome arms, but not enough to withstand the force of the mitotic spindle at the centromere. An alternative rationale for this phenotype could be the highly heterochromatic nature of the centromere which makes it a late replicating region. If NIPBL was removed during S phase, it is possible that cohesion was established in a locus specific manner, occurring first in early replicating regions, but unable to occur once NIPBL was removed at late replicating regions. Antibody staining of centromeric proteins on chromosome spreads would help identify the position of the centromeres and confirm whether there is a correlation between EdU banding patterning (showing late and early replicating regions based on EdU incorporation, centromere locus and lack of cohesion.

Moving to earlier in the cell cycle, in cells where NIPBL was depleted in G1, the levels of cohesion reduced further leading to the highest levels of the railroad phenotype characterised by the parallel attachment of the sister chromatids. Moving earlier again, cells which been depleted of NIPBL in mitosis or in the previous cell cycle had increasing incidences of the severe phenotype of PCS showing total cohesion loss. PCS levels continued to increase the earlier in the cell cycle that NIPBL was depleted, presumably because cohesin was prevented from loading as cells exited mitosis.

Results from this and prior chapters therefore reveal two principles; firstly, that if cohesin is loaded onto DNA, cells will by default build cohesion without strictly requiring NIPBL; and

secondly, that the more cohesin there is on DNA, the more cohesion there will be along the chromosomes. The predominant window in which NIPBL is required for cohesion establishment therefore is as cells exit mitosis during telophase, after which the cell's dependency on NIPBL to build cohesion becomes less important, as long as there is cohesin loaded onto DNA.

Chapter V: Conclusions and Future Directions

NIPBL as an essential protein

In yeast, Scc2 is essential and required for life (Ciosk et al., 2000). Equally in humans the NIPBL gene is essential, as discovered through unsuccessful attempts to deplete NIPBL in human HAP1 (Haarhuis et al., 2017). Why then, was NIPBL deemed potentially non-essential in mammalian systems? Despite NIPBL's known vital roles associating cohesin with DNA and activating its ATPase, knock down studies in mammalian cells had never been able to show that NIPBL was essential for life. Typically, a certain threshold of essential protein is required to remain in the cell in order to do its function, so knock-down behaves like knock-out. Using this principle then, it was suggested that perhaps mammalian cells, which have extra regulatory proteins elsewhere in the cohesion cycle, had developed another system of cohesin loading that was NIPBL independent. Indeed, *in vitro* studies have shown that cohesin is able to topologically load onto DNA in the absence of Scc2, albeit at a much lower level than with Scc2 stimulation (Collier et al., 2020; Murayama & Uhlmann, 2014). Perhaps then, alongside NIPBL loading, cohesin can be independently recruited to DNA and thus when DNA replication takes place, enough cohesin is present still to build WT-like cohesion. In this instance, cohesion would be unaffected but chromatin architecture formed by loop extrusion which requires active ATP hydrolysis by NIPBL would be lost. This model fitted well with the data seen across various experimental results observed (Alonso-Gil et al., 2023; Mitter et al., 2020; Schwarzer et al., 2017).

An alternative possibility was instead that NIPBL was an extremely efficient protein, and that knock down of the protein was not equivalent to knock out. Evidence for this came from the observation in microscopy studies that NIPBL was a highly substoichiometric protein to cohesin, and that it was able to transiently interact with cohesin molecules on the scale of seconds, as opposed to the cohesin residency time of minutes, meaning that NIPBL could hop

between cohesive complexes (Rhodes et al., 2017). If cohesin loading was a singular event, requiring 1 round of ATP hydrolysis, this would also be much more efficiently achieved than loop extrusion that requires constant ATP hydrolysis and continuous NIPBL binding. Low levels of NIPBL would therefore be able to load some cohesin onto DNA, even if they were unable to achieve much loop extrusion. It was previously showed that only a very small amount of cohesin needs to be loaded onto DNA in order for cohesion to be built (Heidinger-Pauli et al., 2010). It is therefore equally possible, that low levels of NIPBL remaining would be sufficient to load low levels of cohesin which would be sufficient to build cohesion. If cohesin's ability to build cohesion is fundamental to life, rather than its ability to loop extrude, then cells would survive.

The previous NIPBL degron publish had targeted NIPBL at the N-terminus. When NIPBL was then degraded through this method which should be complete, even though protein levels were below the level of immunoblot detection, the cells still survived and had WT cohesion (Jan Michael Peters – Personal Communication). Analysis of NIPBL's various isoforms (which can be seen clearly with immunoblots) revealed that this form of tagging would leave some predicted isoforms untagged. Indeed, when cells were analysed by mass spectrometry, it was seen that some protein remained.

Targeting the protein through an internal degron tag demonstrated that all isoforms of NIPBL could be depleted as seen by the major NIPBL band disappearance, as well as the banding patterns below. Depletion of NIPBL using this internal mAID^{int}-NIPBL degron demonstrated for the first time in mammalian cells that NIPBL was essential, and that cells cannot grow and die in NIPBL's absence.

We can therefore draw two conclusions from this first piece of work. Firstly, that NIPBL is essential in mammals, just as Scc2 is essential in yeast. Secondly, that NIPBL is an extremely

efficient protein, and that trace amounts of the protein are sufficient to load cohesin on DNA, and facilitate cohesion.

Last week a pre-print was published where a N-terminal dTAG-NIPBL degron was developed (Hansen et al., 2024). Here, they again found that cells were viable but equally that > 10% of the original protein expression remained after depletion. This was enough to support life, but not enough to promote correct chromatin architecture and gene expression. This corroborates my findings that small amounts of NIPBL may be sufficient to support life, and that cohesion will be established in preference to loop extrusion, probably as a result of the different stoichiometric and temporal requirements of NIPBL of each activity.

NIPBL's role in cohesion loading

NIPBL's role in associating cohesin with DNA is well established, as NIPBL associates cohesin with DNA *in vitro* (Murayama & Uhlmann, 2014), *in vivo* (Hu et al., 2015; Srinivasan et al., 2019), and has many chromatin binding partners for recruitment (Linares-Saldana et al., 2021; Mattingly et al., 2022; Muñoz et al., 2019). Our observations of NIPBL knockdown, both pre-mitosis and at the end of G1, showed a reduction in chromatin-bound cohesin levels as determined by chromatin fractionation. This is line with observations from the Losada, Gerlich and Rowland labs, where knock down's of NIPBL either through degradation tools or destabilisation universally showed a reduction in chromatin-bound SCC1 levels (Alonso-Gil et al., 2023; Haarhuis et al., 2017; Schwarzer et al., 2017).

Surprisingly, depletion in the final 6 hours of G1 had less of a dramatic effect on cohesin levels on DNA than initially expected. This is in contrast to yeast where Scc2 was shown to be essential for cohesin association with DNA in G1, even if the WAPL release pathway was

abrogated (Srinivasan et al., 2019). One explanation for this could be the relatively short depletion time (compared to pre-mitosis depletion). Immunoblots however show the majority of NIPBL is depleted within 2 hours, therefore 6 hours depletion should be in excess, especially if cohesin has a typical residency time on DNA of ~22 minutes (Hansen et al., 2017). By the end of G1 is likely that cohesin turnover is stabilised, as studies using fluoresence recovery after photobleaching (FRAP) showed chromatin-bound cohesin levels reach near-G1 levels already by the end of telophase (Gerlich et al., 2006). Whilst the effects of NIPBL depletion may therefore be more modest by this point, they should still be able to affect cohesin within its average turnover time. This then brings into question whether there is another factor stabilising cohesin on DNA, making it WAPL resistant. Work in the last few years exploring the acetylation activity of Esco1 in G1 might provide an explanation for the body of cohesin remaining. It was observed that some chromatin loops in G1 are established for a much longer period (hours) rather than the usual cohesin turnover (minutes) (Wutz et al., 2020). These loops appear to be dependent on the acetylation activity by Esco1, which stabilises a STAG1 and PDS5-bound version of cohesin at CTCF loops (Bastié et al., 2022; Dauban et al., 2020; van Ruiten et al., 2022). PDS5 displaces NIPBL in these complexes and halts further loop extrusion. It is therefore possible that the modest effects of NIPBL depletion in late G1 are the result of a body of cohesin which is already stabilised and NIPBL / WAPL independent. It would be very interesting to co-deplete PDS5 with NIPBL to see if the remaining cohesin is then lost from DNA in G1.

Depletion of NIPBL prior to mitosis aimed to prevent cohesin-reloading at the very start of the cell cycle, before the window of major cohesin reloading in telophase. Thus, we hoped to prevent even the initial association of cohesin with DNA, and determine whether NIPBL is the sole cohesin loader. This had also been a topic of recent debate in the field as knockdown of

NIPBL using siRNA had shown cell survival, WT cohesion and an increase in STAG1 expression as compensation (Alonso-Gil et al., 2023; Alonso-Gil & Losada, 2023). This had led to the proposal that cohesin could associate with DNA independently from NIPBL using STAG1 which also has a DNA binding site, with NIPBL then aiding cohesin's subsequent translocation. Indeed, background levels of cohesin entrapment are always seen in *in vitro* work, however they are stimulated by the addition of Scc2 (Collier et al., 2020; Collier & Nasmyth, 2022; Murayama & Uhlmann, 2014).

In our experiments depleting NIPBL prior to mitosis, we saw a dramatic reduction in cohesin levels on DNA, showing that NIPBL has a major role in promoting DNA association. There was, however, a small body of cohesin that was chromatin bound, therefore we cannot conclude that NIPBL is the sole method by which cohesin can load. Some practical caveats for this exist however; we saw that the level of chromatin-bound cohesin remaining was not functionally enough to build cohesion, as seen by the major cohesion defects observed when NIPBL was depleted and taken for chromosome spreads under the same conditions. We also observed that cells die without NIPBL and huge aneuploidy is seen within 24 hours of depletion, suggesting that whilst there may be some cohesin able to bind, it is not to a level able to support life. None of these observations were previously possible with other NIPBL knock-down technologies, suggesting that the levels of depletion previously tested were not sufficient. Taken together, it is therefore highly likely that NIPBL is the sole cohesin loader, in order to load <u>functional</u> levels of cohesin onto DNA.

In future work, alternative higher sensitivity techniques will be needed to finally assess whether NIPBL is the sole cohesin loader. Firstly, it must be noted that our cell cycle synchronisation methods were not absolute, synchronising most, but not all of the population. If NIPBL was depleted in out of synch cells in late G1-G2, we would expect some cohesin to remain bound.

Whilst the cell cycle synchronisations were sufficient for cohesion experiments where a proportional change was still indicative of a defect, in the case of the absolute question of whether NIPBL is the sole cohesin loader or not, a more robust method is required. To achieve a more accurate cell synchrony as cell exit mitosis, a mitotic shakeoff could be used. This method however yields very low cell numbers, therefore it would be best combined with techniques that require smaller sample sizes such as IF with pre-extraction to look at chromatin-bound cohesin levels on DNA. Alternatively, with further fluorophore tagging, live cell imaging methods such as FRAP or single molecule tracking could be used to study the chromatin bound / unbound populations of cohesin (see end of discussion). Whilst both IF and chromatin fractionation are useful methods for quantifying protein levels changes, they are not the superlative technique available for quantifying protein levels on DNA. Ideally, a better approach would be to use a calibrated technique such as calibrated ChIP-sequencing to look at absolute levels of cohesin on DNA. This approach however is a bulk assay requiring a lot of sample material, therefore would also be limited by cell synchronisation protocols.

NIPBL's role in cohesion:

1. G1

NIPBL's role in cohesion has remained largely unstudied without the ability to deplete NIPBL acutely throughout the cell cycle, yet it was demonstrated over 20 years ago in yeast that Scc2 was essential for cohesion. It had previously been shown using temperature sensitive mutants that depletion of Scc2 in G1 disrupted sister chromatid cohesion but depletion in G2 did not (Ciosk et al., 2000). These findings were recapitulated in my depletion studies in human cells,

demonstrating that NIPBL is required for the establishment of cohesion but not its maintenance once establishment.

Experiments depleting NIPBL in the final 6 hours of G1 showed significant levels of cohesion defects, albeit mild, and demonstrated that cohesin was required for cohesion establishment - a finding that corroborated in yeast (Ciosk et al., 2000). The question for both, however, remained whether this was a product of NIPBL's role as the cohesin loader, or whether NIPBL was required to directly build cohesion during DNA replication in S phase.

2. Conversion cohesion establishment

To be able to differentiate between these two dependencies, one must somehow separate initial cohesin loading in G1, from fresh loading that could build cohesion in S phase. This was attempted in yeast, using the temperature sensitive Scc2 mutant but changing the arrest cycle so that after arrest in G1 with α- factor, cells were further arrested using the early S phase inhibitor, hydroxyurea (HU) (Lengronne et al., 2006). Between G1 and early S, cells were grown in either permissive or non-permissive temperatures. At early S, the cells that had been grown at permissive temperatures were shifted to non-permissive temperatures as the cells were released through S phase. This ensured that cohesin had been allowed to load throughout G1 prior to Scc2 depletion in S phase. They found that loaded cohesin could build cohesion, albeit not at the level of cells grown in permissible temperatures, and that Scc2 was not required during S phase. Furthermore, they checked that cohesin was not re-loaded in an Scc2 independent manner by depleting Scc2 and then the re-expression a new HA-SCC1 under a GAL promoter. In the absence of Scc2 in S phase, the newly expressed cohesin could not be loaded (Lengronne et al., 2006), therefore the cohesion built was from pre-loaded cohesin. Whilst this experiment supposedly proved that loaded cohesin could be converted into cohesive cohesin, it was later challenged by a similar set of experiments which played with HU arrest

(Nasmyth, 2017). Here, it was found that Scc2 depleted in S phase after 45 minutes HU incubation could not build cohesion, whereas depletion after 90 minutes HU could (as seen in Lengronne et al.,). The difference was that extended HU incubation still allowed some replication to take place, which was confirmed by assessing acetylation levels across the two incubation timepoints. It was argued that cohesion built from background DNA replication during the extended HU incubation accounted for the phenotypes seen, and that Scc2 was in fact essential during S phase to build cohesion.

Whilst in conflict, both of these experiments had the confounding variable of active WAPL release. Therefore, when Scc2 was inactivated, the balance would shift toward an unloaded state, making the observation of conversion very challenging. Furthermore, it was later discovered that cohesin loading in G1 was Scc2 dependent, even in a WAPL depleted background. This WAPL-independent release pathway has yet to be fully understood, however it answering this question in yeast very challenging (Srinivasan et al., 2019). The Srinivasan lab did manage to overcome this dependency through the development of a system where cohesin could be loaded in the prior cell cycle and kept topologically bound throughout DNA replication of the next (Srinivisan et al., 2020). It was elegantly demonstrated here that pre-loaded cohesin could build cohesion in the absence of Scc2, and further revealed this dependency on a number of replication fork associated factors.

In mammalian cells, we did not find the same NIPBL dependency for loading in G1, therefore we were able to deplete the WAPL release factor, and then NIPBL in order to leave a population of cohesin bound to DNA prior to S. We then asked whether this pre-loaded (and non-turning over) cohesin could build cohesion during S phase, even in the absence of NIPBL. Here, we found a complete recovery of cohesion to WT levels, showing that NIPBL was not technically required during S phase to build cohesion and that as long as there was cohesin loaded, it could

be build cohesion. This is line with one other observation in mammalian cells, where cohesin associated with DNA prior to the replication fork, remained associated after its passage, in cells where turnover was stopped with WAPL depletion (Rhodes et al., 2017). These microscopy studies could not however determine whether this cohesin was holding cohesion. With our direct visualisation of cohesion using chromosome spread this is the first time we have been able to detect conversion in mammalian cells.

Critical to this experiment, was the principle that cohesin turnover had been stopped. Prior evidence has shown that depletion of WAPL stops cohesin turnover (Haarhuis et al., 2017; Kueng et al., 2006; Rhodes et al., 2017; Tedeschi et al., 2013). We observed the same phenotype of increased cohesin loading upon WAPL depletion compared to WT cells. In these cells we attempted to observe vermicelli, but due to the haploinsufficiency of NIPBL in our cell line it's likely that not enough cohesin could be extruded to give the full phenotype. Similar studies of WAPL depletion showed that if a destabilised NIPBL was used, vermicelli could not be observed (Haarhuis et al., 2017). Ideally, we would use FRAP to monitor cohesin turnover. FRAP requires fluorophores for live cell imaging however, so we have to further tag a unit of the cohesin complex to track this.

3. *De novo* cohesion establishment

Our experiments exploring the conversion pathway do not exclude the possibility that a *de novo* mechanism for cohesion establishment could be happing also. In yeast, it was found that there was redundancy in the existence of both pathways concurrently (Srinivisan et al., 2020). There is good evidence for the possibility of *de novo* loading, as in *Xenopus* egg extracts Scc2 is recruited to licensed replication forks via Scc4 through its interaction with the Cdc7-Dbf4 kinase, and shown to load cohesin ahead of the replication fork (Gillespie & Hirano, 2004; Takahashi et al., 2004).To explore the possibility of *de novo* loading in mammalian cells, a

simple follow up experiment could be performed using the mAID degron. NIPBL could be depleted pre-mitosis, as shown before until the G/1 boundary using thymidine arrest. NIPBL would then be allowed to re-express as cells are release through G1/S into S phase. This prevent cohesin from loading during G1, and only allow loading during S phase.

4. G2

The finding that NIPBL is dispensable in G2 for cohesion, shows that NIBL is not required for cohesion maintenance which fits into our current understanding of cohesive complexes. Once cohesion is established, acetylated cohesin complexes bind both sororin and PDS5 until mitosis (Lafont et al., 2010; Nishiyama et al., 2010). PDS5 has been shown to bind cohesin in a manner that is mutually exclusive with NIPBL, suggesting that the cohesin complex can only bind to one of these HAWKs at a time (Kikuchi et al., 2016; Petela et al., 2018). The mutual exclusivity of these complexes is unsurprising as these HAWKs have generally opposing regulatory roles. NIPBL forms part of the loading complex and PDS5 forms part of the release complex. Furthermore, chromatin loops that extend in size through loop extrusion when bound to NIPBL, are opposed by PDS5 which inhibits loop extension (Bastié et al., 2022). NIPBL is an ATPase activator, yet PDS5 has no ATPase activity (Bastié et al., 2022; Petela et al., 2018). If it is the case that NIPBL and PDS5 bind cohesin in a mutually exclusive manner, it follows that cohesive complexes bound to PDS5 would most likely not bind NIPBL, and hence NIPBL was unlikely to have a role in maintaining the cohesin complexes when formed. A Hi-C technique was developed called Sister-chromatid-sensitive Hi-C (scs-Hi-C) which could distinguish crosslinks between sister chromatids (*trans*) vs. within a chromatid (*cis*) using 4-thio-thymidine (4sT) labelling, and hence distinguish between cohesive and loop extruding cohesin (Mitter et al., 2020). Using this technique, it was shown that in G2 that both *trans* and *cis* chromatid

contacts exist, and only *cis* contacts are lost when NIPBL is knocked-down, suggesting that NIPBL has a role as a loop extruding complexes but not cohesion maintenance.

5. Pre-Mitosis

The observation that NIPBL was required for cohesion establishment, but not directly required during S phase to build cohesion, suggested that NIPBL's main contribution to cohesion establishment was through its role as a cohesin loader. It was hypothesised then that if NIPBL's role is mostly as a cohesin loader, then depletion of NIPBL prior to cohesin's major re-loading in telophase would have the greatest effect on cohesion. Subsequent depletion experiments using both synchronous and asynchronous conditions confirmed that cohesin struggled to load onto DNA, and consequently the cell has catastrophic cohesion defects.

What was also interesting to observe, was the fact that cohesion defects became less severe the later in G1 cohesin was that NIPBL depleted. This presumably is because of higher levels of cohesin on DNA. As was established from the conversion experiments, if cohesin is loaded onto DNA, the default is that it will build cohesion, even in the absence of NIPBL. Higher levels of cohesin on DNA would lead to more cohesion. This could explain the phenotypes observed. In the case of cells, the PCS phenotype, there is a total lack of cohesion and the sisters are fully separate. In the case of the railroad phenotype, it is likely that there is a very low level of cohesion, which enables the sisters to remain roughly parallel, although the levels of cohesion are unlikely to withstand the spindle microtubule forces and are therefore classed as a cohesion defect. Finally, the newest observed phenotype of centromeric defects, suggests a third tier of cohesin loading where yet more cohesion is built, holding sister chromatids mostly together, aside from the centromere where the greatest spindle pulling forces are experienced. This suggests a linear relationship between cohesin levels and the levels of cohesion built.

Studying NIPBL and cohesin dynamics

In this thesis we have purely explored NIPBL's role in loading and cohesion. Our learnings however suggest on a cellular level that cohesin that is loaded will prioritise building cohesion, with loop extrusion coming secondarily, as evidenced by knock-downs which lose chromatin looping first but not cohesion. This is likely due to the active nature of loop extrusion which requires constitutive NIPBL binding in a 1:1 stoichiometry, and thus requires more molecules of NIPBL, rather than loading which could be a singular event, and cohesion establishment which is definitely a singular event.

Taking these thoughts into account, we must consider what cohesin bound to DNA in G1 is doing prior to cohesion establishment. NIPBL stimulates cohesin's ATPase and thus promotes topological entrapment and / or loop extrusion. Cohesin might be topologically loaded onto a single DNA, a process that requires ATP hydrolysis and NIPBL once to load, but should remain passive and no longer need NIPBL until removed by WAPL/PDS5. In the case of cohesion establishment, it would seem that topological loading onto a single DNA would ensure the highest levels of cohesin ready for cohesion establishment. Alternatively, it has been suggested that all cohesin associated with DNA in G1 is loop extruding (Alonso-Gil & Losada, 2023). If the latter were the case, low levels of NIPBL from knock-down experiments would drastically limit the number of cohesin molecules on DNA if they could only have a 1:1 association with NIPBL, and thus we would have to query whether enough cohesin would be associated with DNA to achieve WT-like cohesion. Microscopy evidence indeed shows that NIPBL hops between cohesin molecules in a "spinning plate" model (Rhodes et al., 2017). It is possible that loops are partially extruded in bursts when NIPBL binds and releases which would allow some NIPBL redundancy.

In order to understand NIPBL as a processivity factor, it would be interesting to use other approaches such as FRAP to investigate cohesin binding dynamics (Gerlich et al., 2006; Rhodes et al., 2017). To this end, a mAID^{int}-NIPBL RAD21-T7-Halo (Heterozygous) cell line was generated, so that cohesin could be imaged in live cells (**Appendix Figure 3**). Future work using this cell line could use FRAP to investigate the proportion of bound / unbound cohesin on DNA. Similarly to FRAP, single molecule tracking could be used to determine the residency time of cohesin molecules to assess the populations of cohesin that are affected as NIPBL is depleted in different stages of the cell cycle. This would provide insight into NIPBL's role as a loader and cohesin loop extrusion dynamics. In future work it would also be interesting to study cohesin dynamics in the context of PDS5 as well as NIPBL, which has been shown to halt loop extrusion during G1 and stabilise chromatin loops .

Closing statement

This body of work has aimed to elucidate NIPBL's role in building and maintaining cohesion across the cell cycle in mammalian cells. Through developing a tool which could conditionally deplete NIPBL in a rapid and complete manner, we were able to demonstrate that NIPBL is an essential protein in mammals. We were able to use this system to identify a role for NIPBL in cohesion establishment during G1 and found that NIPBL's primary contribution to cohesion is through its role as a cohesin loader. Beyond initial loading which occurs as soon as cells exit mitosis, NIPBL was not strictly required during S phase and became refractory to cohesion in G2 where it had no effect on its maintenance. NIPBL's role in cohesion is therefore a simple but very important one: NIPBL loads cohesin onto DNA which is an essential prerequisite to establishing cohesion. This body of work suggests that NIPBL plays no further role in building cohesion beyond this.

Chapter VI: Materials and methods

Cell culture

Human U2OS osteosarcoma cells were cultured Dulbecco's Modified Eagle Medium (DMEM) supplemented with 10% foetal bovine serum (FBS), 1% penicillin-streptomycin. U2OS cells were maintained in a humidified incubator at 37°C with 5% CO2. Cells were passaged at approximately 70-80% confluence to ensure continuous growth. For passaging, cells were rinsed with phosphate-buffered saline (PBS) and detached using 0.25% trypsin-EDTA solution. Trypsinisation was halted by adding an equal volume of complete DMEM media, and cells were then centrifuged at 200 x g for 5 minutes. The cell pellet was resuspended in fresh media and seeded into new culture flasks at the desired density. Cell viability and density were routinely assessed using trypan blue exclusion and a haemocytometer.

Cell cycle synchronisation

A double thymidine block was used to synchronise cells at the G1/S boundary. Cells were treated with 2 mM thymidine (Sigma: T1895) and incubated for 18 hours to initiate the first thymidine block. Following the first block, cells were washed three times with PBS and then released into warm DMEM with 24 μM deoxycytidine for 6 hours to allow progression through S phase. Subsequently, a second thymidine block was applied by re-adding thymidine to a final concentration of 2 mM for an additional 17 hours. Finally, cells were washed three times with PBS and released into fresh DMEM with 24 μM deoxycytidine for synchronization analysis or further experimentation. Cell cycle synchronization was confirmed using flow cytometry analysis to ensure the majority of the population was arrested at the G1/S transition.

CRISPR/ Cas9 gene editing

CRISPR/Cas9 gene editing was employed to target and modify specific genes in human U2OS cells. Guide RNAs (gRNAs) specific to the target gene were designed using the online CRISPOR design tool, ensuring minimal off-target effects. The gRNAs were cloned into the pX459V2 CRISPR/Cas9 plasmid vector containing the Cas9 nuclease and a puromycin resistance marker. U2OS cells were transfected with the CRISPR/Cas9 construct using FuGENE® HD Transfection Reagent (Promega: E2311), following the manufacturer's protocol. Post-transfection, cells were incubated for 18 hours in a humidified incubator at 37°C with 5% CO2. Following incubation, cells were selected with puromycin (2 µg/mL) for 48 hours to enrich for successfully transfected cells. Post-selection, cells were incubated for 48 hours in a humidified incubator at 37°C with 5% CO2 to recover. Puromycin resistant clones were counted and seeded at a low density for single colony growth and grown until colonies were large enough to colony pick. Genomic DNA was extracted from clones, and the target gene modification was confirmed by PCR amplification and subsequent Sanger sequencing. Positive clones were expanded and further analysed to ensure successful gene editing and to assess any potential off-target effects.

Western blotting and chromatin fractionation

To perform western blot analysis, both whole cell extracts and nuclear fractions of U2OS cells were prepared. For whole cell extracts, U2OS cells were lysed in Radioimmunoprecipitation Assay (RIPA) buffer containing 10 mM Tris-HCl (pH 7.5), 150 mM NaCl, 1% NP-40, 1% sodium deoxycholate, 0.1% SDS, 1mM DTT, 10% glycerol and supplemented with protease inhibitors and supernuclease enzyme. Cells were incubated on ice for 20 minutes, and the lysate

was cleared by centrifugation at 14,000 x g for 20 minutes at 4°C. The supernatant was collected as the whole cell extract. For nuclear fractionation, cells were first resuspended in a hypotonic buffer (10 mM HEPES, pH 7.9, 1.5 mM $MgCl_2$, 10 mM KCl, 500mM DTT and protease inhibitors) to permeabilise the membrane and incubated on ice for 15 minutes. Cells were pelleted by centrifugation at 2,000 x g for 5 minutes at 4°C and the supernatant was removed. Cell pellets were resuspended in the hypertonic buffer with detergent (as before + 0.1% NP-40) to remove the cytosolic fraction and incubated on ice for 15 minutes. The lysate was centrifuged at 1,000 x g for 5 minutes at 4°C to pellet the nuclei. Cells were again pelleted by centrifugation at 4,000 x g for 5 minutes at 4°C and the supernatant was removed. The nuclear pellet was then resuspended in RIPA buffer (as before) and incubated and collected as before. The supernatant was collected as the nuclear extract. Chromatin fractionation was performed using the Subcellular Protein Fractionation Kit for Cultured Cells (ThermoFisher Scientific: 78840), following the manufacturers protocol. Protein concentrations were determined using the Bradford assay. Equal amounts of protein were resolved by SDS-PAGE using NuPAGE Novex 3-8% Tris-Acetate gels and transferred onto a nitrocellulose membrane using Transfer buffer (25mM Tris, 190 mM Glycine, 1.5mM EDTA, 20% ethanol) for 16hrs at 25V. Membranes were blocked with 5% non-fat dry milk in PBS-T (Phosphate-buffered saline with 0.05% Tween-20) and probed with specific primary antibodies, followed by HRP-conjugated secondary antibodies. Detection was performed using enhanced chemiluminescence (ECL) reagents, and signals were captured using film exposure or the LI-COR Odyssey FC imaging system. Analysis of band intensities was performed using the local background corrected band volumes taken by the iBright ThermoFisher imaging system, normalised against the loading controls.

Immunofluorescence

Immunofluorescence staining was performed to visualize protein localization in U2OS cells. Cells were grown on glass coverslips in a 24-well plate until they reached approximately 70% confluence. The cells were then fixed with 4% paraformaldehyde (PFA) in phosphate-buffered saline (PBS) for 10 minutes at room temperature. After fixation, cells were washed three times with PBS, to remove PFA, before being permeabilized by PBS with 0.1% Triton X-100 (PBS-Tx; Sigma: X100) for 10 minutes. Following permeabilization, cells were blocked with 5% bovine serum albumin (BSA) in PBS for 1 hour at room temperature to prevent non-specific binding. Primary antibodies, diluted in 1% BSA in PBS-Tx, were applied to the cells and incubated overnight at 4°C in a humidified chamber. After primary antibody incubation, cells were washed three times with PBS-Tx. Secondary antibodies conjugated with a fluorescent dye (e.g., Alexa Fluor dyes) were diluted in 1% BSA in PBS-Tx and applied to the cells for 1 hour at room temperature in the dark. The cells were then washed three times with PBS-Tx to remove unbound secondary antibodies. Finally, the coverslips were mounted onto glass slides using a mounting medium containing DAPI to counterstain the nuclei. Slides were sealed and imaged using the ScanR microscope and analysed to assess the localization and expression patterns of the target proteins.

Image analysis (such as mitotic index)

Image analysis was conducted using Scan R proprietary software for cell segmentation and cell cycle identification based on DAPI staining (see below). FIJI was used for any further analyses and preparation of representative images.

Flow cytometry

Flow cytometry analysis was conducted to assess cell cycle distribution in U2OS cells using ethanol fixation. Cells were harvested by trypsinization, washed twice with cold phosphate-buffered saline (PBS), and centrifuged at 300 x g for 5 minutes. The cell pellet was gently resuspended in 1 mL of cold PBS, and an equal volume of ice-cold 70% ethanol was added dropwise while vortexing gently to ensure even fixation. Cells were fixed at -20°C for at least 2 hours, or overnight, to ensure thorough permeabilization. Following fixation, cells were centrifuged at 300 x g for 5 minutes to remove ethanol and washed twice with cold PBS to rehydrate them. The cell pellet was then resuspended in 500 µL of PBS containing 50 µg/mL propidium iodide (PI) and 100 µg/mL RNase A to stain the DNA and eliminate RNA interference, respectively. Cells were incubated at room temperature in the dark for 30 minutes to allow complete staining. The stained cells were analyzed on a flow cytometer with appropriate settings for PI detection. Data were collected for at least 10,000 events per sample. Flow cytometry data were analyzed using FlowJo to determine cell cycle distribution and quantify the percentage of cells in different phases of the cell cycle.

ScanR cell cycle analysis

Cells were prepared as above in the Immunofluorescence section. DAPI-labelled cells were imaged using a 20x objective, capturing multiple fields per well to ensure comprehensive analysis. The ScanR analysis software was utilized to measure fluorescence intensity, which is proportional to DNA content, allowing differentiation of cell cycle phases (G1, S, and G2/M). Data analysis was carried out using the ScanR software to generate histograms and quantify cell cycle distribution.

Chromosome Spreads

Cells were cultured in appropriate growth medium until they reached 70-80% confluency. To enrich mitotic cells, 100 ng/mL Nocodazole was added to the culture medium for 4-10 hours to arrest cells in metaphase. Post Nocodazole treatment, cells were harvested by trypsinisation and centrifuged at 200 x g for 5 minutes. The cell pellet was gently resuspended in pre-warmed 0.075 M potassium chloride (KCl) solution and incubated at 37°C for 20 minutes to swell the cells. Once cells were swelled, they were fixed by adding a freshly prepared solution consisting of methanol and glacial acetic acid in a 3:1 ratio. This fixation step was repeated three times to ensure thorough permeabilisation and fixation of cellular components. After each addition, cells were centrifuged at 200 x g for 5 minutes and the supernatant was carefully removed. A small volume of the fixed cell suspension was dropped onto clean, wet microscope slides from a height of 30-50 cm to ensure optimal chromosome spreading. Slides were allowed to air dry completely. Following airdrying, the chromosome spreads were mounted VECTASHIELD mounting media with DAPI before being covered by a coverslip and sealed with nail polish.

EdU labelling for Flow cytometry or Chromosome spreads

Cells were cultured with media containing Edu5 (5-ethynyl-2'-deoxyuridine) at a final concentration of 10 µM for the time stated in the figure. Following Edu incorporation during S phase (or lack thereof), cells were prepared as described above in Flow Cytometry/Chromosome spreads with an additional step after fixation and before any other staining. EdU incorporation was detected using the Click-iT™ EdU Imaging Kit (Thermo Fisher Scientific: C10337) according to the manufacturer's instructions. Cells were incubated with the Click-iT™ reaction cocktail, which includes a Alexafluor647 azide dye, for 30

minutes at room temperature in the dark. This reaction covalently labels EdU with a fluorescent dye, allowing visualization of newly synthesized DNA. The samples were further stained or analysed on by flow cytometry/microscopy.

Chapter VII: Appendix

Optimising cell cycle arrest conditions

In order to synchronise cells G1, a CD4/6 inhibitor Palbociclib was used to arrest U2OS. Synchronisation protocols can vary for different cell lines, therefore I wished to establish the optimum arrest protocol for U2OS cells, which provided enough arrest to achieve a good G1 synchronisation, but still allowed for release. FACs was used to assess cell cycle profiles through propidium iodide (PI) staining of DNA. Cells in G2 will have 2n the DNA staining as cells in G1.

Initial tests used the recommended concentration of 1μM along with two other lower concentrations for 24 hours in order to establish the minimum concentration required for G1 arrest (**Appendix Fig. 1-1a**). Cells were also pulse-labelled with EdU in order to mark S phase cells, to help delineate cell cycle phases. Comparison of the cell cycle profiles obtained with PI staining alone compared to an EdU – PI matrix gave similar readings, therefore for easier handling, future cell cycle profiles will be assessed with PI staining alone. Tests showed that whilst cells did arrest with higher concentrations of palbociclib, as much as 10 fold lower concentrations still provided a reasonable arrest of > 85% in G1.

In order to see whether a longer incubation would improve the G1 arrest efficiency, low and high concentrations (0.3μM and 1μM respectively) were tested over different incubation lengths of 18 hours (overnight), 24 hours and 48 hours. Arrest was efficient with as little as 18 hours' incubation with little gain with extended incubations, therefore 18 hours was selected as the minimal arrest length time for optimal arrest (**Appendix Fig. 1-1b**).

In our experiments, we wished to assess cells synchronised in both G1 and G2. In order to synchronise cells in G2, we used a CDK1 inhibitor RO-3306. Testing direct inhibition of U2OS for 18 hours with the recommended concentration of 9 μM, yielded a low arrest efficiency

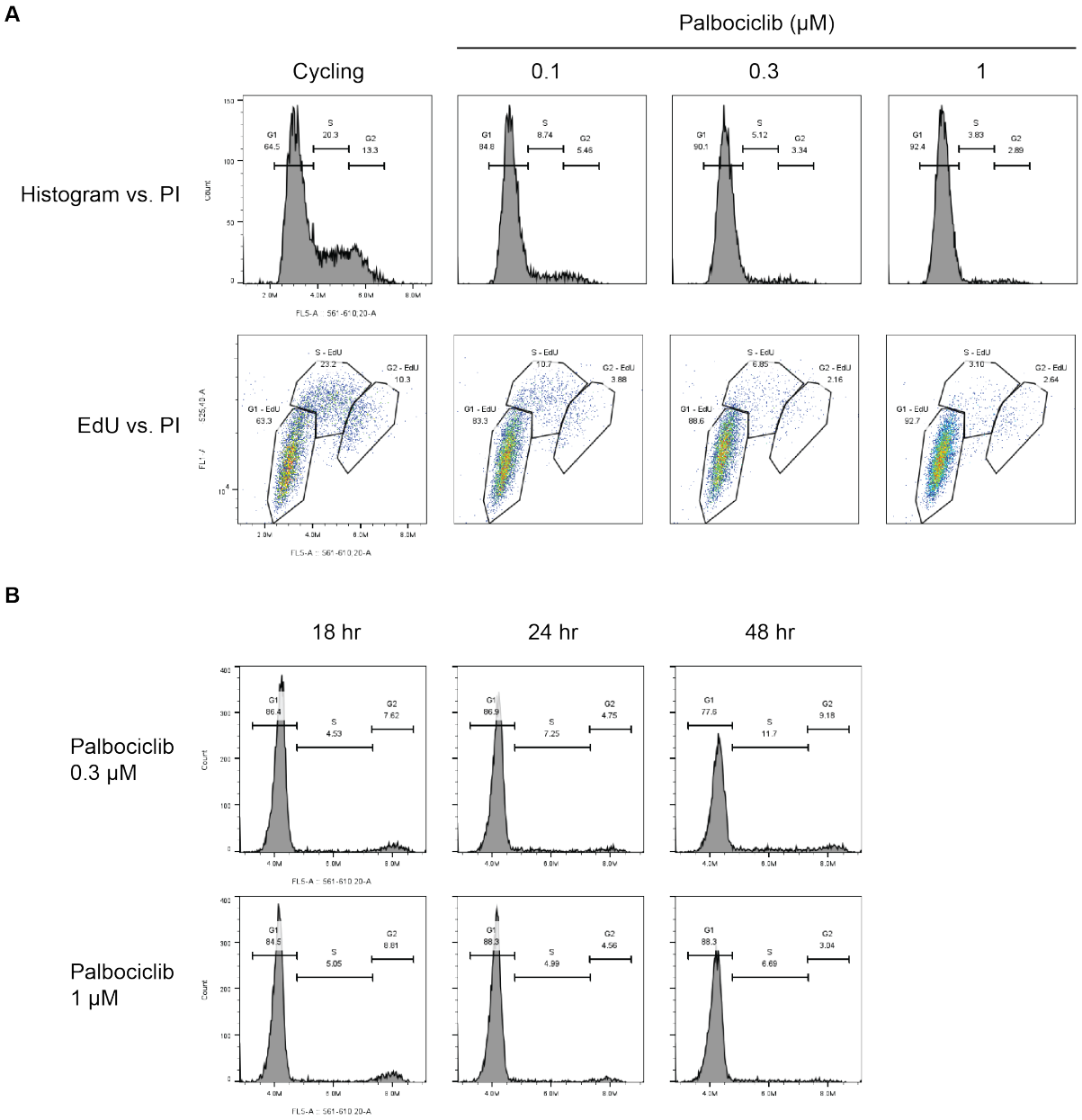

Appendix Figure 1-1. Optimising conditions for G1 arrest. All DNA stained propidium iodide intensities herein are measured with an excitation of 561λ with a bypass filter of 610;20. **(A)** FACs histogram of PI intensity of G1 arrested U2OS under varying palbociclib concentrations arrested for 24 hours. Cell cycle phases are gated according to 1n vs. 2n PI intensities. FACs profile of EdU – propidium iodide matrix. **(B)** FACs testing the optimal length of arrest at either 18 (ON), 24 or 48 hours with a high and low Palbociclib concentration.

(**Appendix Fig. 1-2a**). To improve arrest in G2, we therefore tested initial arrest in G1 with Palbociclib with release into RO-3306 to achieve a better synchrony. Release experiments showed that cells arrested in Palbociclib did not release from G1 for around 8-10 hours after Palbociclib washout, even in lower concentrations with the minimum arrest time of 18 hours (**Appendix Fig. 1-2b**). A 12 hr release window was identified as a good release window to catch cells as they begin to cycle into G2. We therefore tested G2 arrest with Palbociclib incubation for 18 hrs, a 12 hour release window, followed by RO-3306 arrest at different length incubation times of 12 and 24 hr (**Appendix Fig. 1-2c**). 24 hr arrest with RO-3306 was more effective than 12 hr, so the final arrest time selected was 18 hrs so that cells are stressed for a shorter period of time but still achieve an effective arrest of around 70%.

In our experiment depleting NIPBL in G1 and G2, we wished to keep our cell synchrony the same for both conditions and only change the position in which NIPBL is depleted. We therefore wanted to arrest in G1 and release to G2 before releasing finally into mitosis for chromosome spreads. When selecting the final concentration for G1 arrest we therefore had to balance between a good arrest in G1 and the ability to release into G2. The minimum concentration and incubation time for Palbociclib to fulfil both requirements was chosen to be 0.6 μM for 18 hrs. For G2 arrest we would follow this up with 12 hr release into RO-3306 for 18 hrs.

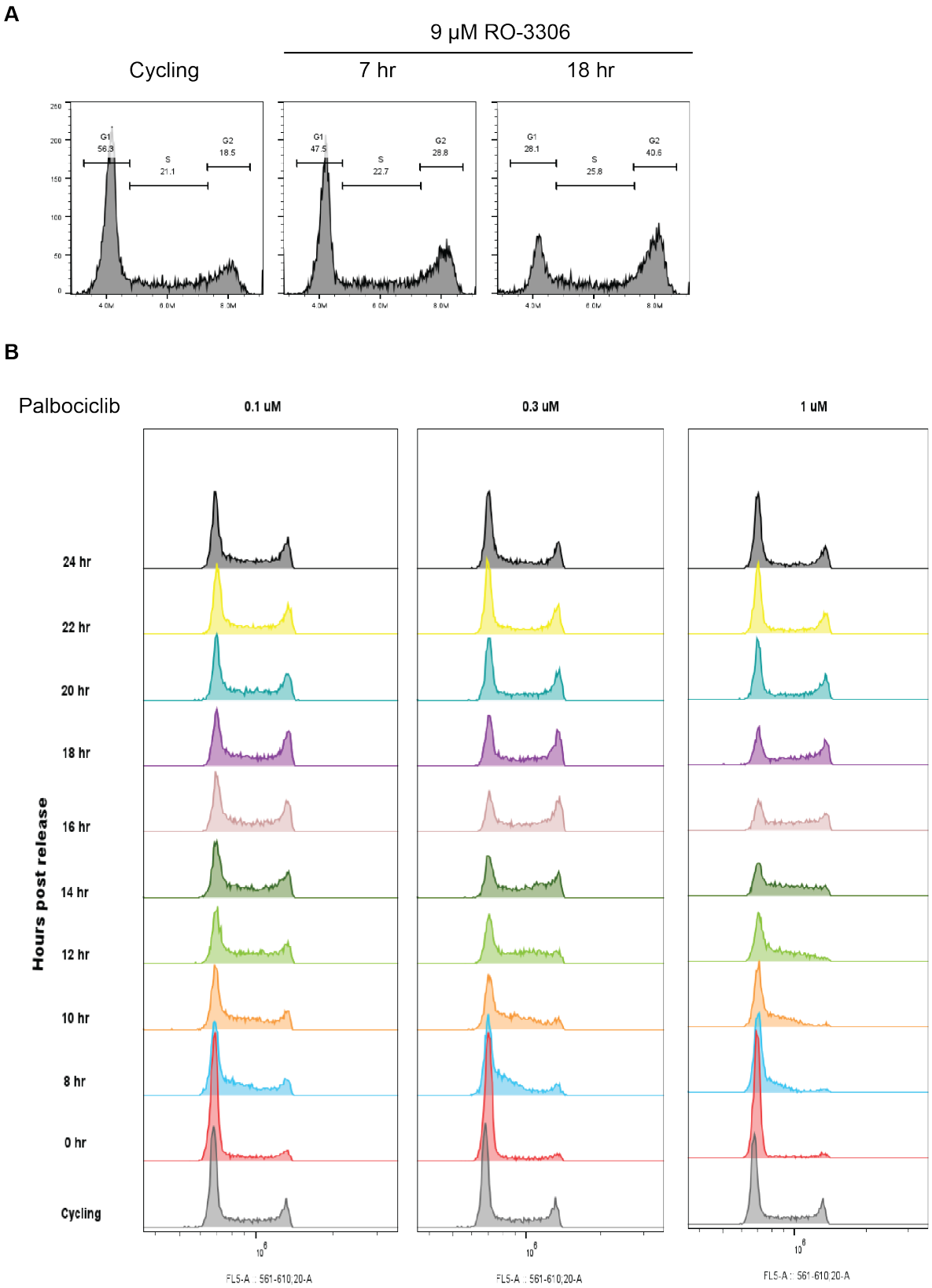

Appendix Figure 1-2. Optimising conditions for G2 release. (A) FACS testing G2 arrest with RO-3306 in stated incubations **(B)** FACS release from Palbo concentrations listed after 18 hr arrest

C

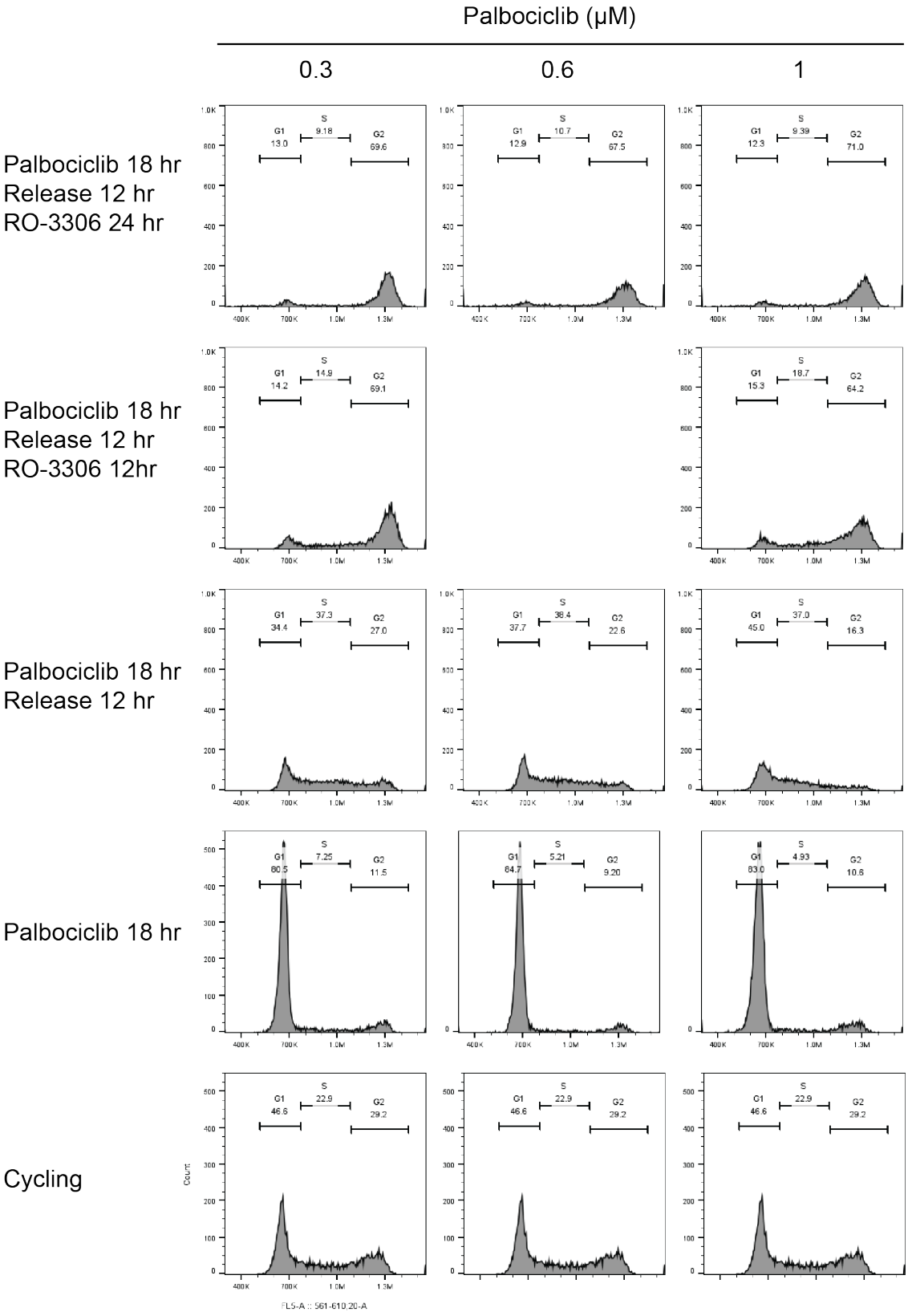

Appendix Figure 1-2 continued. Optimising conditions for G2 release. (C) FACS timecourse testing G2 arrest with Palbociclib arrest into RO-3306 in stated incubations

NIPBL depletion: Length of time vs. the cell cycle phase

We have in Figure 4-2 that depletion of NIPBL before mitosis leads to severe PCS cohesion defect of around 60%. It was unclear, however, whether the increased severity of cohesion defects was due to the extended depletion time of NIPBL rather than the cell cycle position. To address this, we repeated the synchronisation of Figure 4-2a but delayed the depletion to G2 so that NIPBL was fully depleted on the border of mitotic exit / early G1, but still depleted for an excessive period of time (> 18 hrs before S phase) (**Appendix Fig. 2a**). Here, we observe that PCS severe cohesion defects reduce from 60 ± 5% to 31 ± 1 %, with only a 6 hour delay in release (**Appendix Fig. 2b**). As NIPBL depletes fully within 6 hours as seen in Figure 2-8, it is unlikely that the reduction in the severity of cohesion defect is due to not enough depletion time, as NIPBL was depleted 18 hours ahead of S phase in these cells. We therefore conclude that it is indeed the cell cycle phase rather than the length of depletion which is causing these sever cohesion defects.

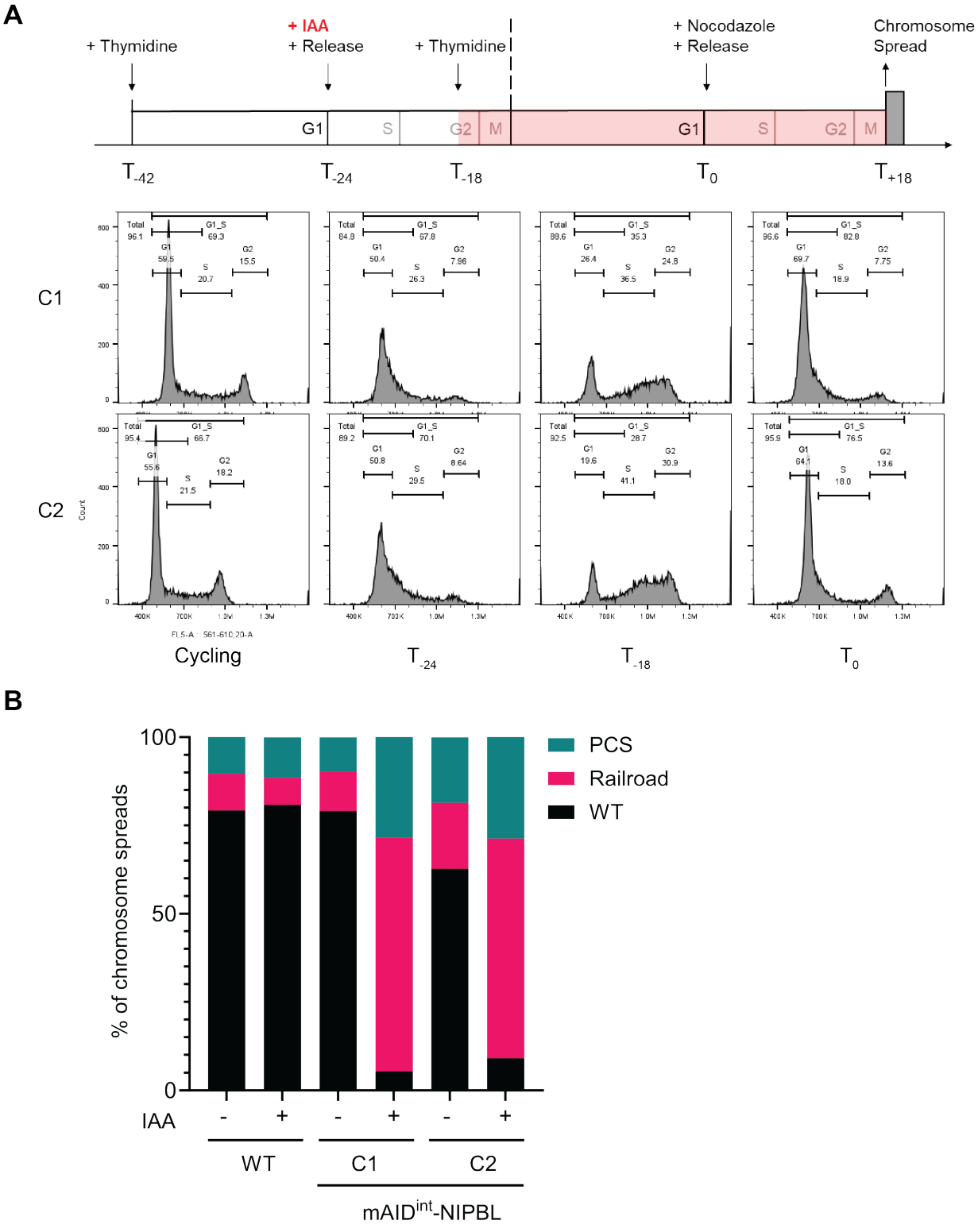

Appendix Figure 2. Length of NIPBL depletion vs cell cycle stage. (A) Experiment schematic of NIPBL depletion 8 hours after arrest in G1/S of the prior cell cycle when cells should be cycling through G2. Cell cycle profile is made using FACS with Propidium iodide staining showing arrest at major experiment time points. **(B)** Quantified cohesion phenotypes of chromosome spreads of experiment outlined in (A). Scoring was performed as in Figure 2-11, n >50 spreads over 2 biological repeats.

Observing cohesin live

Addressing whether NIPBL is the sole loader of cohesin is challenging, as the result must be absolute. If NIPBL predominantly loads as cells exit mitosis, then cells must be synchronised at that point in order to observe this. Synchronisation however is challenging and that means bulk assay approaches will not be clean enough to provide an absolute answer.

In order to observe cohesin on the single cell level, we wished to tag cohesin the mAID^{int}-NIPBL background so that cohesin molecules could be observed live. Live techniques such as FRAP or single molecule tracking can observe the bound / unbound population of a protein and are compatible observing the cell cycle through morphological changes by microscopy.

We targeted mAID^{int}-NIPBL with Rad21-Halo-T7, as Halo is a stable epitope which is able to conjugate with permanent fluorophore ligands for live cell imaging and provides more flexibility than a constitutive fluorophore such as GFP, based on the ligand choice. We also targeted T7 for purification for potential ChIP experiments. Previously, Rad21-Halo cells have been made in U2OS, however we were unable to achieve a homozygous tagging of Rad21-Halo-T7 despite screening over 600 clones. We must conclude that the homozygous version is non-viable, perhaps due to the addition of the T7 tag.

We were able to make several heterozygous clones (**Appendix Fig. 3**). Although it can be argued that the tagged alleles of RAD21 might behave differently to the untagged alleles, we will compare the behaviour of mAID^{int}-NIPBL Rad21-Halo-T7 with Rad21-Halo controls in future experiments as well as untreated and treated auxin controls.

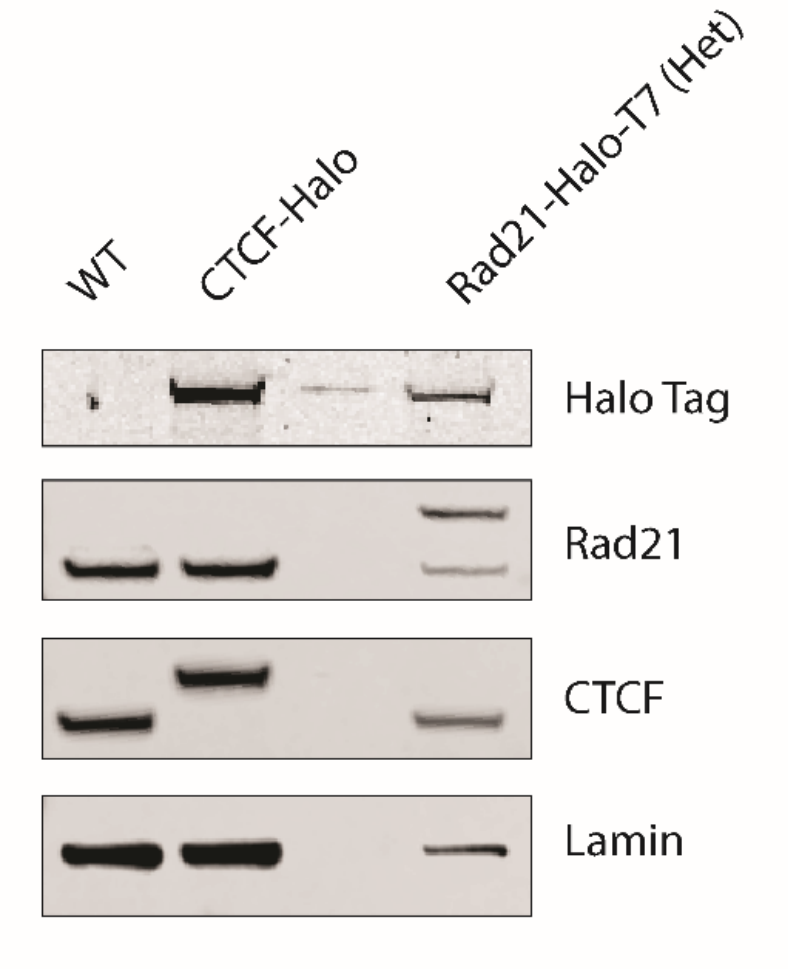

Appendix Figure 3. Tagging Rad21 with Halo-T7. Immunoblot of mAID^{int}-NIPBL cells tagged heterozygously with RAD21-Halo-T7. CTCF is a positive control for Halo Ab.

NIPBL isoform exon map positions (Figure 1.1 sup.)

- Transcript variant A = Exon 1 → 45, 46a, 46c
- Transcript variant B = Exon 1 → 45, 46b
- PREDICTED Transcript variant X1 = Exon 1 → 45, 46a, 46c* (up until where 46b ends)
- PREDICTED Transcript variant X2 = Exon 1 → 45, 46a, 46c-
- PREDICTED Transcript variant X3 = Exon 1 → 45, 46a+, 46c-
- PREDICTED Transcript variant X4 = Exon 1 → 45, 46a+, 46c--
- PREDICTED Transcript variant X5 = Intronic transcript between exon 7 and 8, Exon 8 → 45, 46a, 46c-
- PREDICTED Transcript variant X6 = Exon 1 → 42, 45-
- PREDICTED Transcript variant X7 = Intronic transcript between exon 9 and 10, Exon 10 → 45, 46a, 46c-
- PREDICTED Transcript variant X8 = Exon 1 →9, 11→45, 46a, 46c-

Bibliography

Alberts, B., Johnson, A., Lewis, J., Raff, M., Roberts, K., & Walter, P. (2002). *Chromosomal DNA and Its Packaging in the Chromatin Fiber*. https://www.ncbi.nlm.nih.gov/books/NBK26834/

Alonso-Gil, D., Cuadrado, A., Giménez-Llorente, D., Rodríguez-Corsino, M., & Losada, A. (2023). Different NIPBL requirements of cohesin-STAG1 and cohesin-STAG2. *Nature Communications*, *14*(1), 1–11. https://doi.org/10.1038/s41467-023-36900-7

Alonso-Gil, D., & Losada, A. (2023). NIPBL and cohesin: new take on a classic tale. In *Trends in Cell Biology* (Vol. 33, Issue 10, pp. 860–871). Elsevier Ltd. https://doi.org/10.1016/j.tcb.2023.03.006

Anderson, D. E., Losada, A., Erickson, H. P., & Hirano, T. (2002). Condensin and cohesin display different arm conformations with characteristic hinge angles. *Journal of Cell Biology*, *156*(3), 419–424. https://doi.org/10.1083/jcb.200111002

Arumugam, P., Gruber, S., Tanaka, K., Haering, C. H., Mechtler, K., & Nasmyth, K. (2003). ATP Hydrolysis Is Required for Cohesin's Association with Chromosomes. *Current Biology*, *13*(22), 1941–1953. https://doi.org/10.1016/j.cub.2003.10.036

Ba, Z., Lou, J., Ye, A. Y., Dai, H. Q., Dring, E. W., Lin, S. G., Jain, S., Kyritsis, N., Kieffer-Kwon, K. R., Casellas, R., & Alt, F. W. (2020). CTCF orchestrates long-range cohesin-driven V(D)J recombinational scanning. *Nature*, *586*(7828), 305–310. https://doi.org/10.1038/s41586-020-2578-0

Bastié, N., Chapard, C., Dauban, L., Gadal, O., Beckouët, F., & Koszul, R. (2022). Smc3 acetylation, Pds5 and Scc2 control the translocase activity that establishes cohesin-dependent chromatin loops. *Nature Structural and Molecular Biology*, *29*(6), 575–585. https://doi.org/10.1038/s41594-022-00780-0

Beckouët, F., Hu, B., Roig, M. B., Sutani, T., Komata, M., Uluocak, P., Katis, V. L., Shirahige, K., & Nasmyth, K. (2010). An Smc3 Acetylation Cycle Is Essential for Establishment of Sister Chromatid Cohesion. *Molecular Cell*, *39*(5), 689–699. https://doi.org/10.1016/j.molcel.2010.08.008

Beckouët, F., Srinivasan, M., Roig, M. B., Chan, K. L., Scheinost, J. C., Batty, P., Hu, B., Petela, N., Gligoris, T., Smith, A. C., Strmecki, L., Rowland, B. D., & Nasmyth, K. (2016). Releasing Activity Disengages Cohesin's Smc3/Scc1 Interface in a Process Blocked by Acetylation. *Molecular Cell*, *61*(4), 563–574. https://doi.org/10.1016/j.molcel.2016.01.026

Ben-Shahar, T. R., Heeger, S., Lehane, C., East, P., Flynn, H., Skehel, M., & Uhlmann, F. (2008). Eco1-dependent cohesin acetylation during establishment of sister chromatid cohesion. *Science*, *321*(5888), 563–566. https://doi.org/10.1126/science.1157774

Bermudez, V. P., Maniwa, Y., Tappin, I., Ozato, K., Yokomori, K., & Hurwitz, J. (2003). The alternative Ctf18-Dcc1-Ctf8-replication factor C complex required for sister chromatid cohesion loads proliferating cell nuclear antigen onto DNA. *Proceedings of the National Academy of Sciences of the United States of America*, *100*(18), 10237–10242. https://doi.org/10.1073/pnas.1434308100

Borges, V., Lehane, C., Lopez-Serra, L., Flynn, H., Skehel, M., Ben-Shahar, T. R., & Uhlmann, F. (2010). Hos1 Deacetylates Smc3 to Close the Cohesin Acetylation Cycle. *Molecular Cell*, *39*(5), 677–688. https://doi.org/10.1016/j.molcel.2010.08.009

Bot, C., Pfeiffer, A., Giordano, F., Manjeera, D. E., Dantuma, N. P., & Ström, L. (2017). Independent mechanisms recruit the cohesin loader protein NIPBL to sites of DNA damage. *Journal of Cell Science*, *130*(6), 1134–1146. https://doi.org/10.1242/jcs.197236

Braunholz, D., Hullings, M., Gil-Rodríguez, M. C., Fincher, C. T., Mallozzi, M. B., Loy, E., Albrecht, M., Kaur, M., Limon, J., Rampuria, A., Clark, D., Kline, A., Eckhold, J., Tzschach, A., Hennekam, R., Gillessen-Kaesbach, G., Wierzba, J., Krantz, I. D., Deardorff, M. A., & Kaiser, F. J. (2012). Isolated NIBPL missense mutations that cause Cornelia de Lange syndrome alter MAU2 interaction. *European Journal of Human Genetics*, *20*(3), 271–276. https://doi.org/10.1038/ejhg.2011.175

Buck, S. B., Bradford, J., Gee, K. R., Agnew, B. J., Clarke, S. T., & Salic, A. (2008). Detection of S-phase cell cycle progression using 5-ethynyl-2′- deoxyuridine incorporation with click chemistry, an alternative to using 5-bromo-2′-deoxyuridine antibodies. *BioTechniques*, *44*(7), 927–929. https://doi.org/10.2144/000112812

Carmena, M., Wheelock, M., Funabiki, H., & Earnshaw, W. C. (2012). The chromosomal passenger complex (CPC): From easy rider to the godfather of mitosis. *Nature Reviews Molecular Cell Biology*, *13*(12), 789–803. https://doi.org/10.1038/nrm3474

Chan, K. L., Roig, M. B., Hu, B., Beckouët, F., Metson, J., & Nasmyth, K. (2012). Cohesin's DNA exit gate is distinct from its entrance gate and is regulated by acetylation. *Cell*, *150*(5), 961–974. https://doi.org/10.1016/j.cell.2012.07.028

Chao, W. C. H., Murayama, Y., Muñoz, S., Costa, A., Uhlmann, F., & Singleton, M. R. (2015). Structural Studies Reveal the Functional Modularity of the Scc2-Scc4 Cohesin Loader. *Cell Reports*, *12*(5), 719–725. https://doi.org/10.1016/j.celrep.2015.06.071

Chao, W. C. H., Murayama, Y., Muñoz, S., Jones, A. W., Wade, B. O., Purkiss, A. G., Hu, X. W., Borg, A., Snijders, A. P., Uhlmann, F., & Singleton, M. R. (2017). Structure of the cohesin loader Scc2. *Nature Communications*, *8*, 6–13. https://doi.org/10.1038/ncomms13952

Ciosk, R., Shirayama, M., Shevchenko, A., Tanaka, T., Toth, A., Shevchenko, A., & Nasmyth, K. (2000). Cohesin's binding to chromosomes depends on a separate complex consisting of Scc2 and Scc4 proteins. *Molecular Cell*, *5*(2), 243–254. https://doi.org/10.1016/S1097-2765(00)80420-7

Ciosk, R., Zachariae, W., Michaelis, C., Shevchenko, A., Mann, M., & Nasmyth, K. (1998). An ESP1/PDS1 complex regulates loss of sister chromatid cohesion at the metaphase to anaphase transition in yeast. *Cell*, *93*(6), 1067–1076. https://doi.org/10.1016/S0092-8674(00)81211-8

Cleveland, D. W., Mao, Y., & Sullivan, K. F. (2003). Centromeres and kinetochores: From epigenetics to mitotic checkpoint signaling. In *Cell* (Vol. 112, Issue 4, pp. 407–421). Elsevier B.V. https://doi.org/10.1016/S0092-8674(03)00115-6

Collier, J. E., Lee, B. G., Roig, M. B., Yatskevich, S., Petela, N. J., Metson, J., Voulgaris, M., Llamazares, A. G., Löwe, J., & Nasmyth, K. A. (2020). Transport of DNA within cohesin involves clamping on top of engaged heads by SCC2 and entrapment within the ring by SCC3. *ELife*, *9*, 1–36. https://doi.org/10.7554/ELIFE.59560

Collier, J. E., & Nasmyth, K. A. (2022). DNA passes through cohesin's hinge as well as its Smc3–kleisin interface. *ELife*, *11*. https://doi.org/10.7554/ELIFE.80310

Cortone, G., Zheng, G., Pensieri, P., Chiappetta, V., Tatè, R., Malacaria, E., Pichierri, P., Yu, H., & Pisani, F. M. (2018). Interaction of the Warsaw breakage syndrome DNA helicase DDX11 with the replication fork-protection factor Timeless promotes sister chromatid cohesion. *PLOS Genetics*, *14*(10), e1007622. https://doi.org/10.1371/journal.pgen.1007622

Cundell, M. J., Hutter, L. H., Bastos, R. N., Poser, E., Holder, J., Mohammed, S., Novak, B., & Barr, F. A. (2016). A PP2A-B55 recognition signal controls substrate dephosphorylation kinetics during mitotic exit. *Journal of Cell Biology*, *214*(5), 539–554. https://doi.org/10.1083/jcb.201606033

Dai, H. Q., Hu, H., Lou, J., Ye, A. Y., Ba, Z., Zhang, X., Zhang, Y., Zhao, L., Yoon, H. S., Chapdelaine-Williams, A. M., Kyritsis, N., Chen, H., Johnson, K., Lin, S., Conte, A., Casellas, R., Lee, C. S., & Alt, F. W. (2021). Loop extrusion mediates physiological Igh locus contraction for RAG scanning. *Nature*, *590*(7845), 338–343. https://doi.org/10.1038/s41586-020-03121-7

Dauban, L., Montagne, R., Thierry, A., Lazar-Stefanita, L., Bastié, N., Gadal, O., Cournac, A., Koszul, R., & Beckouët, F. (2020). Regulation of Cohesin-Mediated Chromosome Folding by Eco1 and Other Partners. *Molecular Cell*, *77*(6), 1279-1293.e4. https://doi.org/10.1016/j.molcel.2020.01.019

Davidson, I. F., Bauer, B., Goetz, D., Tang, W., Wutz, G., & Peters, J. M. (2019). DNA loop extrusion by human cohesin. *Science*, *366*(6471), 1338–1345. https://doi.org/10.1126/science.aaz3418

de Wit, E., & Nora, E. P. (2023). New insights into genome folding by loop extrusion from inducible degron technologies. In *Nature Reviews Genetics* (Vol. 24, Issue 2, pp. 73–85). Nature Research. https://doi.org/10.1038/s41576-022-00530-4

Diller, L., Kassel, J., Nelson, C. E., Gryka, M. A., Litwak, G., Gebhardt, M., Bressac, B., Ozturk, M., Baker, S. J., Vogelstein, B., & Friend, S. H. (1990). p53 Functions as a Cell Cycle Control Protein in Osteosarcomas. *Molecular and Cellular Biology*, *10*(11), 5772–5781. https://doi.org/10.1128/mcb.10.11.5772-5781.1990

Dixon, J. R., Selvaraj, S., Yue, F., Kim, A., Li, Y., Shen, Y., Hu, M., Liu, J. S., & Ren, B. (2012). Topological domains in mammalian genomes identified by analysis of chromatin interactions. *Nature*, *485*(7398), 376–380. https://doi.org/10.1038/nature11082

Dohadwala, M., Da Cruz E Silva, E. F., Hall, F. L., Williams, R. T., Carbonaro-Hall, D. A., Nairn, A. C., Greengard, P., & Berndt, N. (1994). Phosphorylation and inactivation of protein phosphatase 1 by cyclin-dependent kinases. *Proceedings of the National Academy of Sciences of the United States of America*, *91*(14), 6408–6412. https://doi.org/10.1073/pnas.91.14.6408

Dreier, M. R., Bekier, M. E., & Taylor, W. R. (2011). Regulation of sororin by cdk1-mediated phosphorylation. *Journal of Cell Science*, *124*(17), 2976–2987. https://doi.org/10.1242/jcs.085431

Earnshaw, W. C., & Laemmli, U. K. (1983). Architecture of metaphase chromosomes and chromosome scaffolds. *Journal of Cell Biology*, *96*(1), 84–93. https://doi.org/10.1083/jcb.96.1.84

Evans, T., Rosenthal, E. T., Youngblom, J., Distel, D., & Hunt, T. (1983). Cyclin: A protein specified by maternal mRNA in sea urchin eggs that is destroyed at each cleavage

division. *Cell*, *33*(2), 389–396. https://doi.org/10.1016/0092-8674(83)90420-8

Fernius, J., Nerusheva, O. O., Galander, S., Alves, F. D. L., Rappsilber, J., & Marston, A. L. (2013). Cohesin-dependent association of Scc2/4 with the centromere initiates pericentromeric cohesion establishment. *Current Biology*, *23*(7), 599–606. https://doi.org/10.1016/j.cub.2013.02.022

Flomerfelt, F. A., & Gress, R. E. (2015). Analysis of cell proliferation and homeostasis using edu labeling. In *T-Cell Development: Methods and Protocols* (Vol. 1323, pp. 211–220). Springer New York. https://doi.org/10.1007/978-1-4939-2809-5_18

Fudenberg, G., Imakaev, M., Lu, C., Goloborodko, A., Abdennur, N., & Mirny, L. A. (2016). Formation of Chromosomal Domains by Loop Extrusion. *Cell Reports*, *15*(9), 2038–2049. https://doi.org/10.1016/j.celrep.2016.04.085

Furuya, K., Takahashi, K., & Yanagida, M. (1998). Faithful anaphase is ensured by Mis4, a sister chromatid cohesion molecule required in S phase and not destroyed in G1 phase. *Genes and Development*, *12*(21), 3408–3418. https://doi.org/10.1101/gad.12.21.3408

Gambus, A., Jones, R. C., Sanchez-Diaz, A., Kanemaki, M., van Deursen, F., Edmondson, R. D., & Labib, K. (2006). GINS maintains association of Cdc45 with MCM in replisome progression complexes at eukaryotic DNA replication forks. *Nature Cell Biology*, *8*(4), 358–366. https://doi.org/10.1038/ncb1382

Gandhi, R., Gillespie, P. J., & Hirano, T. (2006). Human Wapl Is a Cohesin-Binding Protein that Promotes Sister-Chromatid Resolution in Mitotic Prophase. *Current Biology*, *16*(24), 2406–2417. https://doi.org/10.1016/j.cub.2006.10.061

Ganji, M., Shaltiel, I. A., Bisht, S., Kim, E., Kalichava, A., Haering, C. H., & Dekker, C. (2018). Real-time imaging of DNA loop extrusion by condensin. *Science*, *360*(6384), 102–105. https://doi.org/10.1126/science.aar7831

Garcia, P., Fernandez-Hernandez, R., Cuadrado, A., Coca, I., Gomez, A., Maqueda, M., Latorre-Pellicer, A., Puisac, B., Ramos, F. J., Sandoval, J., Esteller, M., Mosquera, J. L., Rodriguez, J., Pié, J., Losada, A., & Queralt, E. (2021). Disruption of NIPBL/Scc2 in Cornelia de Lange Syndrome provokes cohesin genome-wide redistribution with an impact in the transcriptome. *Nature Communications*, *12*(1), 1–15. https://doi.org/10.1038/s41467-021-24808-z

Gerlich, D., Koch, B., Dupeux, F., Peters, J. M., & Ellenberg, J. (2006). Live-Cell Imaging Reveals a Stable Cohesin-Chromatin Interaction after but Not before DNA Replication. *Current Biology*, *16*(15), 1571–1578. https://doi.org/10.1016/j.cub.2006.06.068

Gillespie, P. J., & Hirano, T. (2004). Scc2 couples replication licensing to sister chromatid cohesion in Xenopus egg extracts. *Current Biology*, *14*(17), 1598–1603. https://doi.org/10.1016/j.cub.2004.07.053

Gligoris, T. G., Scheinost, J. C., Bürmann, F., Petela, N., Chan, K.-L., Uluocak, P., Beckouët, F., Gruber, S., Nasmyth, K., & Löwe, J. (2014). Closing the cohesin ring: Structure and function of its Smc3-kleisin interface. *Science*, *346*(6212), 963–967. https://doi.org/10.1126/science.1256917

Grant, G. D., Kedziora, K. M., Limas, J. C., Cook, J. G., & Purvis, J. E. (2018). Accurate delineation of cell cycle phase transitions in living cells with PIP-FUCCI. *Cell Cycle*, *17*(21–22), 2496–2516. https://doi.org/10.1080/15384101.2018.1547001

Gruber, S., Arumugam, P., Katou, Y., Kuglitsch, D., Helmhart, W., Shirahige, K., & Nasmyth, K. (2006). Evidence that Loading of Cohesin Onto Chromosomes Involves Opening of Its SMC Hinge. *Cell*, *127*(3), 523–537. https://doi.org/10.1016/j.cell.2006.08.048

Gruber, S., Haering, C. H., & Nasmyth, K. (2003). Chromosomal cohesin forms a ring. *Cell*, *112*(6), 765–777. https://doi.org/10.1016/S0092-8674(03)00162-4

Guacci, V., Koshland, D., & Strunnikov, A. (1997). A direct link between sister chromatid cohesion and chromosome condensation revealed through the analysis of MCD1 in S. cerevisiae. *Cell*, *91*(1), 47–57. https://doi.org/10.1016/S0092-8674(01)80008-8

Haarhuis, J. H. I., van der Weide, R. H., Blomen, V. A., Yáñez-Cuna, J. O., Amendola, M., van Ruiten, M. S., Krijger, P. H. L., Teunissen, H., Medema, R. H., van Steensel, B., Brummelkamp, T. R., de Wit, E., & Rowland, B. D. (2017). The Cohesin Release Factor WAPL Restricts Chromatin Loop Extension. *Cell*, *169*(4), 693-707.e14. https://doi.org/10.1016/j.cell.2017.04.013

Haering, C. H., Farcas, A. M., Arumugam, P., Metson, J., & Nasmyth, K. (2008). The cohesin ring concatenates sister DNA molecules. *Nature*, *454*(7202), 297–301. https://doi.org/10.1038/nature07098

Haering, C. H., Löwe, J., Hochwagen, A., & Nasmyth, K. (2002). Molecular architecture of SMC proteins and the yeast cohesin complex. *Molecular Cell*, *9*(4), 773–788. https://doi.org/10.1016/S1097-2765(02)00515-4

Haering, C. H., Schoffnegger, D., Nishino, T., Helmhart, W., Nasmyth, K., & Löwe, J. (2004). Structure and stability of cohesin's Smc1-kleisin interaction. *Molecular Cell*, *15*(6), 951–964. https://doi.org/10.1016/j.molcel.2004.08.030

Hansen, A. S., Pustova, I., Cattoglio, C., Tjian, R., & Darzacq, X. (2017). CTCF and cohesin regulate chromatin loop stability with distinct dynamics. *ELife*, *6*, 1–33. https://doi.org/10.7554/elife.25776

Hansen, K. L., Adachi, A. S., Braccioli, L., Kadvani, S., Boileau, R. M., Shah, R., Anderson, E. C., Martinovic, M., Zhang, K., Carel, I., Bonitto, K., Blelloch, R., Fudenberg, G., de Wit, E., Nora, E. P., & Biohub San Francisco, C.-Z. (2024). Synergy between cis-regulatory elements can render cohesin dispensable 1 for distal enhancer function 2 3. *BioRxiv*, 2024.10.04.615095. https://doi.org/10.1101/2024.10.04.615095

Hara, K., Zheng, G., Qu, Q., Liu, H., Ouyang, Z., Chen, Z., Tomchick, D. R., & Yu, H. (2014). Structure of cohesin subcomplex pinpoints direct shugoshin-Wapl antagonism in centromeric cohesion. *Nature Structural and Molecular Biology*, *21*(10), 864–870. https://doi.org/10.1038/nsmb.2880

Hartman, T., Stead, K., Koshland, D., & Guacci, V. (2000). Pds5p is an essential chromosomal protein required for both sister chromatid cohesion and condensation in Saccharomyces cerevisiae. *Journal of Cell Biology*, *151*(3), 613–626. https://doi.org/10.1083/jcb.151.3.613

Hauf, S., Roitinger, E., Koch, B., Dittrich, C. M., Mechtler, K., & Peters, J.-M. (2005). Dissociation of Cohesin from Chromosome Arms and Loss of Arm Cohesion during Early Mitosis Depends on Phosphorylation of SA2. *PLoS Biology*, *3*(3), e69. https://doi.org/10.1371/journal.pbio.0030069

Heidinger-Pauli, J. M., Mert, O., Davenport, C., Guacci, V., & Koshland, D. (2010). Systematic

Reduction of Cohesin Differentially Affects Chromosome Segregation, Condensation, and DNA Repair. *Current Biology*, *20*(10), 957–963. https://doi.org/10.1016/j.cub.2010.04.018

Higashi, T. L., Eickhoff, P., Sousa, J. S., Locke, J., Nans, A., Flynn, H. R., Snijders, A. P., Papageorgiou, G., O'Reilly, N., Chen, Z. A., O'Reilly, F. J., Rappsilber, J., Costa, A., & Uhlmann, F. (2020). A Structure-Based Mechanism for DNA Entry into the Cohesin Ring. *Molecular Cell*, *79*(6), 917-933.e9. https://doi.org/10.1016/j.molcel.2020.07.013

Hinshaw, S. M., Makrantoni, V., Harrison, S. C., & Marston, A. L. (2017). The Kinetochore Receptor for the Cohesin Loading Complex. *Cell*, *171*(1), 72-84.e13. https://doi.org/10.1016/j.cell.2017.08.017

Hinshaw, S. M., Makrantoni, V., Kerr, A., Marston, A. L., & Harrison, S. C. (2015). Structural evidence for Scc4-dependent localization of cohesin loading. *ELife*, *4*(JUNE), 1–15. https://doi.org/10.7554/eLife.06057

Hirano, T., Kobayashi, R., & Hirano, M. (1997). Condensins, chromosome condensation protein complexes containing XCAP- C, XCAP-E and a Xenopus homolog of the Drosophila Barren protein. *Cell*, *89*(4), 511–521. https://doi.org/10.1016/S0092-8674(00)80233-0

Hirano, T., & Mitchison, T. J. (1994). A heterodimeric coiled-coil protein required for mitotic chromosome condensation in vitro. *Cell*, *79*(3), 449–458. https://doi.org/10.1016/0092-8674(94)90254-2

Hu, B., Itoh, T., Mishra, A., Katoh, Y., Chan, K. L., Upcher, W., Godlee, C., Roig, M. B., Shirahige, K., & Nasmyth, K. (2011). ATP hydrolysis is required for relocating cohesin from sites occupied by its Scc2/4 loading complex. *Current Biology*, *21*(1), 12–24. https://doi.org/10.1016/j.cub.2010.12.004

Hu, B., Petela, N., Kurze, A., Chan, K. L., Chapard, C., & Nasmyth, K. (2015). Biological chromodynamics: A general method for measuring protein occupancy across the genome by calibrating ChIP-seq. *Nucleic Acids Research*, *43*(20). https://doi.org/10.1093/nar/gkv670

Isfort, R. J., Cody, D. B., Lovell, G., & Doersen, C. (1995). Analysis of oncogenes, tumor suppressor genes, autocrine growth-factor production, and differentiation state of human osteosarcoma cell lines. *Molecular Carcinogenesis*, *14*(3), 170–178. https://doi.org/10.1002/mc.2940140306

Ivanov, D., & Nasmyth, K. (2005). A topological interaction between cohesin rings and a circular minichromosome. *Cell*, *122*(6), 849–860. https://doi.org/10.1016/j.cell.2005.07.018

Ivanov, D., Schleiffer, A., Eisenhaber, F., Mechtler, K., Haering, C. H., & Nasmyth, K. (2002). Eco1 is a novel acetyltransferase that can acetylate proteins involved in cohesion. *Current Biology*, *12*(4), 323–328. https://doi.org/10.1016/S0960-9822(02)00681-4

Jahnke, P., Xu, W., Wülling, M., Albrecht, M., Gabriel, H., Gillessen-Kaesbach, G., & Kaiser, F. J. (2008). The Cohesin loading factor NIPBL recruits histone deacetylases to mediate local chromatin modifications. *Nucleic Acids Research*, *36*(20), 6450–6458. https://doi.org/10.1093/nar/gkn688

Janssen, A., & Medema, R. H. (2013). Genetic instability: Tipping the balance. In *Oncogene*

(Vol. 32, Issue 38, pp. 4459–4470). Nature Publishing Group. https://doi.org/10.1038/onc.2012.576

Kagey, M. H., Newman, J. J., Bilodeau, S., Zhan, Y., Orlando, D. A., Van Berkum, N. L., Ebmeier, C. C., Goossens, J., Rahl, P. B., Levine, S. S., Taatjes, D. J., Dekker, J., & Young, R. A. (2010). Mediator and cohesin connect gene expression and chromatin architecture. *Nature*, *467*(7314), 430–435. https://doi.org/10.1038/nature09380

Kean, C. M., Tracy, C. J., Mitra, A., Rahat, B., Van Winkle, M. T., Gebert, C. M., Noeker, J. A., Calof, A. L., Lander, A. D., Kassis, J. A., & Pfeifer, K. (2022). Decreasing *Wapl* dosage partially corrects embryonic growth and brain transcriptome phenotypes in *Nipbl* $^{+/-}$ embryos. *Science Advances*, *8*(48), 4136. https://doi.org/10.1126/sciadv.add4136

Kikuchi, S., Borek, D. M., Otwinowski, Z., Tomchick, D. R., & Yu, H. (2016). Crystal structure of the cohesin loader Scc2 and insight into cohesinopathy. *Proceedings of the National Academy of Sciences of the United States of America*, *113*(44), 12444–12449. https://doi.org/10.1073/pnas.1611333113

Kim, Y., Shi, Z., Zhang, H., Finkelstein, I. J., & Yu, H. (2019). Human cohesin compacts DNA by loop extrusion. *Science*, *366*(6471), 1345–1349. https://doi.org/10.1126/science.aaz4475

King, R. W., Peters, J. M., Tugendreich, S., Rolfe, M., Hieter, P., & Kirschner, M. W. (1995). A 20s complex containing CDC27 and CDC16 catalyzes the mitosis-specific conjugation of ubiquitin to cyclin B. *Cell*, *81*(2), 279–288. https://doi.org/10.1016/0092-8674(95)90338-0

Kitajima, T. S., Sakuno, T., Ishiguro, K. I., Iemura, S. I., Natsume, T., Kawashima, S. A., & Watanabe, Y. (2006). Shugoshin collaborates with protein phosphatase 2A to protect cohesin. *Nature*, *441*(1), 46–52. https://doi.org/10.1038/nature04663

Krantz, I. D., McCallum, J., DeScipio, C., Kaur, M., Gillis, L. A., Yaeger, D., Jukofsky, L., Wasserman, N., Bottani, A., Morris, C. A., Nowaczyk, M. J. M., Toriello, H., Bamshad, M. J., Carey, J. C., Rappaport, E., Kawauchi, S., Lander, A. D., Calof, A. L., Li, H. H., … Jackson, L. G. (2004). Cornelia de Lange syndrome is caused by mutations in NIPBL, the human homolog of Drosophila melanogaster Nipped-B. *Nature Genetics*, *36*(6), 631–635. https://doi.org/10.1038/ng1364

Kschonsak, M., Merkel, F., Bisht, S., Metz, J., Rybin, V., Hassler, M., & Haering, C. H. (2017). Structural Basis for a Safety-Belt Mechanism That Anchors Condensin to Chromosomes. *Cell*, *171*(3), 588-600.e24. https://doi.org/10.1016/j.cell.2017.09.008

Kubota, T., Nishimura, K., Kanemaki, M. T., & Donaldson, A. D. (2013). The Elg1 Replication Factor C-like Complex Functions in PCNA Unloading during DNA Replication. *Molecular Cell*, *50*(2), 273–280. https://doi.org/10.1016/j.molcel.2013.02.012

Kueng, S., Hegemann, B., Peters, B. H., Lipp, J. J., Schleiffer, A., Mechtler, K., & Peters, J. M. (2006). Wapl Controls the Dynamic Association of Cohesin with Chromatin. *Cell*, *127*(5), 955–967. https://doi.org/10.1016/j.cell.2006.09.040

Lafont, A. L., Song, J., & Rankin, S. (2010). Sororin cooperates with the acetyltransferase Eco2 to ensure DNA replication-dependent sister chromatid cohesion. *Proceedings of the National Academy of Sciences of the United States of America*, *107*(47), 20364–20369. https://doi.org/10.1073/pnas.1011069107

Lechner, M. S., Schultz, D. C., Negorev, D., Maul, G. G., & Rauscher, F. J. (2005). The mammalian heterochromatin protein 1 binds diverse nuclear proteins through a common motif that targets the chromoshadow domain. *Biochemical and Biophysical Research Communications*, *331*(4), 929–937. https://doi.org/10.1016/j.bbrc.2005.04.016

Lee, M. G., & Nurse, P. (1987). Complementation used to clone a human homologue of the fission yeast cell cycle control gene cdc2. *Nature*, *327*(6117), 31–35. https://doi.org/10.1038/327031a0

Lengronne, A., Katou, Y., Mori, S., Yokabayashi, S., Kelly, G. P., Ito, T., Watanabe, Y., Shirahige, K., & Uhlmann, F. (2004). Cohesin relocation from sites of chromosomal loading to places of convergent transcription. *Nature*, *430*(6999), 573–578. https://doi.org/10.1038/nature02742

Lengronne, A., McIntyre, J., Katou, Y., Kanoh, Y., Hopfner, K. P., Shirahige, K., & Uhlmann, F. (2006). Establishment of Sister Chromatid Cohesion at the S. cerevisiae Replication Fork. *Molecular Cell*, *23*(6), 787–799. https://doi.org/10.1016/j.molcel.2006.08.018

Linares-Saldana, R., Kim, W., Bolar, N. A., Zhang, H., Koch-Bojalad, B. A., Yoon, S., Shah, P. P., Karnay, A., Park, D. S., Luppino, J. M., Nguyen, S. C., Padmanabhan, A., Smith, C. L., Poleshko, A., Wang, Q., Li, L., Srivastava, D., Vahedi, G., Eom, G. H., … Jain, R. (2021). BRD4 orchestrates genome folding to promote neural crest differentiation. *Nature Genetics*, *53*(10), 1480–1492. https://doi.org/10.1038/s41588-021-00934-8

Liu, D., Vader, G., Vromans, M. J. M., Lampson, M. A., & Lens, S. M. A. (2009). Sensing Chromosome Bi-Orientation by Spatial Separation of Aurora B Kinase from Kinetochore Substrates. *Science*, *323*(5919), 1350–1353. https://doi.org/10.1126/science.1167000

Liu, H., Rankin, S., & Yu, H. (2013). Phosphorylation-enabled binding of SGO1-PP2A to cohesin protects sororin and centromeric cohesion during mitosis. *Nature Cell Biology*, *15*(1), 40–49. https://doi.org/10.1038/ncb2637

Liu, N. Q., Maresca, M., van den Brand, T., Braccioli, L., Schijns, M. M. G. A., Teunissen, H., Bruneau, B. G., Nora, E. èP, & de Wit, E. (2021). WAPL maintains a cohesin loading cycle to preserve cell-type-specific distal gene regulation. *Nature Genetics*, *53*(1), 100–109. https://doi.org/10.1038/s41588-020-00744-4

Losada, A., Yokochi, T., Kobayashi, R., & Hirano, T. (2000). Identification and characterization of SA/Scc3p subunits in the Xenopus and human cohesin complexes. *Journal of Cell Biology*, *150*(3), 405–416. https://doi.org/10.1083/jcb.150.3.405

Löwe, J., Cordell, S. C., & Van Den Ent, F. (2001). Crystal structure of the SMC head domain: An ABC ATPase with 900 residues antiparallel coiled-coil inserted. *Journal of Molecular Biology*, *306*(1), 25–35. https://doi.org/10.1006/jmbi.2000.4379

Luna-Peláez, N., March-Díaz, R., Ceballos-Chávez, M., Guerrero-Martínez, J. A., Grazioli, P., García-Gutiérrez, P., Vaccari, T., Massa, V., Reyes, J. C., & García-Domínguez, M. (2019). The Cornelia de Lange Syndrome-associated factor NIPBL interacts with BRD4 ET domain for transcription control of a common set of genes. *Cell Death and Disease*, *10*(8). https://doi.org/10.1038/s41419-019-1792-x

Mach, P., Kos, P. I., Zhan, Y., Cramard, J., Gaudin, S., Tünnermann, J., Marchi, E., Eglinger, J., Zuin, J., Kryzhanovska, M., Smallwood, S., Gelman, L., Roth, G., Nora, E. P., Tiana, G., & Giorgetti, L. (2022). Cohesin and CTCF control the dynamics of chromosome folding. *Nature Genetics*, *54*(12), 1907–1918. https://doi.org/10.1038/s41588-022-01232-

Mahdessian, D., Cesnik, A. J., Gnann, C., Danielsson, F., Stenström, L., Arif, M., Zhang, C., Le, T., Johansson, F., Shutten, R., Bäckström, A., Axelsson, U., Thul, P., Cho, N. H., Carja, O., Uhlén, M., Mardinoglu, A., Stadler, C., Lindskog, C., … Lundberg, E. (2021). Spatiotemporal dissection of the cell cycle with single-cell proteogenomics. *Nature*, *590*(7847), 649–654. https://doi.org/10.1038/s41586-021-03232-9

Mannini, L., Cucco, F., Quarantotti, V., Krantz, I. D., & Musio, A. (2013). Mutation Spectrum and Genotype-Phenotype Correlation in Cornelia de Lange Syndrome. *Human Mutation*, *34*(12), 1589–1596. https://doi.org/10.1002/humu.22430

Mattingly, M., Seidel, C., Muñoz, S., Hao, Y., Zhang, Y., Wen, Z., Florens, L., Uhlmann, F., & Gerton, J. L. (2022). Mediator recruits the cohesin loader Scc2 to RNA Pol II-transcribed genes and promotes sister chromatid cohesion. *Current Biology*, *32*(13), 2884-2896.e6. https://doi.org/10.1016/j.cub.2022.05.019

Michaelis, C., Ciosk, R., & Nasmyth, K. (1997). Cohesins: Chromosomal proteins that prevent premature separation of sister chromatids. *Cell*, *91*(1), 35–45. https://doi.org/10.1016/S0092-8674(01)80007-6

Mitter, M., Gasser, C., Takacs, Z., Langer, C. C. H., Tang, W., Jessberger, G., Beales, C. T., Neuner, E., Ameres, S. L., Peters, J. M., Goloborodko, A., Micura, R., & Gerlich, D. W. (2020). Conformation of sister chromatids in the replicated human genome. *Nature*, *586*(7827), 139–144. https://doi.org/10.1038/s41586-020-2744-4

Muñoz, S., Minamino, M., Casas-Delucchi, C. S., Patel, H., & Uhlmann, F. (2019). A Role for Chromatin Remodeling in Cohesin Loading onto Chromosomes. *Molecular Cell*, *74*(4), 664-673.e5. https://doi.org/10.1016/j.molcel.2019.02.027

Murayama, Y., Samora, C. P., Kurokawa, Y., Iwasaki, H., & Uhlmann, F. (2018). Establishment of DNA-DNA Interactions by the Cohesin Ring. *Cell*, *172*(3), 465-477.e15. https://doi.org/10.1016/j.cell.2017.12.021

Murayama, Y., & Uhlmann, F. (2014). Biochemical reconstitution of topological DNA binding by the cohesin ring. *Nature*, *505*(7483), 367–371. https://doi.org/10.1038/nature12867

Murayama, Y., & Uhlmann, F. (2015). DNA Entry into and Exit out of the Cohesin Ring by an Interlocking Gate Mechanism. *Cell*, *163*(7), 1628–1640. https://doi.org/10.1016/j.cell.2015.11.030

Musacchio, A. (2015). The Molecular Biology of Spindle Assembly Checkpoint Signaling Dynamics. In *Current Biology* (Vol. 25, Issue 20, pp. R1002–R1018). Cell Press. https://doi.org/10.1016/j.cub.2015.08.051

Nabet, B., Roberts, J. M., Buckley, D. L., Paulk, J., Dastjerdi, S., Yang, A., Leggett, A. L., Erb, M. A., Lawlor, M. A., Souza, A., Scott, T. G., Vittori, S., Perry, J. A., Qi, J., Winter, G. E., Wong, K. K., Gray, N. S., & Bradner, J. E. (2018). The dTAG system for immediate and target-specific protein degradation. *Nature Chemical Biology*, *14*(5), 431–441. https://doi.org/10.1038/s41589-018-0021-8

Nagasaka, K., Davidson, I. F., Stocsits, R. R., Tang, W., Wutz, G., Batty, P., Panarotto, M., Litos, G., Schleiffer, A., Gerlich, D. W., & Peters, J. M. (2023). Cohesin mediates DNA loop extrusion and sister chromatid cohesion by distinct mechanisms. *Molecular Cell*, *83*(17), 3049-3063.e6. https://doi.org/10.1016/j.molcel.2023.07.024

Nasmyth, K. A. (2017). Scc2-mediated loading of cohesin onto chromosomes in G1 yeast cells is insufficient to build cohesion during S phase. *BioRxiv*, 123596. https://doi.org/10.1101/123596

Natsume, T., Kiyomitsu, T., Saga, Y., & Kanemaki, M. T. (2016). Rapid Protein Depletion in Human Cells by Auxin-Inducible Degron Tagging with Short Homology Donors. *Cell Reports*, *15*(1), 210–218. https://doi.org/10.1016/j.celrep.2016.03.001

Nicklas, R. B. (1997). How Cells Get the Right Chromosomes. *Science*, *275*(5300), 632–637. https://doi.org/10.1126/science.275.5300.632

Nishimura, K., Fukagawa, T., Takisawa, H., Kakimoto, T., & Kanemaki, M. (2009). An auxin-based degron system for the rapid depletion of proteins in nonplant cells. *Nature Methods*, *6*(12), 917–922. https://doi.org/10.1038/nmeth.1401

Nishimura, K., & Kanemaki, M. T. (2014). Rapid depletion of budding yeast proteins via the fusion of an auxin-inducible degron (AID). *Current Protocols in Cell Biology*, *2014*, 20.9.1-20.9.16. https://doi.org/10.1002/0471143030.cb2009s64

Nishiyama, T., Ladurner, R., Schmitz, J., Kreidl, E., Schleiffer, A., Bhaskara, V., Bando, M., Shirahige, K., Hyman, A. A., Mechtler, K., & Peters, J. M. (2010). Sororin mediates sister chromatid cohesion by antagonizing Wapl. *Cell*, *143*(5), 737–749. https://doi.org/10.1016/j.cell.2010.10.031

Nora, E. P., Lajoie, B. R., Schulz, E. G., Giorgetti, L., Okamoto, I., Servant, N., Piolot, T., Van Berkum, N. L., Meisig, J., Sedat, J., Gribnau, J., Barillot, E., Blüthgen, N., Dekker, J., & Heard, E. (2012). Spatial partitioning of the regulatory landscape of the X-inactivation centre. *Nature*, *485*(7398), 381–385. https://doi.org/10.1038/nature11049

Novak, B., Tyson, J. J., Gyorffy, B., & Csikasz-Nagy, A. (2007). Irreversible cell-cycle transitions are due to systems-level feedback. In *Nature Cell Biology* (Vol. 9, Issue 7, pp. 724–728). Nature Publishing Group. https://doi.org/10.1038/ncb0707-724

Ochs, F., Green, C., Szczurek, A. T., Pytowski, L., Kolesnikova, S., Brown, J., Gerlich, D. W., Buckle, V., Schermelleh, L., & Nasmyth, K. A. (2024). Sister chromatid cohesion is mediated by individual cohesin complexes. *Science*, *383*(6687), 1122–1130. https://doi.org/10.1126/science.adl4606

Oka, Y., Suzuki, K., Yamauchi, M., Mitsutake, N., & Yamashita, S. (2011). Recruitment of the cohesin loading factor NIPBL to DNA double-strand breaks depends on MDC1, RNF168 and HP1γ in human cells. *Biochemical and Biophysical Research Communications*, *411*(4), 762–767. https://doi.org/10.1016/j.bbrc.2011.07.021

Oliveira, R. A., Hamilton, R. S., Pauli, A., Davis, I., & Nasmyth, K. (2010). Cohesin cleavage and Cdk inhibition trigger formation of daughter nuclei. *Nature Cell Biology*, *12*(2), 185–192. https://doi.org/10.1038/ncb2018

Olley, G., Ansari, M., Bengani, H., Grimes, G. R., Rhodes, J., Von Kriegsheim, A., Blatnik, A., Stewart, F. J., Wakeling, E., Carroll, N., Ross, A., Park, S. M., Bickmore, W. A., Pradeepa, M. M., & Fitzpatrick, D. R. (2018). BRD4 interacts with NIPBL and BRD4 is mutated in a Cornelia de Lange-like syndrome. *Nature Genetics*, *50*(3), 329–332. https://doi.org/10.1038/s41588-018-0042-y

Ouyang, Z., Zheng, G., Song, J., Borek, D. M., Otwinowski, Z., Brautigam, C. A., Tomchick, D. R., Rankin, S., & Yu, H. (2013). Structure of the human cohesin inhibitor Wapl.

Proceedings of the National Academy of Sciences of the United States of America, *110*(28), 11355–11360. https://doi.org/10.1073/pnas.1304594110

Ouyang, Z., Zheng, G., Tomchick, D. R., Luo, X., & Yu, H. (2016). Structural Basis and IP6 Requirement for Pds5-Dependent Cohesin Dynamics. *Molecular Cell*, *62*(2), 248–259. https://doi.org/10.1016/j.molcel.2016.02.033

Palecek, J. J. (2019). SMC5/6: Multifunctional player in replication. In *Genes* (Vol. 10, Issue 1, p. 7). MDPI AG. https://doi.org/10.3390/genes10010007

Panizza, S., Tanaka, T., Hochwagen, A., Eisenhaber, F., & Nasmyth, K. (2000). Pds5 cooperates with cohesion in maintaining sister chromatid cohesion. *Current Biology*, *10*(24), 1557–1564. https://doi.org/10.1016/S0960-9822(00)00854-X

Parelho, V., Hadjur, S., Spivakov, M., Leleu, M., Sauer, S., Gregson, H. C., Jarmuz, A., Canzonetta, C., Webster, Z., Nesterova, T., Cobb, B. S., Yokomori, K., Dillon, N., Aragon, L., Fisher, A. G., & Merkenschlager, M. (2008). Cohesins Functionally Associate with CTCF on Mammalian Chromosome Arms. *Cell*, *132*(3), 422–433. https://doi.org/10.1016/j.cell.2008.01.011

Petela, N. J., Gligoris, T. G., Metson, J., Lee, B. G., Voulgaris, M., Hu, B., Kikuchi, S., Chapard, C., Chen, W., Rajendra, E., Srinivisan, M., Yu, H., Löwe, J., & Nasmyth, K. A. (2018). Scc2 Is a Potent Activator of Cohesin's ATPase that Promotes Loading by Binding Scc1 without Pds5. *Molecular Cell*, *70*(6), 1134-1148.e7. https://doi.org/10.1016/j.molcel.2018.05.022

Petryk, N., Dalby, M., Wenger, A., Stromme, C. B., Strandsby, A., Andersson, R., & Groth, A. (2018). MCM2 promotes symmetric inheritance of modified histones during DNA replication. *Science*, *361*(6409), 1389–1392. https://doi.org/10.1126/science.aau0294

Rankin, S., Ayad, N. G., & Kirschner, M. W. (2005). Sororin, a substrate of the anaphase-promoting complex, is required for sister chromatid cohesion in vertebrates. *Molecular Cell*, *18*(2), 185–200. https://doi.org/10.1016/j.molcel.2005.03.017

Rao, S. S. P., Huang, S. C., Glenn St Hilaire, B., Engreitz, J. M., Perez, E. M., Kieffer-Kwon, K. R., Sanborn, A. L., Johnstone, S. E., Bascom, G. D., Bochkov, I. D., Huang, X., Shamim, M. S., Shin, J., Turner, D., Ye, Z., Omer, A. D., Robinson, J. T., Schlick, T., Bernstein, B. E., … Aiden, E. L. (2017). Cohesin Loss Eliminates All Loop Domains. *Cell*, *171*(2), 305-320.e24. https://doi.org/10.1016/j.cell.2017.09.026

Rhodes, J., Haarhuis, J. H. I., Grimm, J. B., Rowland, B. D., Lavis, L. D., & Nasmyth, K. A. (2017). Cohesin Can Remain Associated with Chromosomes during DNA Replication. *Cell Reports*, *20*(12), 2749–2755. https://doi.org/10.1016/j.celrep.2017.08.092

Rhodes, J., Mazza, D., Nasmyth, K., & Uphoff, S. (2017a). Scc2/Nipbl hops between chromosomal cohesin rings after loading. *ELife*, *6*, 1–20. https://doi.org/10.7554/eLife.30000

Rhodes, J., Mazza, D., Nasmyth, K., & Uphoff, S. (2017b). Scc2/Nipbl hops between chromosomal cohesin rings after loading. *ELife*, *6*. https://doi.org/10.7554/eLife.30000

Rowland, B. D., Roig, M. B., Nishino, T., Kurze, A., Uluocak, P., Mishra, A., Beckouët, F., Underwood, P., Metson, J., Imre, R., Mechtler, K., Katis, V. L., & Nasmyth, K. (2009). Building Sister Chromatid Cohesion: Smc3 Acetylation Counteracts an Antiestablishment Activity. *Molecular Cell*, *33*(6), 763–774. https://doi.org/10.1016/j.molcel.2009.02.028

Sakaue-Sawano, A., Kurokawa, H., Morimura, T., Hanyu, A., Hama, H., Osawa, H., Kashiwagi, S., Fukami, K., Miyata, T., Miyoshi, H., Imamura, T., Ogawa, M., Masai, H., & Miyawaki, A. (2008). Visualizing Spatiotemporal Dynamics of Multicellular Cell-Cycle Progression. *Cell*, *132*(3), 487–498. https://doi.org/10.1016/j.cell.2007.12.033

Salic, A., & Mitchison, T. J. (2008). A chemical method for fast and sensitive detection of DNA synthesis in vivo. *Proceedings of the National Academy of Sciences of the United States of America*, *105*(7), 2415–2420. https://doi.org/10.1073/pnas.0712168105

Sanborn, A. L., Rao, S. S. P., Huang, S. C., Durand, N. C., Huntley, M. H., Jewett, A. I., Bochkov, I. D., Chinnappan, D., Cutkosky, A., Li, J., Geeting, K. P., Gnirke, A., Melnikov, A., McKenna, D., Stamenova, E. K., Lander, E. S., & Aiden, E. L. (2015). Chromatin extrusion explains key features of loop and domain formation in wild-type and engineered genomes. *Proceedings of the National Academy of Sciences of the United States of America*, *112*(47), E6456–E6465. https://doi.org/10.1073/pnas.1518552112

Santaguida, S., & Amon, A. (2015). Short- and long-term effects of chromosome mis-segregation and aneuploidy. In *Nature Reviews Molecular Cell Biology* (Vol. 16, Issue 8, pp. 473–485). Nature Publishing Group. https://doi.org/10.1038/nrm4025

Schwarzer, W., Abdennur, N., Goloborodko, A., Pekowska, A., Fudenberg, G., Loe-Mie, Y., Fonseca, N. A., Huber, W., Haering, C. H., Mirny, L., & Spitz, F. (2017). Two independent modes of chromatin organization revealed by cohesin removal. *Nature*, *551*(7678), 51–56. https://doi.org/10.1038/nature24281

Seitan, V. C., Banks, P., Laval, S., Majid, N. A., Dorsett, D., Rana, A., Smith, J., Bateman, A., Krpic, S., Hostert, A., Rollins, R. A., Erdjument-Bromage, H., Tempst, P., Benard, C. Y., Hekimi, S., Newbury, S. F., & Strachan, T. (2006). Metazoan Scc4 Homologs Link Sister Chromatid Cohesion to Cell and Axon Migration Guidance. *PLoS Biology*, *4*(8), e242. https://doi.org/10.1371/journal.pbio.0040242

Sender, R., & Milo, R. (2021). The distribution of cellular turnover in the human body. *Nature Medicine*, *27*(1), 45–48. https://doi.org/10.1038/s41591-020-01182-9

Shi, Z., Gao, H., Bai, X. C., & Yu, H. (2020). Cryo-EM structure of the human cohesin-NIPBL-DNA complex. *Science*, *368*(6498), 1454–1459. https://doi.org/10.1126/science.abb0981

Shintomi, K., & Hirano, T. (2009). Releasing cohesin from chromosome arms in early mitosis: Opposing actions of Wapl-Pds5 and Sgo1. *Genes and Development*, *23*(18), 2224–2236. https://doi.org/10.1101/gad.1844309

Shirayama, M., Tóth, A., Gálová, M., & Nasmyth, K. (1999). APCCdc20 promotes exit from mitosis by destroying the anaphase inhibitor Pds1 and cyclin Clb5. *Nature*, *402*(6758), 203–207. https://doi.org/10.1038/46080

Skibbens, R. V., Corson, L. B., Koshland, D., & Hieter, P. (1999). Ctf7p is essential for sister chromatid cohesion and links mitotic chromosome structure to the DNA replication machinery. *Genes and Development*, *13*(3), 307–319. https://doi.org/10.1101/gad.13.3.307

Smith, J. R., Maguire, S., Davis, L. A., Alexander, M., Yang, F., Chandran, S., ffrench-Constant, C., & Pedersen, R. A. (2008). Robust, Persistent Transgene Expression in Human Embryonic Stem Cells Is Achieved with AAVS1-Targeted Integration. *Stem Cells*, *26*(2), 496–504. https://doi.org/10.1634/stemcells.2007-0039

Soppa, J. (2001). Prokaryotic structural maintenance of chromosomes (SMC) proteins: Distribution, phylogeny, and comparison with MukBs and additional prokaryotic and eukaryotic coiled-coil proteins. *Gene*, *278*(1–2), 253–264. https://doi.org/10.1016/S0378-1119(01)00733-8

Srinivasan, M., Petela, N. J., Scheinost, J. C., Collier, J., Voulgaris, M., Roig, M. B., Beckouët, F., Hu, B., & Nasmyth, K. A. (2019). Scc2 counteracts a wapl-independent mechanism that releases cohesin from chromosomes during G1. *ELife*, *8*. https://doi.org/10.7554/eLife.44736.001

Srinivasan, M., Scheinost, J. C., Petela, N. J., Gligoris, T. G., Wissler, M., Ogushi, S., Collier, J. E., Voulgaris, M., Kurze, A., Chan, K. L., Hu, B., Costanzo, V., & Nasmyth, K. A. (2018). The Cohesin Ring Uses Its Hinge to Organize DNA Using Non-topological as well as Topological Mechanisms. *Cell*, *173*(6), 1508-1519.e18. https://doi.org/10.1016/j.cell.2018.04.015

Srinivisan, M., Fumasoni, M., Petela, N., Murray, A. W., & Nasmyth, K. A. (2020). *Cohesion is established during DNA replication by converting pre-existing chromosomal cohesin into cohesive structures as well as by de novo loading of cohesin onto nascent DNAs*. 1–27.

Stemmann, O., Zou, H., Gerber, S. A., Gygi, S. P., & Kirschner, M. W. (2001). Dual Inhibition of Sister Chromatid Separation at Metaphase. *Cell*, *107*(6), 715–726. https://doi.org/10.1016/S0092-8674(01)00603-1

Strunnikov, A. V., Larionov, V. L., & Koshland, D. (1993). SMC1: An essential yeast gene encoding a putative head-rod-tail protein is required for nuclear division and defines a new ubiquitous protein family. *Journal of Cell Biology*, *123*(6 PART 2), 1635–1648. https://doi.org/10.1083/jcb.123.6.1635

Sumara, I., Vorlaufer, E., Gieffers, C., Peters, B. H., & Peters, J. M. (2000). Characterization of vertebrate cohesin complexes and their regulation in prophase. *Journal of Cell Biology*, *151*(4), 749–761. https://doi.org/10.1083/jcb.151.4.749

Suryadinata, R., Sadowski, M., & Sarcevic, B. (2010). Control of cell cycle progression by phosphorylation of cyclin-dependent kinase (CDK) substrates. In *Bioscience reports* (Vol. 30, Issue 4, pp. 243–255). Portland Press. https://doi.org/10.1042/BSR20090171

Takahashi, T. S., Yiu, P., Chou, M. F., Gygi, S., & Walter, J. C. (2004). Recruitment of Xenopus Scc2 and cohesin to chromatin requires the pre-replication complex. *Nature Cell Biology*, *6*(10), 991–996. https://doi.org/10.1038/ncb1177

Tanaka, T. U. (2010). Kinetochore-microtubule interactions: Steps towards bi-orientation. *EMBO Journal*, *29*(24), 4070–4082. https://doi.org/10.1038/emboj.2010.294

Tanaka, T. U., & Desai, A. (2008). Kinetochore-microtubule interactions: the means to the end. In *Current Opinion in Cell Biology* (Vol. 20, Issue 1, pp. 53–63). Elsevier Current Trends. https://doi.org/10.1016/j.ceb.2007.11.005

Tanaka, T. U., Rachidi, N., Janke, C., Pereira, G., Galova, M., Schiebel, E., Stark, M. J. R., & Nasmyth, K. (2002). Evidence that the Ipl1-Sli15 (Aurora Kinase-INCENP) complex promotes chromosome bi-orientation by altering kinetochore-spindle pole connections. *Cell*, *108*(3), 317–329. https://doi.org/10.1016/S0092-8674(02)00633-5

Tedeschi, A., Wutz, G., Huet, S., Jaritz, M., Wuensche, A., Schirghuber, E., Davidson, I. F.,

Tang, W., Cisneros, D. A., Bhaskara, V., Nishiyama, T., Vaziri, A., Wutz, A., Ellenberg, J., & Peters, J. M. (2013). Wapl is an essential regulator of chromatin structure and chromosome segregation. *Nature*, *501*(7468), 564–568. https://doi.org/10.1038/nature12471

Tonkin, E. T., Wang, T. J., Lisgo, S., Bamshad, M. J., & Strachan, T. (2004). NIPBL, encoding a homolog of fungal Scc2-type sister chromatid cohesion proteins and fly Nipped-B, is mutated in Cornelia de Lange syndrome. *Nature Genetics*, *36*(6), 636–641. https://doi.org/10.1038/ng1363

Tóth, A., Ciosk, R., Uhlmann, F., Galova, M., Schleiffer, A., & Nasmyth, K. (1999). Yeast cohesin complex requires a conserved protein, Eco1p(Ctf7), to establish cohesion between sister chromatids during DNA replication. *Genes and Development*, *13*(3), 320–333. https://doi.org/10.1101/gad.13.3.320

Uhlmann, F., Lottspelch, F., & Nasmyth, K. (1999). Sister-chromatid separation at anaphase onset is promoted by cleavage of the cohesin subunit Scc1. *Nature*, *400*(6739), 37–42. https://doi.org/10.1038/21831

Uhlmann, F., & Nasmyth, K. (1998). Cohesion between sister chromatids must be established during DNA replication. *Current Biology*, *8*(20), 1095–1102. https://doi.org/10.1016/s0960-9822(98)70463-4

Uhlmann, F., Wernic, D., Poupart, M. A., Koonin, E. V., & Nasmyth, K. (2000). Cleavage of cohesin by the CD clan protease separin triggers anaphase in yeast. *Cell*, *103*(3), 375–386. https://doi.org/10.1016/S0092-8674(00)00130-6

Ünal, E., Heidinger-Pauli, J. M., Kim, W., Guacci, V., Onn, I., Gygi, S. P., & Koshland, D. E. (2008). A molecular determinant for the establishment of sister chromatid cohesion. *Science*, *321*(5888), 566–569. https://doi.org/10.1126/science.1157880

van Ruiten, M. S., van Gent, D., Sedeño Cacciatore, Á., Fauster, A., Willems, L., Hekkelman, M. L., Hoekman, L., Altelaar, M., Haarhuis, J. H. I., Brummelkamp, T. R., de Wit, E., & Rowland, B. D. (2022). The cohesin acetylation cycle controls chromatin loop length through a PDS5A brake mechanism. *Nature Structural and Molecular Biology*, *29*(6), 586–591. https://doi.org/10.1038/s41594-022-00773-z

Verma, R., Mohl, D., & Deshaies, R. J. (2020). Harnessing the Power of Proteolysis for Targeted Protein Inactivation. In *Molecular Cell* (Vol. 77, Issue 3, pp. 446–460). Cell Press. https://doi.org/10.1016/j.molcel.2020.01.010

Vian, L., Pękowska, A., Rao, S. S. P., Kieffer-Kwon, K. R., Jung, S., Baranello, L., Huang, S. C., El Khattabi, L., Dose, M., Pruett, N., Sanborn, A. L., Canela, A., Maman, Y., Oksanen, A., Resch, W., Li, X., Lee, B., Kovalchuk, A. L., Tang, Z., … Casellas, R. (2018). The Energetics and Physiological Impact of Cohesin Extrusion. *Cell*, *173*(5), 1165-1178.e20. https://doi.org/10.1016/j.cell.2018.03.072

Waizenegger, I. C., Hauf, S., Meinke, A., & Peters, J. M. (2000). Two distinct pathways remove mammalian cohesin from chromosome arms in prophase and from centromeres in anaphase. *Cell*, *103*(3), 399–410. https://doi.org/10.1016/S0092-8674(00)00132-X

Wang, M. D. (2021). Ruler of life. *Nature Physics*, *17*(8), 976. https://doi.org/10.1038/s41567-021-01300-5

Wang, Y., Wang, F., Wang, R., Zhao, P., & Xia, Q. (2015). 2A self-cleaving peptide-based

multi-gene expression system in the silkworm Bombyx mori. *Scientific Reports*, *5*(1), 1–10. https://doi.org/10.1038/srep16273

Watrin, E., Schleiffer, A., Tanaka, K., Eisenhaber, F., Nasmyth, K., & Peters, J. M. (2006). Human Scc4 Is Required for Cohesin Binding to Chromatin, Sister-Chromatid Cohesion, and Mitotic Progression. *Current Biology*, *16*(9), 863–874. https://doi.org/10.1016/j.cub.2006.03.049

Webb, C. D., Teleman, A., Gordon, S., Straight, A., Belmont, A., Lin, D. C. H., Grossman, A. D., Wright, A., & Losick, R. (1997). Bipolar localization of the replication origin regions of chromosomes in vegetative and sporulating cells of B. subtilis. *Cell*, *88*(5), 667–674. https://doi.org/10.1016/S0092-8674(00)81909-1

Weitzer, S., Lehane, C., & Uhlmann, F. (2003). A Model for ATP Hydrolysis-Dependent Binding of Cohesin to DNA. *Current Biology*, *13*(22), 1930–1940. https://doi.org/10.1016/j.cub.2003.10.030

Wells, J. N., Gligoris, T. G., Nasmyth, K. A., & Marsh, J. A. (2017). Evolution of condensin and cohesin complexes driven by replacement of Kite by Hawk proteins. In *Current Biology* (Vol. 27, Issue 1, pp. R17–R18). Cell Press. https://doi.org/10.1016/j.cub.2016.11.050

Wendt, K. S., Yoshida, K., Itoh, T., Bando, M., Koch, B., Schirghuber, E., Tsutsumi, S., Nagae, G., Ishihara, K., Mishiro, T., Yahata, K., Imamoto, F., Aburatani, H., Nakao, M., Imamoto, N., Maeshima, K., Shirahige, K., & Peters, J. M. (2008). Cohesin mediates transcriptional insulation by CCCTC-binding factor. *Nature*, *451*(7180), 796–801. https://doi.org/10.1038/nature06634

Wutz, G., Ladurner, R., St Hilaire, B. G., Stocsits, R. R., Nagasaka, K., Pignard, B., Sanborn, A., Tang, W., Varnai, C., Ivanov, M. P., Schoenfelder, S., Van Der Lelij, P., Huang, X., Durnberger, G., Roitinger, E., Mechtler, K., Finley Davidson, I., Fraser, P., Lieberman-Aiden, E., & Peters, J. M. (2020). ESCO1 and CTCF enable formation of long chromatin loops by protecting cohesinstag1 from WAPL. *ELife*, *9*. https://doi.org/10.7554/eLife.52091

Wutz, G., Várnai, C., Nagasaka, K., Cisneros, D. A., Stocsits, R. R., Tang, W., Schoenfelder, S., Jessberger, G., Muhar, M., Hossain, M. J., Walther, N., Koch, B., Kueblbeck, M., Ellenberg, J., Zuber, J., Fraser, P., & Peters, J. (2017). Topologically associating domains and chromatin loops depend on cohesin and are regulated by CTCF, WAPL, and PDS5 proteins. *The EMBO Journal*, *36*(24), 3573–3599. https://doi.org/10.15252/embj.201798004

Xu, H., Boone, C., & Brown, G. W. (2007). Genetic Dissection of Parallel Sister-Chromatid Cohesion Pathways. *Genetics*, *176*(3), 1417–1429. https://doi.org/10.1534/genetics.107.072876

Yang, H., Wang, H., Shivalila, C. S., Cheng, A. W., Shi, L., & Jaenisch, R. (2013). XOne-step generation of mice carrying reporter and conditional alleles by CRISPR/cas-mediated genome engineering. *Cell*, *154*(6), 1370. https://doi.org/10.1016/j.cell.2013.08.022

Yatskevich, S., Rhodes, J., & Nasmyth, K. (2019). Organization of Chromosomal DNA by SMC Complexes. *Annual Review of Genetics*, *53*(1), 445–482. https://doi.org/10.1146/annurev-genet-112618-043633

Yesbolatova, A., Saito, Y., Kitamoto, N., Makino-Itou, H., Ajima, R., Nakano, R., Nakaoka,

H., Fukui, K., Gamo, K., Tominari, Y., Takeuchi, H., Saga, Y., Hayashi, K. ichiro, & Kanemaki, M. T. (2020). The auxin-inducible degron 2 technology provides sharp degradation control in yeast, mammalian cells, and mice. *Nature Communications*, *11*(1). https://doi.org/10.1038/s41467-020-19532-z

Yu, C., Gan, H., Serra-Cardona, A., Zhang, L., Gan, S., Sharma, S., Johansson, E., Chabes, A., Xu, R.-M., & Zhang, Z. (2018). A mechanism for preventing asymmetric histone segregation onto replicating DNA strands. *Science*, *361*(6409), 1386–1389. https://doi.org/10.1126/science.aat8849

Zhang, J., Shi, X., Li, Y., Kim, B. J., Jia, J., Huang, Z., Yang, T., Fu, X., Jung, S. Y., Wang, Y., Zhang, P., Kim, S. T., Pan, X., & Qin, J. (2008). Acetylation of Smc3 by Eco1 Is Required for S Phase Sister Chromatid Cohesion in Both Human and Yeast. *Molecular Cell*, *31*(1), 143–151. https://doi.org/10.1016/j.molcel.2008.06.006

Zheng, G., Kanchwala, M., Xing, C., & Yu, H. (2018). MCM2–7-dependent cohesin loading during s phase promotes sister-chromatid cohesion. *ELife*, *7*. https://doi.org/10.7554/eLife.33920

Zhu, Y., Denholtz, M., Lu, H., & Murre, C. (2021). Calcium signaling instructs NIPBL recruitment at active enhancers and promoters via distinct mechanisms to reconstruct genome compartmentalization. *Genes and Development*, *35*(1), 65–81. https://doi.org/10.1101/GAD.343475.120

Zielke, N., & Edgar, B. A. (2015). FUCCI sensors: Powerful new tools for analysis of cell proliferation. In *Wiley Interdisciplinary Reviews: Developmental Biology* (Vol. 4, Issue 5, pp. 469–487). John Wiley and Sons Inc. https://doi.org/10.1002/wdev.189

Zuin, J., Franke, V., van IJcken, W. F. J., van der Sloot, A., Krantz, I. D., van der Reijden, M. I. J. A., Nakato, R., Lenhard, B., & Wendt, K. S. (2014). A Cohesin-Independent Role for NIPBL at Promoters Provides Insights in CdLS. *PLoS Genetics*, *10*(2), e1004153. https://doi.org/10.1371/journal.pgen.1004153